TRANS-TIBIAL SOCKET DESIGN VARIATIONS AND THEIR INFLUENCE ON STATIC AND DYNAMIC PRESSURE PATTERNS

by

Ronald Hulshof

This thesis is submitted in partial fulfilment of the requirements for the degree of Master of Philosophy in Prosthetics and Orthotics

National Centre for Training and Education
in Prosthetics and Orthotics
University of Strathclyde
Glasgow, Scotland, United Kingdom.

March, 1995

ABSTRACT

The aim of this study was to test whether the distal end loading in a trans-tibial socket is affected by modifications in the patellar tendon, medial tibial flare and lateral tibial flare areas.

The Strathclyde CAD/CAM system was used to design and manufacture six sockets for one patient. Four sockets had modifications in the above mentioned areas, increasing in depth and volume from 0% to 150% of the reference socket modifications. Two additional sockets were designed to be equal in volume but different in proximal shape. This meant that the effect of shape changes on the distal end pressure could be separated from the effect of volume changes.

The patellar tendon, medial tibial flare, lateral tibial flare and the distal end of the sockets were instrumented with pressure transducers, incorporated in the socket wall. Series of static and dynamic tests were performed on all six sockets. Static pressures and peak dynamic pressures were selected to base the socket comparisons on.

In the static tests, the proximal modifications led to small, but significant decreases in distal end pressure. In the dynamic tests, there was no clear correlation between proximal modifications and distal end pressure.

ACKNOWLEDGEMENTS

I would like to thank all the staff in the National Centre for their contributions at various stages of this research project. Without the facilities and the support from the Centre, this project would never have taken place.

In particular, I would like to thank:

- Derek Jones, for stimulating me to do a M. Phil. and for making everything happen
- Peter Convery, for his suggestions and prompt reviews of each section of the thesis
- Jack Taylor, for his companionship and extensive knowledge of the history of prosthetics
- Bo Klasson, for his insight into both the practical and biomechanical aspects of prosthetic design
- Frank Larkin, for the carving of all the socket models
- the staff from the library, audiovisual and printing unit for their support and access to their resources

Last but not least, I would like to thank my wife Lydia for her encouragement at the times that the writing of this thesis seemed to take forever.

DEDICATION

To my parents:

for their courage in difficult times

and the freedom they have given me to lead my own life

CONTENTS

CHAPTER 1

GENERAL INTRODUCTION

Designing a comfortable prosthesis for a patient with a trans-tibial amputation is not an easy task. The prosthetist has no control over the quality or type of amputation nor over the general health of the patient. The typical patient in the industrialised countries is an elderly person, suffering from peripheral vascular disease. This generally results in a poorly vascularised stump, ill equipped to support full body weight.

Yet, many patients walk day in, day out on their artificial limbs without great difficulties. Clearly, a well designed socket and prosthesis can succeed in providing a reasonable mobility.

A major problem in prosthetic socket design is that there is no general agreement on how a good prosthetic socket should be designed. Current knowledge about the nature of force transfer between socket and skeleton through the intermediate tissues is very limited. The allowable normal and shear stress levels in tissues are not known. The influence of socket design on stump perfusion is not known. In other words, it is not yet possible to design prosthetic sockets to specific standards.

However, it *is* possible to investigate some claims of existing socket design concepts. New tools, such as CAD/CAM systems, allow the prosthetist to quantify and record socket designs in ways that were not possible in the traditional design process. Both volume and shape of the socket and its modifications can be recorded and reproduced.

These facilities simplify quantified socket design research considerably. In this project, the Strathclyde CAD/CAM system was used to investigate the effectiveness of the traditional patellar tendon, medial tibial flare and lateral tibial flare modifications in offloading the distal end. This was done by creating volume and shape controlled sockets and instrumenting these with pressure transducers in the areas of interest.

Six socket design variations were tested on one patient in both standing and walking trials. The results are limited in significance as only one subject was used. However, the methodology appeared to be successful and the trends observed might be indicative of the limitations of the PTB modifications.

CHAPTER 2

THE TRANS-TIBIAL AMPUTATION LEVEL

2.1 Introduction

An optimal socket design allows the transfer of support and control forces from the socket of a prosthesis to the skeleton of an amputee without tissue damage or discomfort. There is no consensus about optimal socket design because there is little knowledge about the way forces are transmitted through the stump's tissues.

In chapter 2 the functional anatomy of the stump is explored to investigate whether the assumptions of old and new socket design concepts are correct and what the consequences of these assumptions are. The need for various types of research is defined as a result of this examination.

Special attention is paid to the suitability of the patellar tendon as a load bearing structure. The feasibility of hydrostatic force transfer through soft tissues is examined and it's effect on the local circulation assessed.

2.2 Detailed anatomy of the trans-tibial stump

The anatomy of the trans-tibial stump is of particular importance for a prosthetist. Large forces need to be transferred between skeleton and socket without causing tissue damage. As the skeleton is the structural element with the highest rigidity, most of the body weight will be transferred from bone to bone across the intermediate joints. In a normal subject this link ends distally with the foot bones. The calcaneus and the metatarsal heads are separated from the supporting surface by only a few millimetres of specialised skin, with suitable load bearing characteristics. The only skin on the stump that is specialised to take some load is located at the patellar tendon area.

After a trans-tibial amputation the amputee is left with less than half the original length of the tibia and fibula. The fibula is generally left about 1 cm shorter than the tibia. Some mobility of the distal end of the fibula is usually present.

Of the skeletal elements proximal to that level, the femur and the pelvis are of prosthetic significance. The distal end of the femur flares out to form two bearing surfaces: the femoral condyles. The upper sloping surface of the medial femoral condyle can be used to prevent downward displacement of the socket relative to the stump during swing phase (supracondylar suspension). Historically, the thigh and the ischial tuberosity were used to provide additional weight bearing areas because the stump alone was deemed unfit to take all the load. In cases of severe stump problems or extreme loading of the limb such as in heavy manual work, thigh corsets and ischial gluteal bearing structures can still be added to a trans-tibial prosthesis.

The addition of prosthetic segments proximal to the knee joint causes a considerable mechanical problem. The knee joint is not a single axis joint but one in which the instantaneous centre of rotation varies which each degree of flexion (Murphy, 1954). This means that the addition of side steels with knee joints causes a discrepancy between the movement of prosthetic segments and anatomical segments resulting in potentially damaging shear forces at the knee joint.

On the anterior and medial side, the tibia is only covered by skin. Posteriorly, some muscle bulk of the gastrocnemius and sometimes the soleus is present, depending on the type of amputation. If the gastrocnemius is sutured to the distal end of the tibia, it retains it's function as a knee flexor as it originates on the distal end of the femur. All muscles *originating* on the tibia lose their function and are either excised at the amputation or atrophy over time. The result is a stump that is very asymmetrical in its mechanical properties. Only two areas remain that can significantly change their shape and mechanical properties *actively:* the posterior aspect overlying the gastrocnemius and the patellar tendon area (due to the activity of the quadriceps).

The blood supply for the leg passes through the popliteal artery, which divides into three arteries just below the level of the fibular head: the anterior and posterior tibial artery and the peroneal artery. Two venous systems are present in the leg: the deep system and the superficial system. The deep

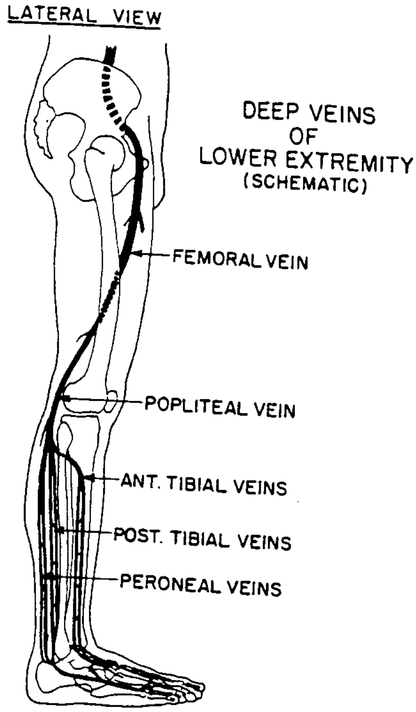

Fig. 2.2.1 (Reproduced from Radcliffe, 1961)

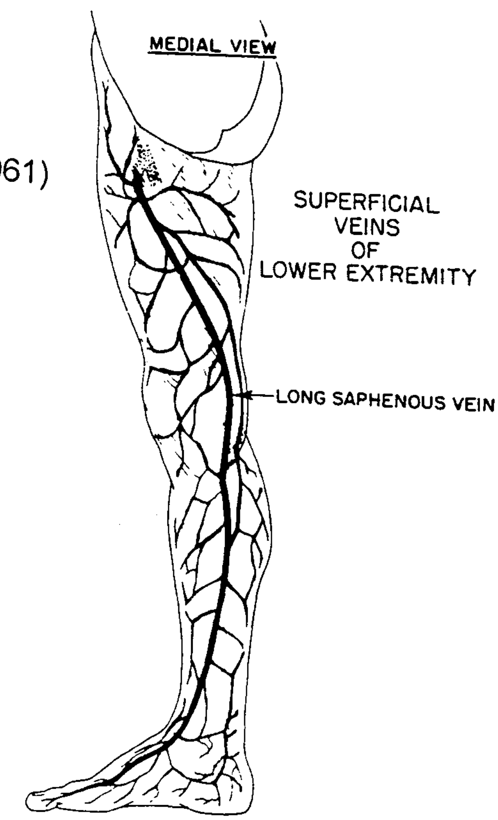

Fig. 2.2.2 (Reproduced from Radcliffe, 1961)

system accompanies the arterial system and has a similar nomenclature (fig. 2.2.1). Most of the blood circulating through the musculature returns through this system. Of the superficial system, the main vein is the long saphenous vein. Most of the blood supply of the skin and subcutaneous tissues returns through this system (fig. 2.2.2). Both the deep and superficial systems are accompanied by lymph vessels.

In the healthy leg, contraction of musculature next to veins is thought to increase the venous return. One way valves, of which there are more in the deep system than in the superficial system, prevent any reverse flow taking place. After amputation many muscles will become nonfunctional and atrophy, thus reducing their effect on the venous return.

In the stump, the cyclic pressure applied by the stump to the socket during walking is thought to enhance the circulation. This would only occur if:

1) the pressure in the stump tissue would decrease from distal to proximal
2) there is less resistance to flow in the venous direction than in the arterial direction.

The latter condition is likely to be fulfilled due to structural differences in arteries and veins such as wall thickness and elasticity and the presence of one way valves. The former condition is more difficult to fulfill, it depends on socket design, loading patterns and local pressure variations due to differences in the mechanical characteristics of all the tissues involved.

The lymphatic system returns interstitial fluid to the circulatory system.

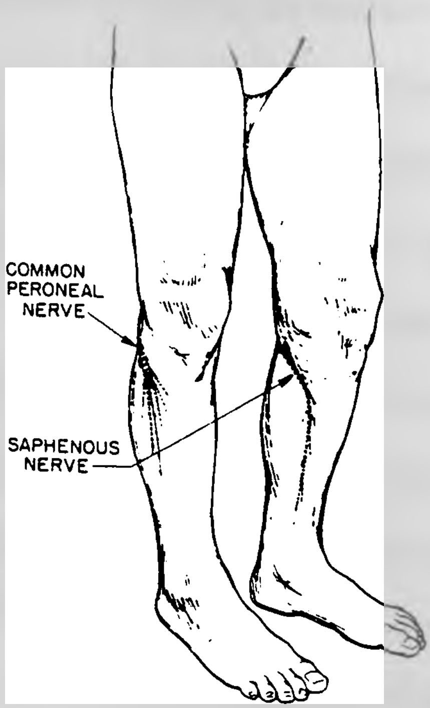

Fig. 2.2.3 (Reproduced from Radcliffe, 1961)

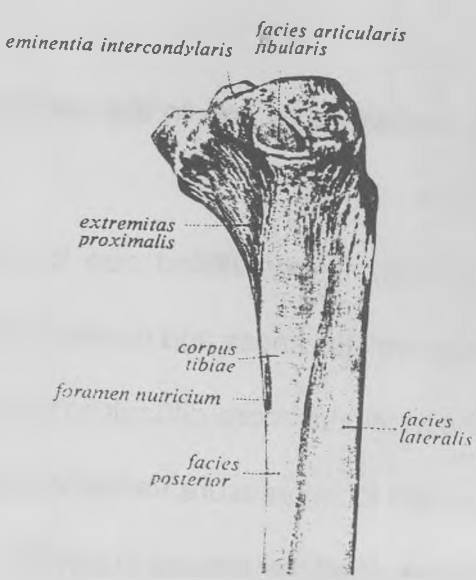

Fig. 2.2.4 (Reproduced from Sobotta, 1982)

When this system is dysfunctional or overloaded, edema is the result. Edema in stumps is mainly associated with a lack of total contact such as in the open-ended sockets commonly used in the past. The primary amputee always suffers to some extent from edema when healing of the stump takes place. Good volume control with the help of rigid dressings or elasticated bandages is vital in preparing the stump for its first prosthesis.

The nerve supply of the lower limb originates from the femoral and the sciatic nerve. Two branches are of clinical importance to the prosthetist: the common peroneal nerve originating from the sciatic nerve and the saphenous nerve originating from the femoral nerve (fig. 2.2.3). The common peroneal nerve passes anteriorly over the distal part of the head of the fibula and is easily irritated and injured by external forces. The saphenous nerve passes on the medial flare of the tibia, is less easily irritated but located in an area normally used to apply pressure to.

In the average trans-tibial amputee, the tibia is the bone through which most of the body weight must be transferred during stance phase. The tibia has a triangular shape in the transverse plane and decreases in cross-sectional area from proximal to distal. The centre of the proximal end is located posterior to the centre of the shaft (fig. 2.2.4). This creates sloping surfaces on the medial, lateral and posterior side of the proximal end. From 5 cm distal to the tibial plateau the angle of the sloping surfaces increases rapidly to a maximum of about 45 degrees to the central axis of the tibia. The maximum proximal cross-sectional area is about seven times the cross-sectional area halfway down the tibia.

The medial and lateral flare have traditionally been regarded as biomechanically advantageous areas to transfer weight bearing forces. Socket designs have reflected this by matching the socket shape in those areas to the underlying bony anatomy. The posterior flare has not been emphasized due to the amount of soft tissue in this area. However, it is likely that compressed tissue between posterior socket wall and posterior tibial flare will exert a significant amount of pressure on this area. Because of the size and the inclination of the area, considerable axial support could be provided (see section 2.4.1).

Flexion and extension of the knee are controlled by the hamstrings and the quadriceps respectively. In the normal trans-tibial amputee both the hamstrings and the quadriceps remain completely intact. The hamstrings consist of three muscles, the semitendinosus, the semimembranosus and the biceps femoris named after its two heads: the short head originates from the posterior aspect of the lower part of the femur and the long head originates from the ischial tuberosity, in common with the two semi's. The semi's insert on the medial side of the tibia and are capable of hip extension, knee flexion and internal rotation of the leg. The biceps femoris inserts mainly on the head of the fibula and generates hip extension, knee flexion and external rotation of the leg.

The quadriceps consists of four muscle groups: the vastus medialis, lateralis, intermedius and rectus femoris. Their tendons merge into one single tendon containing a sesamoid bone: the patella. The patellar tendon originates

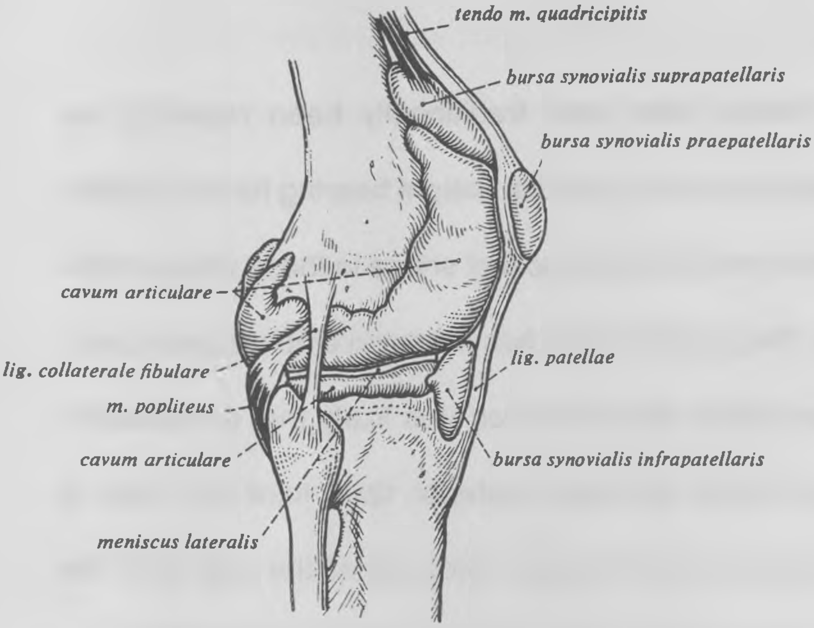

Fig. 2.2.5 (Reproduced from Sobotta, 1982)

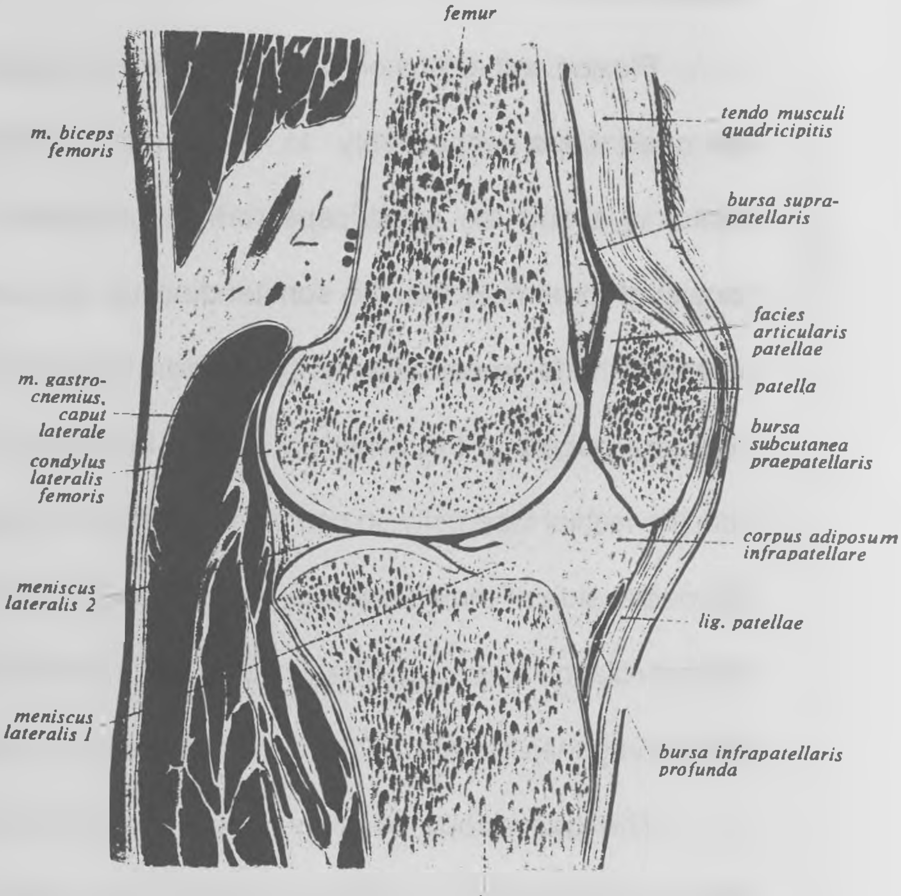

Fig. 2.2.6 (Reproduced from Sobotta, 1982)

from the distal surface of the patella and inserts on the tibial tubercle. The patella has a posterior articulating surface, the facies patellaris, which articulates with a depression between the medial and lateral femoral condyles. The synovial membrane of the knee extends proximally between patellar tendon, patella and femur to form the bursa suprapatellaris (fig. 2.2.5). Distal to the patella lies the bursa infrapatellaris profunda (between patellar tendon and the corpus adiposum infra patellare). The bursa subcutanea infra patellaris is situated between skin and patellar tendon.

The space between patellar tendon and tibial and femoral condyles is filled with the corpus adiposum infrapatellare (fig. 2.2.6). This space increases in size when the knee flexes (Lohman, 1980). The large amount of synovial bursae and adipose bodies in this area allows considerable movement and tissue deformation to take place without the creation of potentially damaging shear forces.

2.3 Changes in muscular activity as a result of trans-tibial amputation

In a normal subject with an average walking speed the quadriceps will be active during the first 20% of the gait cycle. The peak of activity occurs at about 8% of the gait cycle. Initially the quadriceps control the rate of knee flexion by contracting eccentrically. Shortly after foot flat, concentric contraction of the quadriceps extends the knee as the body progresses over the foot. During the last 10% of stance phase they are moderately active to prevent excessive knee flexion.

The hamstrings start to decelerate the forward motion of the shank at the end of swing phase. During the first 15% of the gait cycle they are still active, possibly to assist in hip extension. (Inman, 1981).

The gastrocnemius is active during a large part of stance phase, from about 16 to 60% of the gait cycle. The peak of activity occurs at about 45% when the heel starts to rise and plantarflexion begins. The importance of the plantarflexors for propulsion is illustrated by the fact that they are responsible at push off for over 80% of the mechanical power generated during a gait cycle. (Winter, 1988).

The tibialis anterior is active at the start of the gait cycle to control the plantarflexion of the foot and during swing phase to maintain ground clearance of the foot. After a trans-tibial amputation, the quadriceps and hamstrings are still completely intact but the gastrocnemius now only works across the knee joint. The tibialis anterior has lost its function as have all other muscles with their origin on the tibia.

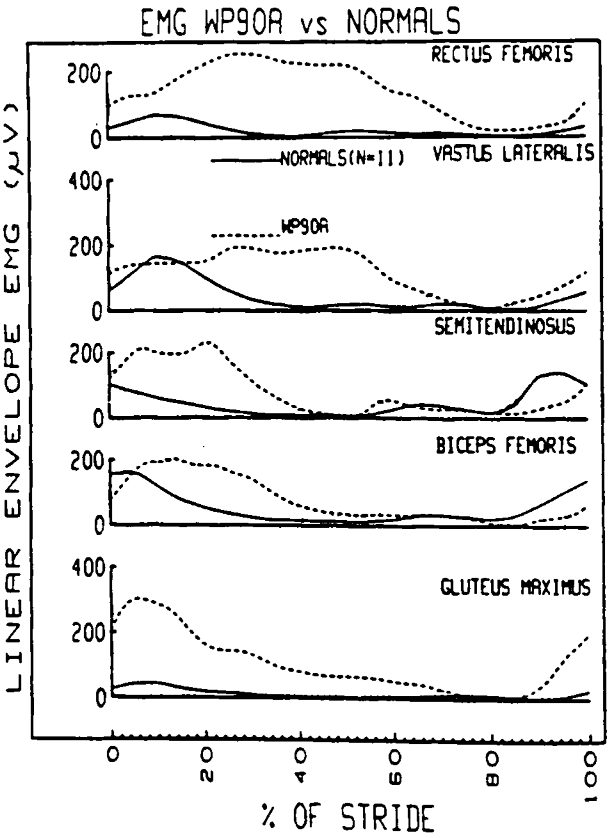

Fig. 2.3.1 (Reproduced from Winter, 1988
WP90A is the amputee's EMG)

The functional loss of the ankle and foot on the amputated side affects muscle activity in both lower limbs (Breakey, 1976; Winter, 1988; Pinzur; 1991). The amputated side shows an increase in activity of the gluteus maximus, quadriceps and the hamstrings during the gait cycle. The exact increase in duration and activity level of the muscle groups is difficult to establish with the electro myographic method and depends on factors such as: the activity level of the amputee (Pinzur, 1991), the type of terminal device used (Breakey, 1976) and the type of suspension used (Grevsten, 1978).

Dynamic EMG measurements of the residual musculature such as the gastrocnemius and the tibialis anterior are hardly reported at all. In a study by Grevsten (1978) the supracondylar strap suspended PTB was compared with a trans-tibial suction prosthesis. Surface electrodes were used to record gastrocnemius and tibialis anterior activity. Differences were found in the amount of simultaneous contraction of antagonistic muscles. This happened more frequently in the strap suspended prostheses during swing phase than in the suction prostheses. It was interpreted as a defence mechanism against slippage between stump and socket during swing phase.

Most authors agree that the activity level of both the quadriceps and the hamstrings is increased during normal gait in a trans-tibial amputee (fig. 2.3.1). Some suggest that the hyperactivity of the quadriceps is caused by the need to compensate for the lack of indirect knee extension, resulting from the absent contraction of the gastrocnemius (Breakey, 1976). Others conclude that abnormal hip extensor activity, partially achieved by hamstrings action resulting in a knee flexion moment, needs to be cancelled out via co-contracting the quadriceps (Winter, 1988)

The increased level of muscle activity in the trans-tibial amputee will greatly affect certain aspects of socket design, e.g. the patellar tendon area. However, the changing properties of the patellar tendon during gait are hardly ever mentioned in discussions of the patellar tendon weight bearing principle or in finite element simulations of the patellar tendon bearing socket and stump. These dynamic characteristics should be taken into consideration, even though this aspect of socket design complicates biomechanical modelling and theorising considerably.

2.4 Socket design for the trans-tibial level of amputation

In 1954 Eugene F. Murphy wrote: 'One must concede at once a considerable confusion and lack of basic knowledge in the entire field of fitting a socket to a stump. Some limb makers and surgeons argue for uniform distribution of pressure over the stump; other believe in supporting high pressures on certain areas considered physiologically and anatomically suitable, while reducing pressure correspondingly on other areas of greater sensitivity and protecting completely some regions thought to be particularly sensitive to pressure.' Forty years later, little has changed. The knowledge of the forces generated by standing and walking on a prosthesis has increased thanks to kinetic and kinematic analyses. Attempts have been made to measure pressures arising between socket and stump in localised areas (see section 3.2.1). The forces that have to be accommodated by the stump during gait have been investigated with strain gauged shank sections and force plates (see sections 2.3 and 2.4.1) However, a clear definition of an optimal socket shape has not been achieved.

The main debate in socket design is still about high localized pressure versus uniform pressure. The former can be said to be represented by the Patellar Tendon Bearing (PTB) concept as advocated by Radcliffe and Foort and the latter by the hydrostatic concept as advocated for both trans-femoral and trans-tibial levels by Isherwood (1971), Redhead (1979) and Kristinsson (1993).

Others such as Murdoch (1965, 1968), Hayes (1975) and Staats (1987) have promoted the use of accurate casting techniques to achieve a more uniform pressure distribution. Murdoch and Staats aimed to some extent for both surface and volume matching (with slight modifications in the patellar tendon area) whereas Hayes used his alginate method mainly for surface matching (but modified 'sensitive areas' at the casting stage by applying buildups).

2.4.1 The patellar tendon bearing concept

In April 1957, Professor C.W. Radcliffe called together a group of knowledgeable prosthetists and educators to systematize trans-tibial socket design and disseminate the resulting information. Until that time, most sockets were of the open-ended type, made from leather or wood. A thigh corset connected to the socket by two side steels with single axis joints provided additional weight bearing and stability. Many patients had stump problems, mainly at the distal end and the head of the fibula. The amputee population was fairly young and consisted mainly of war veterans.

Prosthetic research was done at places such as the Navy Prosthetic Research Laboratory in Oakland reflecting the military cause of most amputations. This laboratory developed and tested various prosthetic procedures and components such as the below-the-knee, closed-end, soft socket (Bleck, 1963). The use of cushioning materials and air-cushions was already patented early this century according to the records of the American patent office. After the second world war, plastics started to be used in prosthetics to increase hygiene and comfort of the amputees.

According to Foort (1984), the Berkeley team derived their information from various sources. The use of the patellar tendon bar as a weight bearing surface was based on German practice, total contact was already used at research level to control edema and the technique for making soft (Kemblo) liners was based on Shindler's technique. Some centres provided selected amputees with the Muley prostheses, prostheses without a thigh lacer but with a soft leather cuff.

A good example of the teams' practical approach is the following anecdote: 'When one of our test amputees rebelled at having the corset-joint system added to his prosthesis following successful trials without, the switch was made to what is now the PTB below-knee prosthesis.' The result of this approach was a manual titled 'The Patellar-Tendon-Bearing Below-Knee Prosthesis'. The manual contained a detailed section on the anatomy of the stump. It also contained a general introduction to the principles of biomechanics and the application of it to the gait of normal subjects and amputees. The analysis of stump socket forces was *theoretical* and based on the assumption that the below-knee amputee can be expected to walk similarly to a normal person. Most of the manual was taken up by a description of practical procedures such as taking a wrap cast, modifying the positive model, manufacturing the socket and static and dynamic alignment of the prosthesis.

The practical nature of the information and the combination of new promising ideas from various sources contributed to the success and the lasting popularity of the method. However, the information on optimum socket design was fairly scarce. In the anatomy section a superficial description of 'pressure tolerant' and 'pressure sensitive' areas was given. In the biomechanics section vertical support was stated to consist of (1) patellar tendon pressure, (2) pressure against the medial flare of the tibial condyle and (3) partial end-bearing. At the time, the partial end-bearing concept was criticised by many who were used to fitting open-ended sockets. Others questioned the effectiveness of the patellar tendon bar in providing vertical support.

Foort himself conducted experiments in the early sixties with locally adjustable PTB's. The experiments were conducted to research the possibilities of standardisation and modularisation of trans-tibial sockets. His results were published at the University of Strathclyde in 1984(!). Two of his findings were contradictory to the guidelines published in the manual:

'1) pressure into the popliteal area of the stump caused a painful sensation that the amputee interpreted as distal discomfort

2) increased pressure on the patellar tendon bar did not improve weight bearing. Less PTB pressure seemed required than was advocated at the time.'

Murdoch conducted experiments with a hydrostatic casting technique and concluded in a discussion of the method in 1965: 'With stumps of the osteo-myo-plastic variety little or no patellar tendon bar is required'. (A detailed description of this method is found in section 2.4.2)

Besser experimented with an adjustable patellar tendon bar section and claimed in 1992 that up to 45% of the body weight can be supported on the patellar tendon (see section 3.2.1). Clearly, there is a wide variety of opinion on the subject.

The mechanism of force transfer between patellar tendon bar and the residual skeleton has not been explored in any depth in the literature. Nor has the degree of vertical load transferred through the patellar bar been measured extensively. In the next section an attempt is made to analyse the

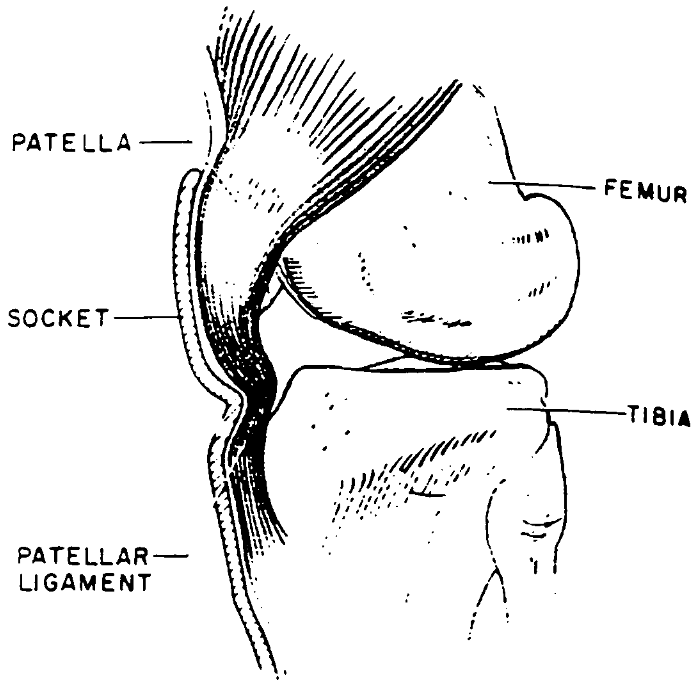

Fig. 2.4.1.1 (Reproduced from Murphy, 1961)

biomechanical effects of the patellar tendon modification in as much detail as current anatomical knowledge and published research allows.

Radcliffe and Foort attributed the capacity of the patellar tendon to contribute to weight bearing to the structural properties of the tendon and the inclined support surface that can be created. Five degrees of initial flexion was recommended as a bench alignment to increase the inclination of the upper surface of the patellar tendon bar relative to the vertical axis. Dr. Eugene Murphy, one of the project group members, published in 1961 a drawing of the way the patellar tendon was supposed to conform to the shape of the socket in that area, illustrating the biomechanical advantage of inclined support surfaces (fig. 2.4.1.1). No attempt was made to assess the influence of quadriceps activity on the patellar tendon and its mechanical properties.

To assess the suitability of the patellar tendon for weight-bearing (or more exactly: for providing a vertically directed support force) two questions need to be answered:

1) is the tissue of that area suitable for taking a high level of load?
2) how are the vertically directed support forces transferred from socket wall to skeletal structure?

When these questions are answered, a third question needs to be raised:

3) how does the force at the patellar tendon bar influence force patterns in other regions of the socket?

Few of these questions have been explored in any depth in the literature.

Due to the large amount of synovial bursae and adipose bodies around

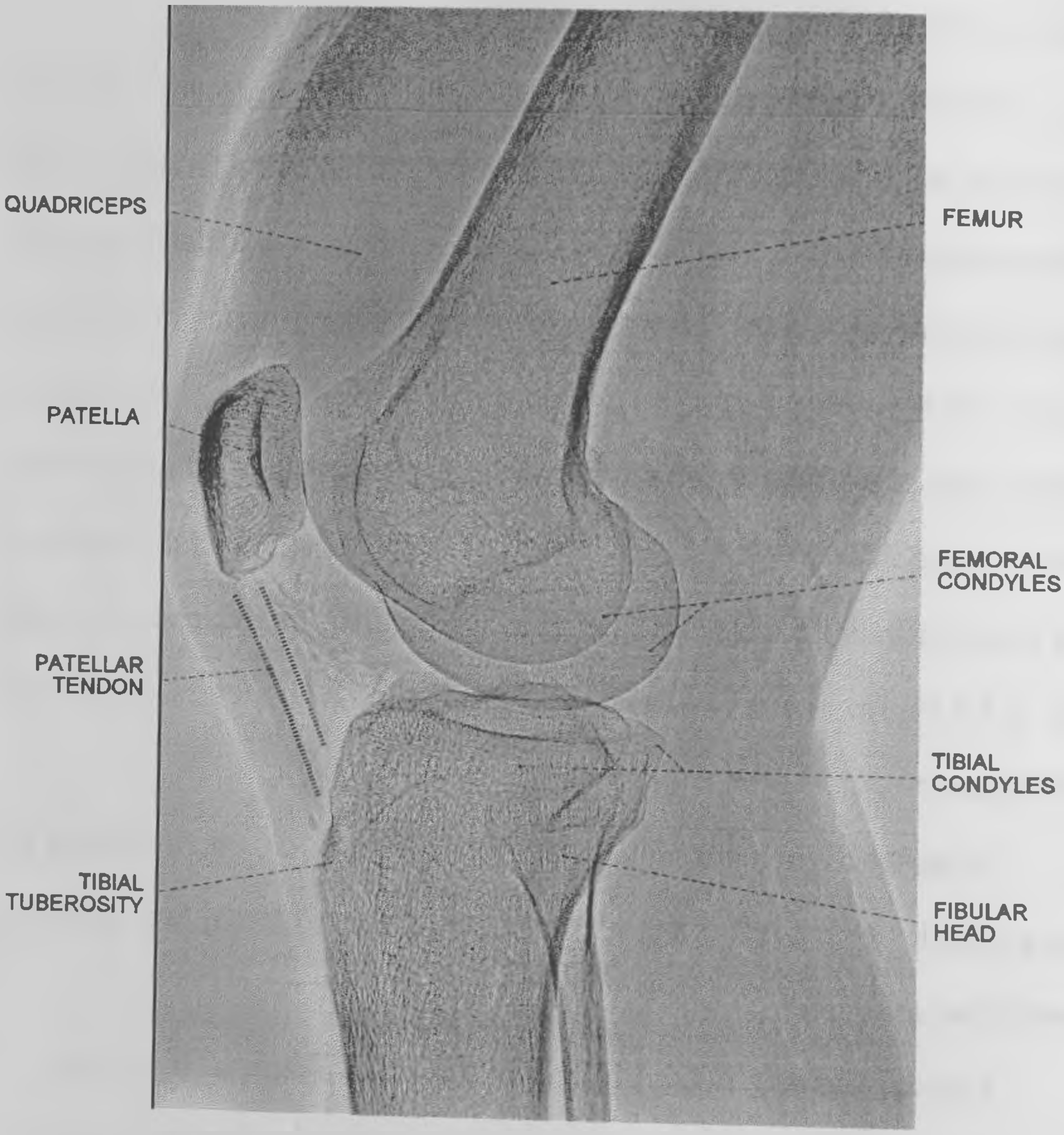

Fig. 2.4.1.2 (Reproduced from Sobotta, 1982)

the patellar tendon (see section 2.2), it is very unlikely that shear stresses of any magnitude can be generated between skin and tendon, and tendon and bone. This prevents the generation of tissue damaging shear forces parallel to the patellar tendon. The tough, flexible structure of the tendon allows the application of large normal stresses without the generation of very localised peak pressures. The skin in this area is more suitable to transmit forces than in other areas of the stump. Thus the answer to question one is positive: the local anatomy is suited to withstanding high levels of loading.

The amount of adipose tissue and the size of the space between patellar tendon and femoral condyles makes direct contact between the patellar tendon and the femoral intercondylar surface unlikely (fig. 2.4.1.2). Because the tendon is a flexible structure and the skin can slide freely over the tendon, the indentation can be displaced along the tendon in the axial direction without immediately generating a vertical support force. Once the indentation comes close to the lower edge of the patella the stump starts to be supported vertically. This is because further downward displacement of the stump could only occur if posterior displacement would take place as well. The latter is resisted by a counterforce provided by the posterior wall. This means that the vertical supporting force in the patellar tendon area is achieved by 'hooking underneath' the inferior edge of the patella and transmitting the support force from the lower edge of the patella as a tensile force through the tendon to the tibial tubercle.

Thus far the patellar tendon has been regarded as a tough but pliable structure. This might be a good approximation for a static situation such as standing. Research has shown that during standing the musculature of the lower limb is hardly active at all (Inman, 1981). It is essentially a balancing act with as little muscular involvement as possible. The trans-tibial amputee must use more of his thigh musculature for this balancing act because of the loss of ankle control and proprioception. However, the control forces are likely to be of a small magnitude compared to those arising during gait.

The increased level of quadriceps activity during the gait of an amputee (see section 2.3) has a profound influence on the mechanical properties of the patellar tendon during stance phase (see section 6.2.4). Instead of behaving like a tough but pliable structure that follows whatever socket contour is created in the area, it offers strong resistance to being indented.

The exact amount of tensile force exerted on the tendon is difficult to determine. Two approaches have been tried: combining force plate and kinematic data to calculate knee moments and measuring the cross-section of the muscle concerned and combining this with ratios of measured EMG signal to maximum EMG signal.

The maximum flexion moment to be opposed by the action of the quadriceps is reported to be 40-60 Nm (Inman 1981, Gowitzke 1988). The moment arm of the quadriceps is reported to be 4.4 cm. This would suggest a tensile force of 50/0.044=1136N. Before the maximum moment, the flexion moment is less but the co-contraction of the hamstrings has to be opposed as

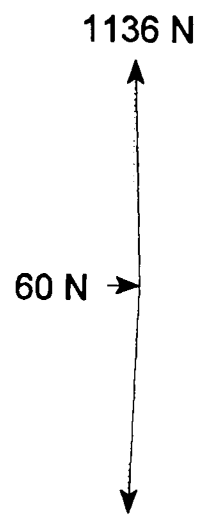

Fig. 2.4.1.3 (Not drawn on scale)

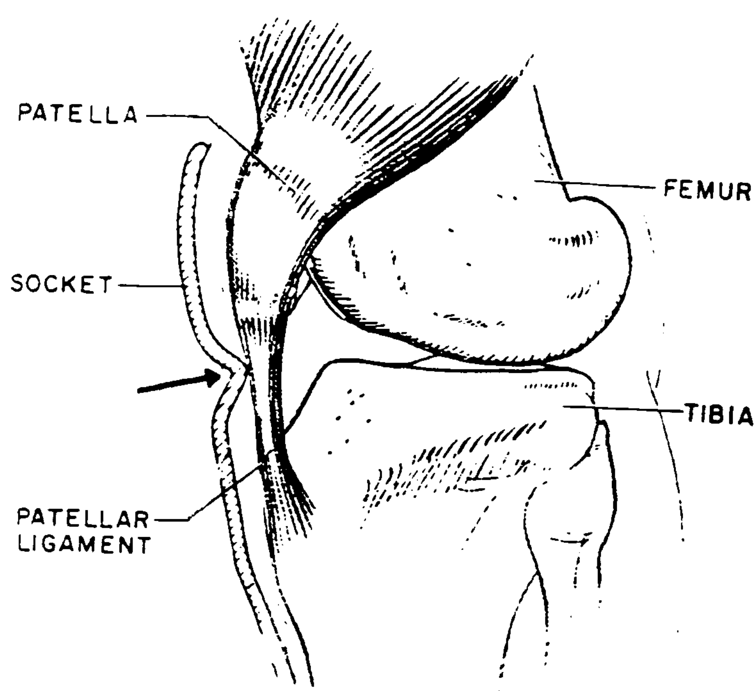

Fig. 2.4.1.4 (Adapted from Murphy, 1961)

well. This means that the calculated force based on kinematic data is an underestimate of the true force required. Peak pressure measurements on the patellar tendon vary, but about 100-200 kPa is commonly reported (see section 3.2.1). If 200 kPa would be uniformly applied to a tendinous area of 1.5 by 2cm =3 cm^2, the force would be $200*10^3*3*10^{-4}=60$ N. Vector analysis shows that the resulting deformation of the patellar tendon is about 1.5 degrees (fig. 2.4.1.3). This clearly illustrates that during critical moments in the stance phase, such as early stance, the tendon does not follow the contour of the patellar tendon bar and cannot be supported on the whole top surface of the bar. Instead, near point loading will take place at the deepest point of the patellar tendon bar (fig. 2.4.1.4).

Another result of the tensioning of the tendon is the posterior displacement of the proximal section of the stump relative to the socket until an equal and opposite counterforce is reached in the popliteal area. The stress levels inside the soft tissue, posterior to the tibia, increase as a result. Because of the size and the inclination of the posterior aspect of the tibial condyles, considerable axial support could be provided. Instead of direct anterior axial support at the patellar tendon itself, an indirect increase in axial support at the proximal posterior section of the tibia would be created (fig. 2.4.1.5).

However, there are several disadvantages related to this posterior displacement of the proximal stump. The stump socket contact at the antero lateral tibial flare is decreased as demonstrated by Isherwood (1978) and by section 7.4. This decreases the possibility of deriving axial support from this

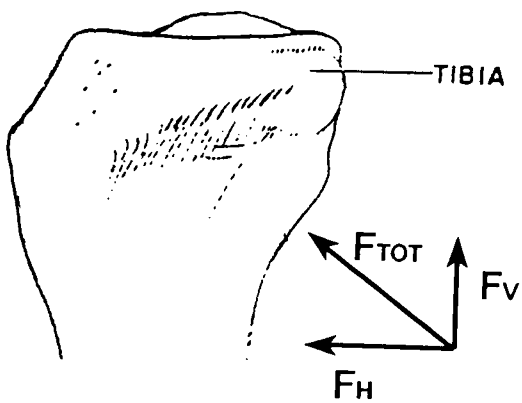

Fig. 2.4.1.5

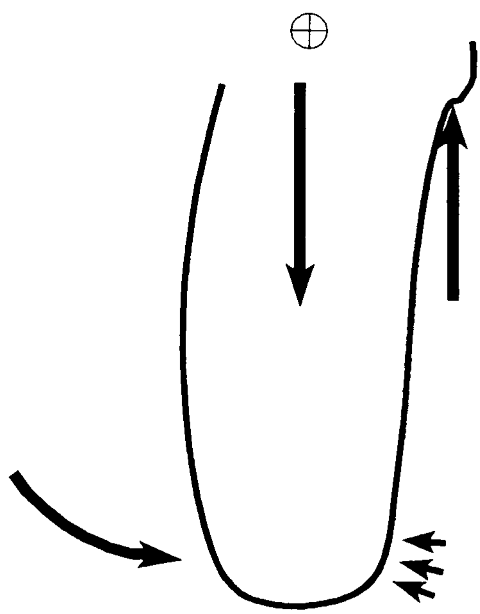

Fig. 2.4.1.6

area. Furthermore, the pressure on the antero-distal aspect will increase for two reasons:

1) the change in angle between anterior socket wall and the anterior surface of the tibia decreases the area of contact between the antero distal end of the tibia and the socket
2) if a considerable axial support force does exist at the patellar tendon, the difference in the line of action of the anteriorly located support force and the centrally oriented body weight will create a moment that rotates the stump relative to the socket in the sagittal plane (fig. 2.4.1.6).

Quadriceps activity increases the pressure on the anterior distal end considerably at the start of stance phase to control the rate of knee flexion. The combination of these effects explains the high pressures measured in this area by various investigators over the past 30 years (see section 3.2.1). The anterior distal end has always been regarded as a problem area requiring buildups to relieve the pressure in this area. It is possible that this is partially caused by modifications in the patellar tendon area. Research is required that investigates the relationship between variations in socket design and pressure patterns resulting from them in the areas modified *and in other critical regions of the socket.*

2.4.2 Controlled pressure casting methods

Individuals who produce statements such as 'instead of loading localised areas the whole surface of the stump is loaded thereby lowering unit pressures' seem to expect the soft tissues to transfer vertical support forces in a hydrostatic manner. Usually no explanation is offered as to how exactly the load is transferred from the surface of the skin to the skeleton.

Questions that need to be asked are:

1) do pressure casting methods apply a (relatively) uniform pressure distribution?
2) what conditions need to be satisfied to create the conditions for hydrostatic weight bearing and what effect do these conditions have on the stump?

The first question is addressed below, the second in section 2.4.3.

Several methods aimed at producing a relatively uniform pressure distribution at the casting stage have been described over the past 40 years. However, none of these methods succeeds in applying a uniform pressure over the whole stump surface. One of the earliest and most interesting casting methods was described by Murdoch (1965). It was actually described as an attempt to eliminate all factors relating to manual dexterity in the casting process. The PTB concept had just been introduced and the lack of experience with this method made it difficult to consistently produce satisfactory sockets.

In this method, a hydrostatic tank was sealed at the top with a double nylon sheet. The patient's stump was covered with socks impregnated with plaster and he was asked to put half his bodyweight on the amputated side. The weight applied was checked by having him stand on a set of scales on his sound side. The supporting force was provided by increasing the water pressure in the tank until the patient was balanced. The pressures quoted were 2 to 6 psi (14-41 kPa). Equal weight bearing commonly required about 14 kPa. The stump was immersed to a level of 7.5 cm above knee level.

If half of the amputees bodyweight had to be suspended by hydrostatic pressure only, the pressures quoted are rather low. An average amputee has a supra patellar cross-sectional area of about 105 cm^2 (0.0105 m^2)[1] and weighs about 80 kg (half body weight: 40 kg). The hydrostatic pressure applied to the stump creates a vertical support force of F=P*A 14000*0.0105=147 N. This corresponds with 147/9.81=15 kg, less than one fifth of the body weight.

Because the hydrostatic pressure is also applied to the sheet material between the leg and the edge of the tank, a tensile stress will develop in the nylon sheet. This tensile stress would have been transferred as a combination of shear stress (to the plaster impregnated socks and the stump) and compressive stress (mainly to the distal end of the stump). The amount of tensile stress generated, depends on the closeness of the fit between the tank and the leg. The smaller the area between leg and tank, the smaller the tensile stress in the sheet and the larger the amount of vertical support force is provided by hydrostatic pressure directly applied to the stump. By incorporating

[1] measured with the Strathclyde CAD/CAM system

an adjustable top a nearly hydrostatic casting method could be achieved.

Water filled bags have been used to produce relatively uniform pressures in localised areas. Isherwood (1971) described the 'controlled pressure distribution' system as consisting of five shaped bags to load the patellar tendon, medial tibial shaft and flare, antero-lateral tibial area, fibular shaft and popliteal area. A sixth bag located at the distal end was added at a later stage (Isherwood, 1978). Because the water was restrained by the material of the bag, it is doubtful whether the pressure applied over the area was uniform. The shape, size and bag material characteristics will have had considerable influence on the pressure patterns created during weight bearing.

Several air pressure casting methods have been reported. None of these aim at a completely uniform pressure distribution. Gardner (1968) reported the use of a rigid plaster distal end cup and latex inserts at the patellar tendon and the popliteal area to redistribute the air pressure applied and Kristinsson (1993) leaves the distal end of the stump outside the pressurised zone.

Alginate is commonly used to increase the accuracy of fit of for example check sockets (Hayes, 1975; Staats 1987). The patient inserts the stump into a socket partially filled with alginate. Excess alginate is squeezed out and total contact is achieved. The pressure distribution is not really controlled although the total contact achieved will decrease shear stress in the underlying tissue.

Most of the methods discussed above do not achieve or aim at a completely uniform pressure distribution. If a uniform pressure distribution is the aim, the Dundee method modified with an adjustable top would be the most successful approach.

2.4.3 Hydrostatic weight bearing?

Very little is known about how the support forces are transferred from the stump surface to the skeleton. The complex structure of several layers of different types of tissue (mainly skin, connective tissue and muscle) makes it very difficult to predict how the tissue is going to behave under load. Soft tissues' resistance to shape change (shear stiffness) is much less than the resistance to volume change (bulk stiffness). Such materials are often called virtually incompressible. This does not mean that the material is incompressible but that volume changes occurring during deformation are negligible in comparison to shape changes (Vannah, 1993).

The mechanical characteristics of soft tissue are very time dependant. Over a very short time (seconds to minutes) the tissues' mechanical properties can change because of muscle contractions. Over short periods (from minutes to hours) the volume of the soft tissue can change due to the migration of fluid through the lymphatic and venous system. Over longer periods such as weeks and months, tissues can alter in shape, volume and mechanical characteristics by responding to internal, biological influences and external loading patterns. These factors make it inherently impossible to describe *the* mechanical characteristics of a stump. All that can be done is to make simplified models of stumps and test the usefulness of those models by comparing predicted interface pressures with measured interface pressures.

For hydrostatic weight bearing at least two conditions need to be satisfied :

Fig. 2.4.3.1

1) no fluid loss from the stump

2) no soft tissue displacement between bone and socket in the proximal direction

The extent to which condition one can be fulfilled depends partially on the degree of fluid confinement. Soft tissues can be said to consist of three fluid containing compartments: the intravascular, the interstitial and the intracellular compartment. The ratio of intracellular to intravascular and interstitial water is roughly 2:1. This means that about one third of the water content can migrate proximally through the venous and lymphatic system (disregarding osmotic pressures). If some hydrostatic weight transfer is to take place between skeleton and soft tissue, it either:

1) has to be of a very short duration so that only a small percentage of fluid can be displaced proximally or

2) the pressure at the proximal end of the stump on the venous and lymphatic system has to be higher than the pressure in the remainder of the stump.

The degree of soft tissue containment depends on the size of the cross-sectional area between bone and the proximal end of the socket and the local resistance to soft tissue deformation and displacement. At the trans-tibial level, the posterior wall needs to enclose the largest cross-sectional area of the tibial condyles to decrease the area of 'tissue extrusion' (fig. 2.4.3.1). The socket design aimed at transferring loads to selected areas, the PTB design, also produces high pressures in both the popliteal and the medial tibial flare area.

This prevents or limits the escape of fluid through respectively the popliteal vein and lymph duct and the long saphenous vein and accompanying lymph ducts. Another way of increasing proximal pressure and decreasing tissue extrusion would be to contract the residual gastrocnemius. EMG studies have indicated an increase in activity of stump musculature during swing phase, but not necessarily during stance phase (see section 2.3).

The pressure on these areas could also interfere with the circulation, especially if there is insufficient pressure relief during swing phase and/or sitting with the prosthesis. Subcutaneous pressures as low as 4-5 kPa are reported to be sufficient to occlude blood flow in the skin (Sangeorzan, 1989). The normal systolic arterial blood pressure is 16 kPa, which drops to 2 kPa in the venous network. Pressures in the popliteal area have been reported to be between 15 and 95 kPa for 95% of the stance phase (Sanders, 1993). Static pressure values in the same area can be about 80 kPa (Isherwood, 1978). This suggests that during those phases, the arterial blood pressure is too low to force blood into the stump, in fact, a limited amount of reverse flow is likely to take place as there are no valves in the arterial network to prevent this from happening. Because the flow resistance in the arteries is larger than that in the venous and lymphatic system, more fluid will be forced downstream than upstream. Whether this happens in reality depends on the direction of the pressure gradient created in the limb.

2.4.4 Consequences for dysvascular patients

As 85% of the amputations in the Western World are caused by vascular diseases, socket designs should pose as little obstruction to blood and lymph flow as possible. This means that having a high proximal pressure to prevent fluid loss might improve hydrostatic weight transfer but would adversely affect the stump's circulation. It seems that when tissue viability is taken into account, hydrostatic weight transfer, if at all, can and should only exist for a short period of time.

For an optimal circulation, socket designs should create decreasing pressure levels from distal to proximal during weight bearing and virtually no pressure on vascular areas during swing phase and sitting. Research should be directed at correlating modifications in socket design to rates of blood and lymph flow. Good socket design might be determined by balancing the biomechanical requirements of prosthetic support and control with the vascular limitations of the patient concerned.

CHAPTER 3

PRESSURE MEASUREMENTS IN PROSTHETIC RESEARCH

3.1 Introduction

This chapter provides an overview of the history of stump-socket interface pressure measurements. Special attention is paid to pressure measurements performed at the trans-tibial amputation level. Advantages and disadvantages of the types of transducers used, will be discussed in relation to the choice made for this project.

The majority of research has been focused at measuring normal (perpendicular) stresses at skin-socket interface. In recent years, attempts have been made to measure normal as well as shear stress to determine each contribution to control and support forces.

3.2 Stress measurements at the trans-tibial level

Stress is defined as the amount of force applied per area. Two types of stress are usually distinguished: normal and shear stress. Normal stress arises when the opposing force works along the same line of action, shear stress arises when the opposing force is parallel to the original force but works along a different line of action. In prosthetic research, the term normal stress (sometimes called *pressure* if the stress is compressive) is usually defined as the stress applied perpendicular to the stump surface and shear stress as the stress applied parallel to the surface.

However, shear stress can and does arise in all three planes. Wherever there are variations in stress levels, shear stress will arise as a consequence of it. Shear stress induces displacement of tissue relative to itself or other tissues with the risk of 'tearing type' of injuries. It is therefore important to keep shear stresses as low as possible.

The stump tissues can slide relative to each other almost without friction over a limited range. The amount of frictionless movement possible, depends on the degree to which scar tissue and adhesions exist. Within the range of frictionless movement, hydrostatic force transfer could be possible. In a truly hydrostatic medium, there would be an absence of shear stress. However, it is important to realise that the pressure distribution on the 'bag' containing the medium (the skin of the stump) is *not* necessarily uniform (see section 2.4.2).

Both normal and shear stress are clinically relevant entities. Research has shown that relatively low levels of normal stress (6-9 kPa) are sufficient to reduce the skin blood flow to dangerous levels (Sangeorzan, 1989). Others have shown that in the presence of shear stress, the normal stress required to occlude blood flow drops by 50% (Bennet, 1979). Sangeorzan demonstrated that *subcutaneous* levels of pressure required to stop blood flow are similar in different areas but that the *external force* required depends on the mechanical properties of underlying anatomical structures.

Most of the pressure oriented research in lower limb prosthetics has been focused on normal stress. There are two reasons for that:

1) normal stress is easier to measure, commercially available load cells can be used without much modification, few modifications to the socket are required
2) shear stress was always thought to be of minimal influence on the support forces distribution due to the ease with which layers of tissue can slide relative to each other and the stretchability of the skin

Recent research has modified the views on item two (Sanders, 1992; Williams, 1993). The results of both types of stress measurements at the trans-tibial level are discussed in section 3.2.1 and 3.2.2.

3.2.1 Normal stress measurements at the trans-tibial level

The ranges of stress reported over the past 30 years differ considerably. Many factors influence the level of normal stress measured. The most important ones are:

Socket related:

- socket design
- socket materials

Patient related:

- stump anatomy
- tissue characteristics
- weight of amputee
- gait of amputee

Method related:

- size of transducer
- localisation of transducer
- accuracy of transducer
- sampling frequency

As far as dynamic measurements are concerned, most researchers report the peak pressures measured. Peak values are clearly identifiable critical moments in the stump socket interaction. Both positioning and size of the transducer have a major influence on the peak values measured. Most research suggests that the pressure distribution in a trans-tibial socket is not uniform. Sharp pressure gradients exist over small areas (Rae & Cockrell, 1971).

The larger the transducer is, the lower the peak value will be due to an averaging effect. With smaller transducers 'true' peak values can be measured but they are extremely site dependant.

Over the years, each research group tended to follow their own approach depending on their particular interest. All these factors make it difficult to compare the results of various studies in an absolute sense. An overview of relevant pressure research from the period 1970-1994 is given below.

In the early seventies, pressure oriented research was stimulated by Rae (1971), who developed, with the help of Kulite Semiconductor Products, miniature pressure transducers with a 3mm diameter. The pressure measurement section was a strain-gauged diaphragm. The transducers could be taped to the patients skin and were used by other groups such as Pearson (1973), Burgess (1977) and (more recently in a new version) Steege (1992). Rae reported peak pressures of 100 to 280 kPa for the anterior distal end and the patellar tendon area respectively. Problems associated with this type of transducer are mainly related to inaccuracies in the location of the transducers and the inevitable disturbance of the measurement area by the introduction of transducers and connecting wires.

The effects of variations in muscle activity and prosthesis alignment on stump-socket interface pressure was investigated by Pearson (1973) et al. They found that tensing the stump musculature could double the pressures measured during postural stance. The effects were most pronounced at the patellar tendon area and the anterior distal end. Both translational and rotational

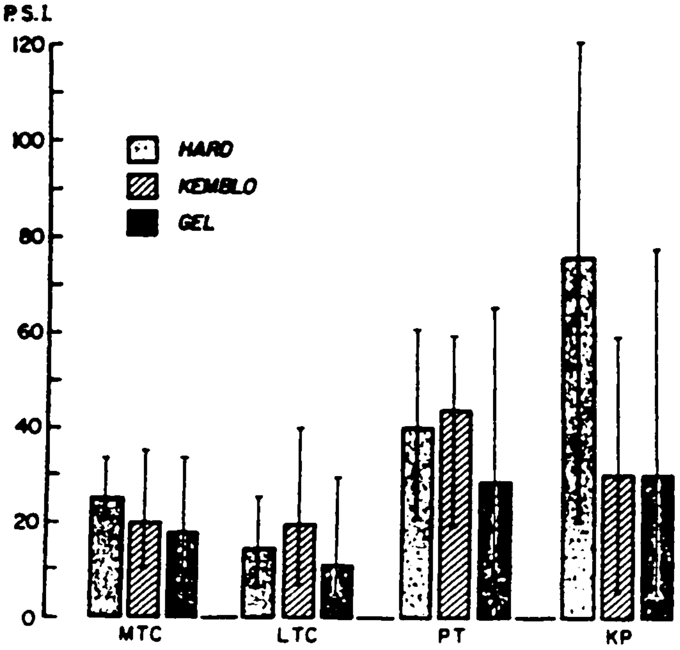

Fig. 3.2.1.1 (Reproduced form Sonck, 1970)

alignment adjustments in the sagittal plane had a significant effect on the pressure levels recorded at the anterior distal end. A change in angular alignment from 10° plantarflexion to 10° dorsiflexion increased the anterior distal end pressure from 160 to 380 kPa. The other areas (patellar tendon, medial tibial condyle, lateral tibial condyle) were not significantly affected. Ad- and abduction affected both the anterior distal end and the lateral tibial condyle. Adduction decreased the pressures recorded in both areas. The medial tibial condyle pressure was not sensitive to any variations in alignment.

One study tested the effect of different liner materials on the pressures measured (Sonck, 1970). Four areas were monitored: patellar tendon, medial tibial condyle, lateral tibial condyle and anterior distal tibia (kick point). A hard socket was compared with a Kemblo (sponge rubber) and silicone gel liner (fig. 3.2.1.1). Kulite transducers of 3mm diameter were used. The most significant reduction in peak pressure was achieved with both the Kemblo and gel liner in the distal anterior area. The lowest overall pressures were measured with the gel liner. The pressure studies were conducted with three *different* groups of patients of unequal size. It is possible that different pressure levels would have been recorded with the *same* liner.

Very few studies have looked into pressure variations resulting from variations in socket design. Isherwood (1971) devised the controlled pressure distribution system (see section 2.4.2). With this, he measured the hydraulic

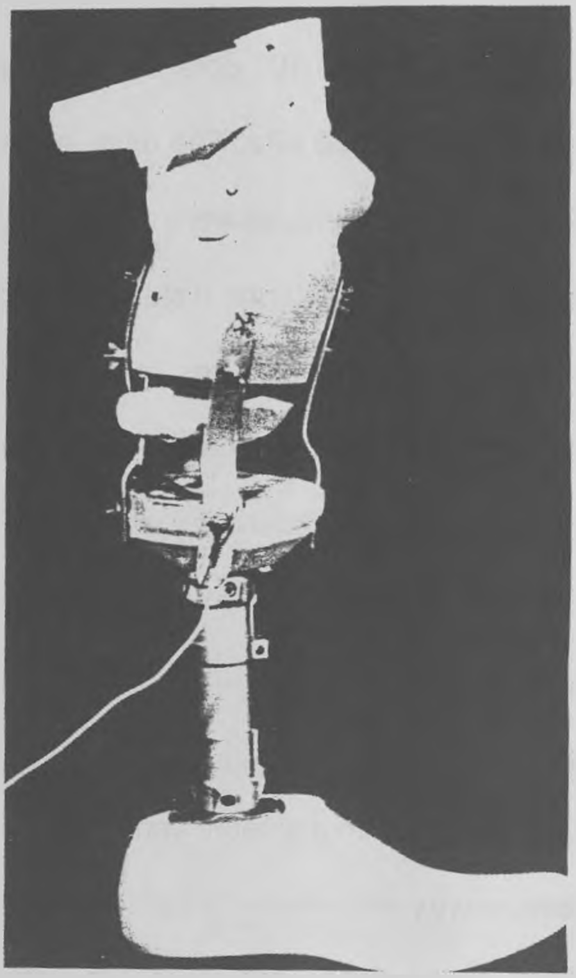

Fig. 3.2.1.2 (Reproduced from Katz, 1979)

pressure of water bags located in selected areas[2]. The pressures measured were an indication of the pressures applied to fairly large areas, from 17 to 58 cm^2 (Isherwood, 1978). In 1979, results were published that included a study of the effect of high patellar tendon (PT) pressure on other areas of the stump. A dynamic test was done on one patient with the PT bag set first at a low pressure (34 kPa) and then at a higher pressure (82.7 kPa). As a result there was a slight increase in popliteal pressure, a slight decrease in distal end pressure and a considerable decrease in pressure at the antero-lateral tibial condyle (exact pressure levels could not be determined from the diagrams). Isherwood concluded that there was no clear advantage to increasing the load on the patellar tendon.

Katz, Susak, Seliktar and Najenson (1979) investigated quantitatively the ability of the distal end to take load. They designed an experimental prosthesis that was split at the distal end to allow free movement of the distal end cap relative to the rest of the socket (fig. 3.2.1.2). The load on the distal end cap during standing and walking was measured with a load cell and the total load on the artificial leg was measured with a force plate. The load taken by the distal end without pain was expressed as a percentage of the total vertical force measured. For the six amputees involved, this varied from 13 to 48% of the total load. As the amputees walked on this experimental leg only for the duration of the test, the results cannot be generalised to a real life situation.

---

[2] the patellar tendon, medial tibial condyle, lateral tibial condyle, popliteal area, fibular shaft and distal end of the stump

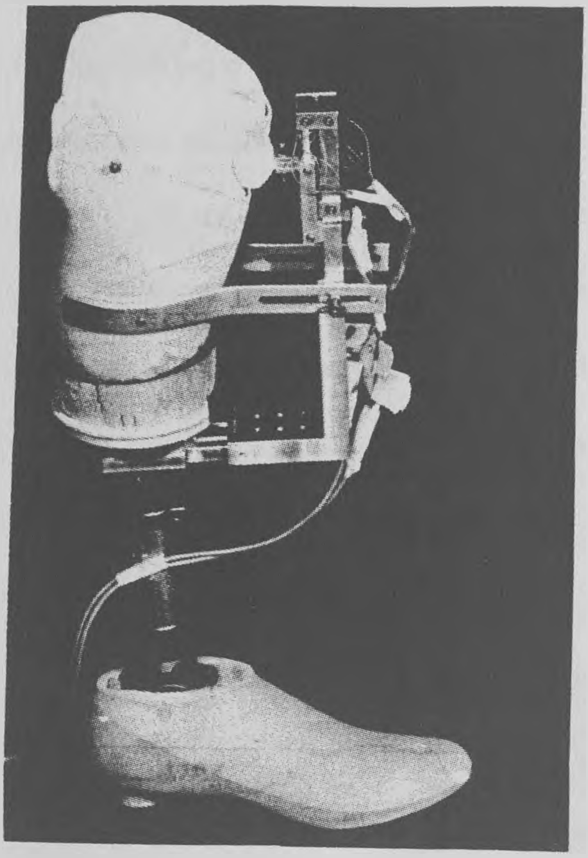

Fig. 3.2.1.3 (Reproduced from Mizrahi, 1985)

They do suggest that the distal end can take a considerable amount of load.

Up till 1992, members of the group have continued publishing results of further investigations. Susak, Seliktar, Najenson published with Mizrahi (1985) studies of the degree of load the patellar tendon takes in a PTB-style socket. Mizrahi and his co-workers fitted an experimental prosthesis with a two-directional load cell, attached to an adjustable mounting frame. The PT area was cut out of the hard shell (but the liner was left *intact*) and connected to the load cell (fig. 3.2.1.3). Adjustments to the PT area's position were made in the sagittal plane. Judging by the picture of the whole assembly, the socket was set in a considerable degree of flexion (13-17°).

The degree of abnormalities in the force plate data were assumed to indicate more, or less desirable positions of the patellar tendon bar. The opinion of the amputee about socket comfort correlated to some extent with criteria such as the timing of vertical braking forces. Because of the high degree of flexion and the intactness of the liner it is not clear whether the forces they measured on the patellar bar cutout truly represent the forces transferred from patellar tendon to socket in an average PTB socket.

In 1992, Besser presented the results of a study on six subjects with the experimental prosthesis described above. This time the distal end load was varied by pressurising an inflatable pneumatic bladder from 0 to 30% of body weight. The conclusions were that both the patellar tendon and the distal end are under utilised as load bearing zones. Maximum load bearing for the patellar tendon was reported to be 30.5 to 53.7% of body weight, for the distal end 17.5

to 68.6% of body weight. The main methodological problems were the fact that the liner was left intact and the short duration of the tests. It is not so useful to know the maximum force an amputee can withstand if the time for which this can be tolerated is not known.

A growing interest in modelling stump behaviour with the help of Finite Element Analysis led to a revival of pressure measurements in prosthetic research. Steege (1992) measured pressures in the sockets of two trans-tibial amputees to obtain reference data for finite element analysis models of their stumps. He used 4mm diameter Kulite transducers embedded in and flush with the socket wall. The (Pelite) liner was left intact and the transducers were calibrated in a simulated socket/liner environment. Pressures were measured during postural double support. The experimental pressure range was from 0 to 105 kPa. Measured and predicted values differed considerably but further improvement was expected.

The first combined normal and shear stress transducers were published in 1992 by Sanders and Williams. Sanders (1992, 1993) developed a transducer with a sensing surface diameter of 6.35 mm. Pressures were measured on two sides medial and two sides lateral to the tibia and on two sides on the posterior aspect of the stump. The normal stresses varied between 20 and 200 kPa during the prosthetic stance phase of walking, shear stresses varied from 5 to 40 kPa (measured on two patients). The patients' stump was in direct contact with the Pelite liner.

Williams (1992) also developed a combined normal and shear stress transducer but with a much larger sensing surface (16mm diameter). This makes it difficult to incorporate it in curved areas with a small radius. Tests on one amputee showed normal stresses of up to 150 kPa lateral to the tibia. The shear stresses are discussed in more detail in section 3.2.2.

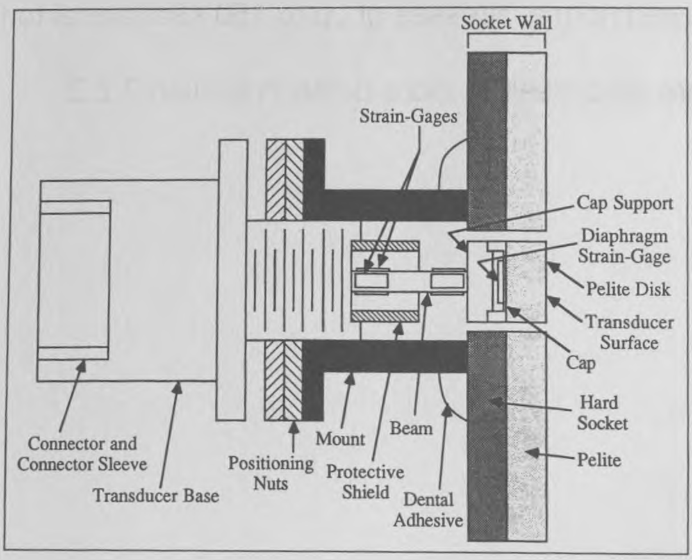

Fig. 3.2.2.1 (Reproduced from Sanders, 1992)

3.2.2 Shear stress measurements at the trans-tibial level

The first attempts of measuring shear in prosthetics were made in 1970 by Appoldt et al. at the trans-femoral level. Measurement of shear stress at trans-femoral level is easier than at the trans-tibial level. More patients wear suction sockets with a direct contact between skin and socket wall and the radius of curvature is generally much larger than in the trans-tibial socket. The latter means that the size of the transducer is less critical and disturbance of the original socket contour is less likely. Appoldt reported shear stresses up to 25 kPa.

Sanders (1992, 1993) claimed to be the first to measure shear stress at the trans-tibial level. The transducer used strain gauges fixed to a beam for biaxial shear stress measurements and a diaphragm strain gauge for normal stress measurements (fig. 3.2.2.1). The top surface had a disc of Pelite attached to it that corresponded to a cut out in the liner. The liner itself may have been fixed inside the socket to prevent it from shearing off the Pelite discs. The socket was designed to be smaller than usual because the amputee was required to wear the limb without any socks. In a normal situation, the amputee wears at least one (cotton or wool) sock over the stump, then the liner, then a smooth nylon sock that is in contact with the outer socket. Because all these layers can slide relative to each other the shear stress between the inner sock and skin in real life is probably much lower than that between skin and Pelite liner in the experimental setup. As a consequence, the shear stresses measured were considered to be higher than normal. These levels

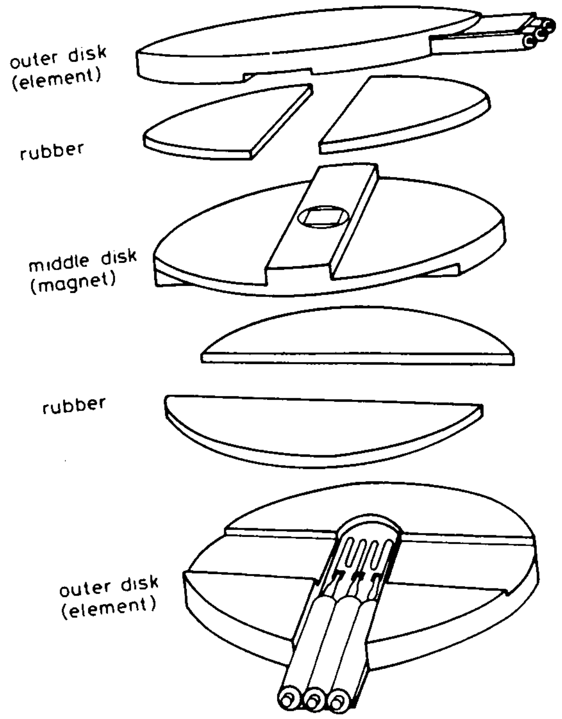

Fig. 3.2.2.2 (Reproduced from Williams, 1993)

might be indicative of the shear stresses arising in skin suspension systems such as the Iceross system.

Large shear stresses were measured at the posterior proximal area: up to 40.7 kPa early in stance. During stance phase, the anterior shear stresses caused the skin to be stretched over the tibial crest and to be forced in the proximal direction. The magnitudes on the tibial flares ranged from 5.6 to 39 kPa for the two subjects measured.

The normal and shear stresses measured were not evenly distributed and there were large local differences in the (calculated ?) coefficients of friction: from 0.01 to 0.55. According to Sanders this can lead to local in-plane tension with a risk of tissue break down. As stated before, in the sock-liner-sock-socket situation the shear stresses and variations in coefficient of friction are likely to be much smaller. In case of a total contact silicon sleeve, the friction should be relatively uniform and high so that the skin can hardly move relative to the liner. The problem area in that case is the proximal end. Where the sleeve-skin contact is lost, shear and in-plane tensioning is likely to occur (sometimes resulting in friction blisters (Kristinsson, 1993)).

Williams (1993) designed a triaxial stress transducer with a diameter of 16mm. Instead of a strain gauged beam, magnetoresistors and rubber were used to create the shear measurement sections (fig. 3.2.2.2).The accuracy of the shear section did not meet the original design specification (0.5 N or +/- 5% of indicated load (whichever is greater)) but it was deemed acceptable for clinical use. A pilot study on one amputee yielded shear forces of up to 35 kPa at the popliteal area. The methodological criticisms stated with respect to Sanders' study are equally applicable to Williams' setup. An additional problem is the size of the transducer: it may be more suitable for trans-femoral type sockets.

Shear stress measurement methods clearly are not very well developed. For the skin-sock-liner-sock-socket type of prosthesis it might be nearly impossible to measure shear stress at the skin without disturbing the interface dramatically. In suction sockets there is a better chance of measuring 'true' shear stresses because of the direct contact between liner/socket wall and skin. Because of the high coefficient of friction between skin and liner, high levels of shear stress can occur when the maximum skin displacement is reached. This maximum displacement is much lower when adherent scar tissue is present, thereby increasing the likelihood of tissue damage.

CHAPTER 4

METHODOLOGY OF THE PILOT AND COMPARISON TESTS

4.1 Introduction

The aim of the study was to test whether the amount of distal end loading correlates to variations in socket design. The design variations researched were those described in the Patellar Tendon Bearing Below Knee Prosthesis (Radcliffe & Foort, 1961). In this manual, the patellar tendon, the medial tibial condyle and the distal end of the tibia are recommended as areas suitable for supporting the body weight. To date, nobody has proven *quantitatively* what proportion of the body weight these areas do support.

Because so little is known about the nature of force transfer between socket and stump, it is important to control and quantify the socket design variations applied. By using the Strathclyde CAD/CAM system as a design tool, this author was able to quantify both shape and volume of the modifications implemented. Sockets were created that were equal in volume but different in shape. Pressure transducers were located at critical areas to determine the effects of design modifications. The relationship between proximal design aspects and distal end loading was investigated for several design configurations.

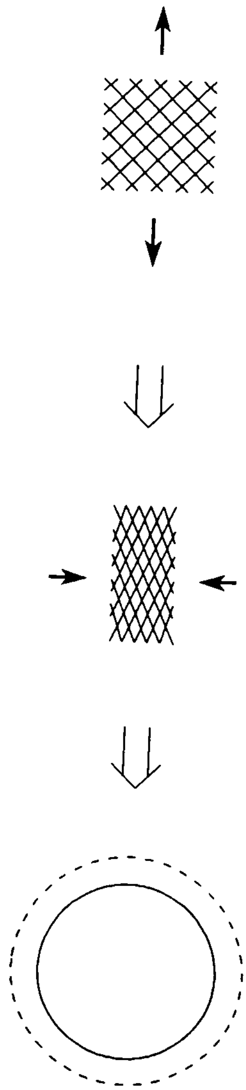

Fig. 4.2.1

4.2 The Strathclyde CAD/CAM system

The Strathclyde CAD/CAM system consists of a laser scanner, a computer and a computer numerically controlled (CNC) four-axis milling machine. The laser scanner[3] serves as the data input device. It scans the patient's stump in four seconds, during which the limb must maintain its position. The distal tip of the stump has to be positioned in the centre of the scanner to prevent a loss of data in that region. The stump is supported by a white nylon sock. By applying his body weight, the amputee preloads his stump. Because of the cross-weave of the sock, axial loading is partially converted to radial loading (fig. 4.2.1). Bony landmarks are identified at this stage by marking them with a black dot of 5-10 mm diameter.

The resolution of the image file from the scanner is in the order of 1.7 mm along the vertical axis and 1.7 degrees rotationally. From the scanner driver, the data is transferred to the computer[4]. At this stage, the validity of the data is tested and the amount of data reduced to 10° rotationally and 3.2 mm axially (to improve object manipulation speed). The operator can visually inspect the quality of the scan, e.g. to check whether significant movement has occurred during the scanning process. If the quality of the image is sufficient and all the landmarks are identified, the image is ready to be modified.

The flexibility of the graphical (computer) tools allows the creation of

---

[3]Cyberware Inc.

[4]Hewlett/Packard Apollo Series 400

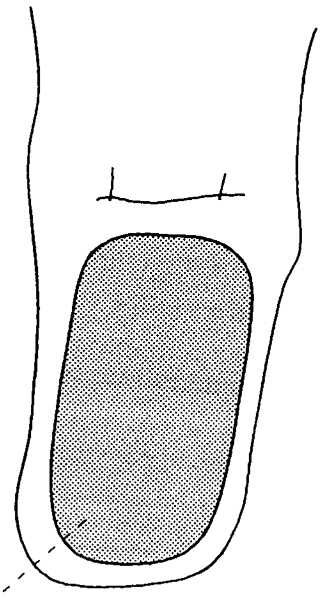

Fig.4.4.2

virtually any type of shape modification. For this project, volume determination of both the total socket shape and of the modifications was important. The aims were to create different sockets with the same volume and a range of sockets increasing in depth of modification. It was decided to use the socket design taught in the National Centre[5] as the reference socket. The modifications were stored as the '100% modifications' and used to create variations of this design. By scaling the reference modifications to 0%, 50% and 150%, a range of four sockets was created increasing in rectification from 0 to 150% and decreasing in volume from 0 to 3% of the total socket volume. Two more socket designs were created equalling in volume, but differing in shape, with the 0 and 100% rectified sockets. This was done by replacing the key modifications at the patellar tendon bar, medial tibial condyle and lateral tibial condyle with an equivalent volume reduction over the posterior aspect of the stump (fig. 4.2.2).

All sockets were used to investigate the effect of the amount of proximal modification on the distal end pressure. The four sockets were used to check whether the pressure in the rectified areas appears directly related to the amount of modification and the two additional sockets were used to check whether a possible effect on the distal end pressure was due to either the type of proximal rectification or the volume reduction that went along with it.

The CAD/CAM system allowed accurate volume control. It also enabled the exact positioning of the transducers, a common problem in prosthetic

---

[5] a modified version of the PTB-concept

research. Because of the small active area of the transducers (20 mm^2), consistent positioning on all six sockets was very important.

The socket models were carved from plaster blanks on a CNC milling machine[6]. The carving pitch for the helical tool path was changed from 2.5 to 1.5 mm to achieve a high quality reproduction of the shape. The cutter used, was a 10 mm diameter ballnose cutter. The 'facet interference' program automatically created the best toolpath for each individual shape. Because of the high resolution chosen and the limited memory capacity of the CNC machine, the carving was carried out in two stages. All six shapes were carved without a change in the settings of the CNC machine to ensure maximum consistency.

The alignment of the six sockets needed to be identical to minimize alignment related influences on the pressure levels recorded. The reference socket was aligned both statically and dynamically until it was considered satisfactory. It was then clamped in a modified transfer jig and the points of contact between the socket and the jig were recorded with the CNC machine. Subsequent sockets were marked with the same coordinates so that they could be identically positioned in the transfer jig (the complete procedure is described in appendix 4.2).

All six sockets were fitted with Berkeley alignment jigs to allow for adjustments potentially required because of the different socket shapes. In

---

[6] Deckel FP4 NC

practice none of the sockets necessitated a change of alignment. The same Otto Bock dynamic foot was used in each test as well as the same shoe (Clarks, air cushion).

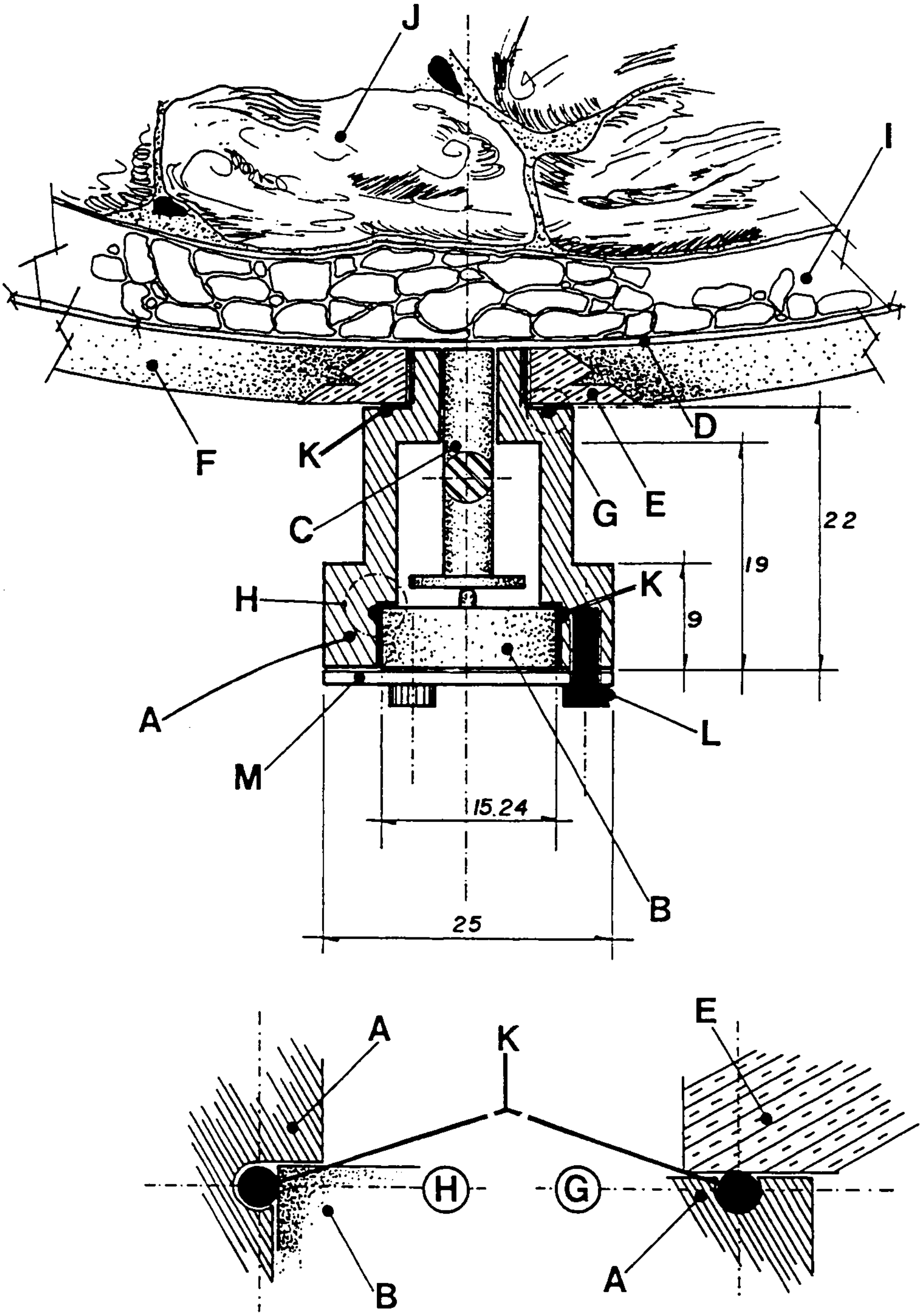

A) Transducer housing,
B) Load cell,
C) Solid cylindrical piston,
D) Skin layer,
E) Metallic insert,
F) Prosthetic socket,
G) "O"-ring, mount/insert seal,
H) "O"-ring, load cell/mount seal,
I) Superficial fascia,
J) Musculature,
K) Sealing "O"-rings,
L) Allen screw,
M) Housing cover.

Fig. 4.3.1 (Reproduced from Torres-Moreno, 1991)

4.3 Test socket design

It was decided to use hard shell, supracondylar sockets made from acrylic laminate. The laminate allowed an accurate reproduction of the socket contours with very little risk of shrinkage or deformation over the test periods. The hardness of the material was similar to that of the aluminium from the transducer housing. This ensured that there were no sudden changes in socket wall characteristics that could have influenced the pressure patterns. The supracondylar inserts were manufactured of Pelite.

At the carving stage, the plaster model was marked by the CNC machine to indicate the location of the four pressure transducers. When the sockets were manufactured, the inserts were fixed to these locations by threaded pins. Some problems were encountered at the patellar tendon bar. The deepest rectifications had small radii of curvature so that it was difficult to blend the flat transducer surface with the curved socket wall. Because of the small diameter of the contact area (5mm sensing surface + 3mm collar) the socket contours were not significantly altered in general.

The inserts were machined to the same depth as the threaded collar of the transducer so that the surfaces were flush once the transducers were fully inserted (fig. 4.3.1). After socket manufacture, the inner socket surface near the inserts was inspected to check for a smooth transition from laminate to insert.

4.4 Subject selection and characteristics

The subject chosen was a male, 56 years old, whose amputation was due to an accident six years ago. His state of health was good and he was an active walker. His weight was 91 kg and his height 1.72 m.

The patient's stump was in good condition with a length of 19 cm from the tibial plateau. There was an average amount of soft tissue and no particular stump problems. He was used to wearing a supracondylar suspension with a suprapatellar section. The patient's opinion of the six sockets was not sought in a *formal* sense as he was only wearing them for a short period. He was able to walk on all six sockets without noticeable discomfort (at least over a one hour test). He did express slight preferences for some sockets but these varied with the months the tests were conducted.

All sockets were worn with one towelling sock. The 0 to 3% volume differences in some sockets did not seem to necessitate a change in the number of socks the patient was wearing (again: at least for the time he was wearing the prosthesis during the tests). The length of the walkway allowed the subject to take 14 steps of which the middle three prosthetic steps were monitored. His stride length was 1.30 m, velocity 1.18 ms^{-1} and cadence 109 steps min^{-1}.

Nonlinearity	± 0.5% Full scale
Hysteresis	± 0.5% Full scale
Frequency range	0 to 900 Hz
Load range	0 to 8.8995 N
Over range	0 to 17.7990 N
Full scale sensitivity	8 mV
Input impedance	600 ohm
Output impedance	600 ohm
Thermal sensitivity	± 1%/55°C

Table 4.5.1

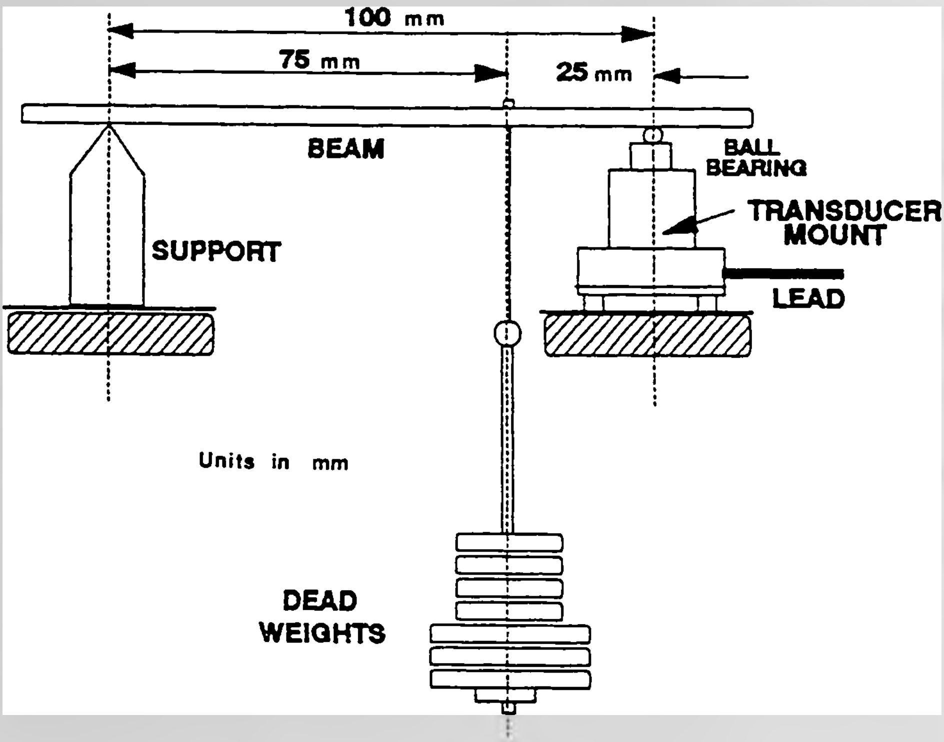

Fig. 4.5.1 (Reproduced from Torres-Moreno, 1991)

4.5 The pressure transducers, load cell and force plate

The aim of the project was to correlate proximal socket design modifications to distal end pressure. The pressure transducers selected for this task, needed to fulfill certain criteria:

- contacting surface (sensor + collar) less than 1cm diameter to prevent changes in the socket contours
- pressure range form 0 to 400 kPa (see section 3.2.1)
- high sensitivity, linearity and frequency response
- low hysteresis and (temperature) drift

The transducers chosen were Entran load cells (ELM-400-2 Series). Four transducers were available in housings designed and tested by Torres-Moreno (1991) (fig. 4.3.1). In this arrangement the load is transmitted from the stump socket interface to the transducer by a piston. By dividing the load applied, by the surface area of the head of the piston, an average pressure over that area can be calculated.

The transducers were originally used in trans-femoral prosthetic sockets. The transducer and housing assembly conformed to the above specifications apart from the socket inserts. These were modified for use in the trans-tibial sockets by scaling them down to the appropriate size. The specification of the transducers is listed in table 4.5.1.

The four transducers were calibrated in their housings by loading the head of the piston through a ball bearing (fig. 4.5.1). A series of known weights was hung from a horizontal beam supported on a knife edge on one end and

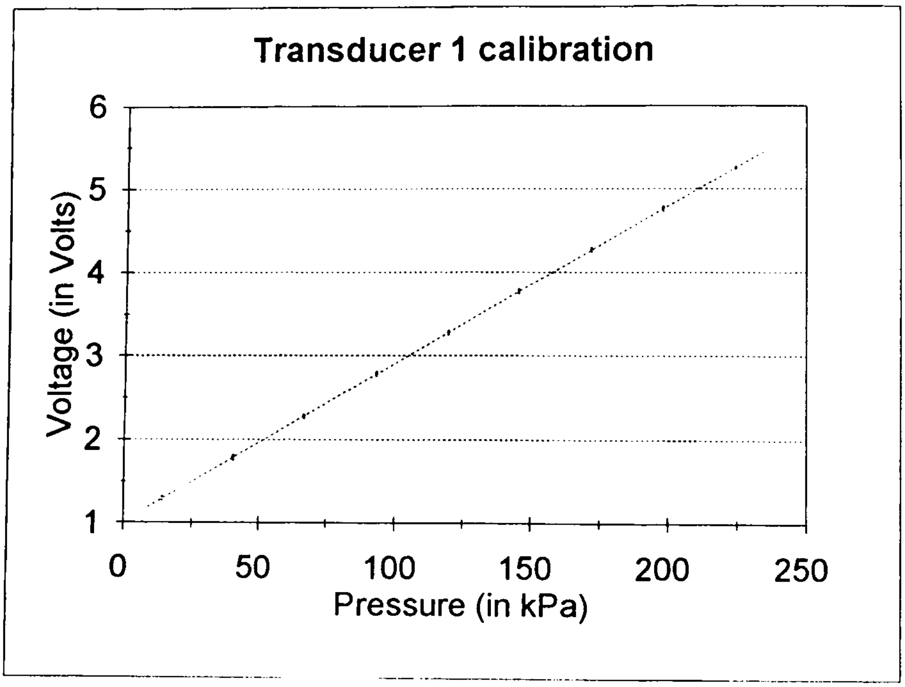
Transducer 1 calibration
Voltage (in Volts)
6
5
4
3
2
1
0
50
100
150
200
250
Pressure (in kPa)

Fig. 4.5.2

the piston head on the other. Amplifiers were connected to each of the four transducers. The output signals were monitored on computer by using Kistler BioWare 2 software. The beam was loaded and unloaded three times by sequentially placing eight weights on the vertical support. The voltage level was read after about ten seconds when the value had stabilised. The resulting data was used to determine a straight line fit through linear regression (fig. 4.5.2). Before each new period of measurements, all the housings were taken apart and cleaned to prevent any friction between the pistons and the housing. After assembly the transducers were recalibrated.

Ideally, the axial load on the socket would have been measured throughout the gait cycle. This would have given an indication of the loading conditions affecting the distal end pressure. An attempt to do this was made by placing a ring shaped load cell[7] between the alignment unit and the foot. A special adaptor was designed to hold the load cell in place, while allowing all the load to be taken by the load cell. The load cell also served as a timing device identifying heel strike and toe off. In practice, the load cell proved to be too sensitive to moments applied during the gait cycle. The output was a summation of the true axial load and the moment applied. As the proportion of each could not be determined, the load cell was unable to monitor axial load.

The ground reaction force was monitored with a Kistler forceplate[8] and the signals of both the forceplate and the transducers and load cell were

---

[7] Kistler Type 9031A

[8] Kistler Type 9281B11

recorded with BioWare 2 software. All data files were exported to a spreadsheet for further analysis.

The sample rate for all channels was 50 Hz for the standing tests and 250 Hz for the walking tests. A high frequency was chosen for the walking tests because of the interest in peak pressures. Too low a sample rate might have resulted in measurements being taken just before or after the peak pressure occurred (aliasing).

4.6 Test protocols

The first series of tests were conducted in January 1994. Both the equipment and the first version of the protocol were tested. Most of the tests were concerned with the repeatability of the measurements and were conducted with the reference socket. The last series of tests were done with an unrectified socket to assess whether there were significant differences in pressure levels between the two types of socket.

Two types of tests were done with the patient: static and dynamic tests. For the static tests, the patient was asked to stand on his prosthetic leg for 5 seconds and then unload his prosthetic leg. The loading conditions were monitored with a force plate. In the first series of tests, the patient supported half his body weight on the prosthesis, in the second series full body weight. The position of both feet was recorded so that each test was done in exactly the same position. When full body weight was applied (standing on the prosthetic leg) the patient was allowed to stabilize himself with a horizontally outstretched arm against the wall. The measurement interval (10 s) was started with the patient in a stable position *on* the force plate. After 5 seconds, the patient was asked to step *off* the plate and to offload his artificial leg for 5 seconds. This procedure ensured two stable signal levels.

For the dynamic walking tests the subject walked along a walkway of 9 m length. The middle three prosthetic steps were used for analysis. The middle step of these three steps landed on the force plate. Peak pressures were determined to base the socket comparisons on.

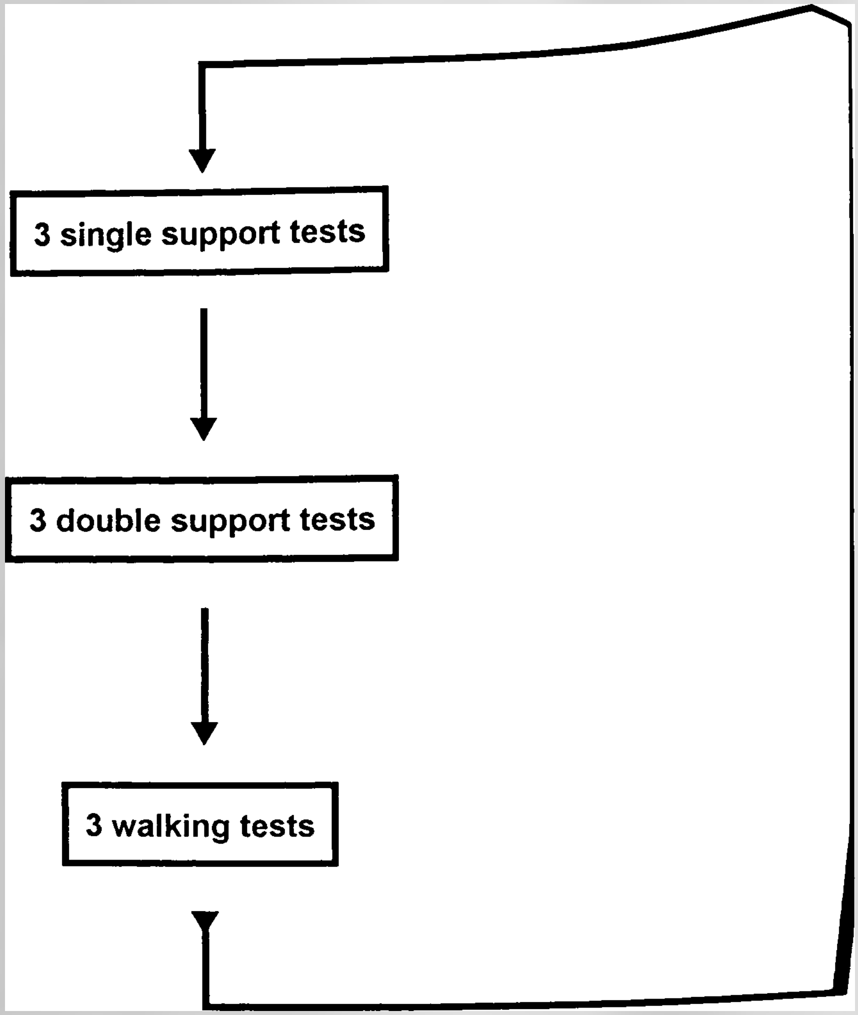

Fig 4.6.1

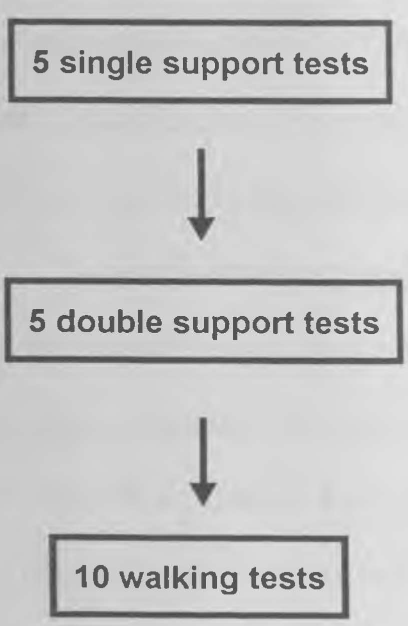

Fig 4.6.2

On a typical test day the protocol would have been as follows:

- all electronic equipment switched on one hour in advance to reach stable operating conditions
- patient dons socket and walks up and down until he feels he is settled in the prosthesis (typically about 15 min)
- series of standing tests with half body weight
- series of standing tests with full body weight
- series of walking tests

The test sessions could then be repeated in the same order.

In the pilot series of tests, each type of test was repeated three times before going on to the next type of test: e.g. three half body weights, three full body weights, three walking tests (fig 4.6.1). The results of these tests were averaged and compared with results from the same and other days.

The results of the pilot tests led to one modification of the protocol: the number of repeat tests for the standing tests increased from 3 to 5 times and the number of repeat tests for the walking tests increased from 3 to 10 tests (fig 4.6.2).

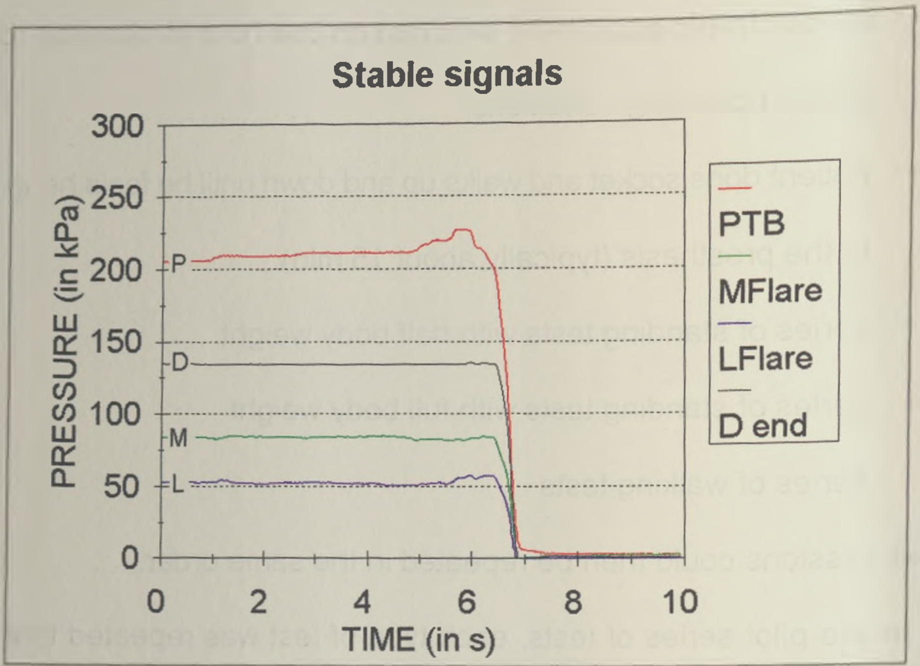

Fig 4.7.1

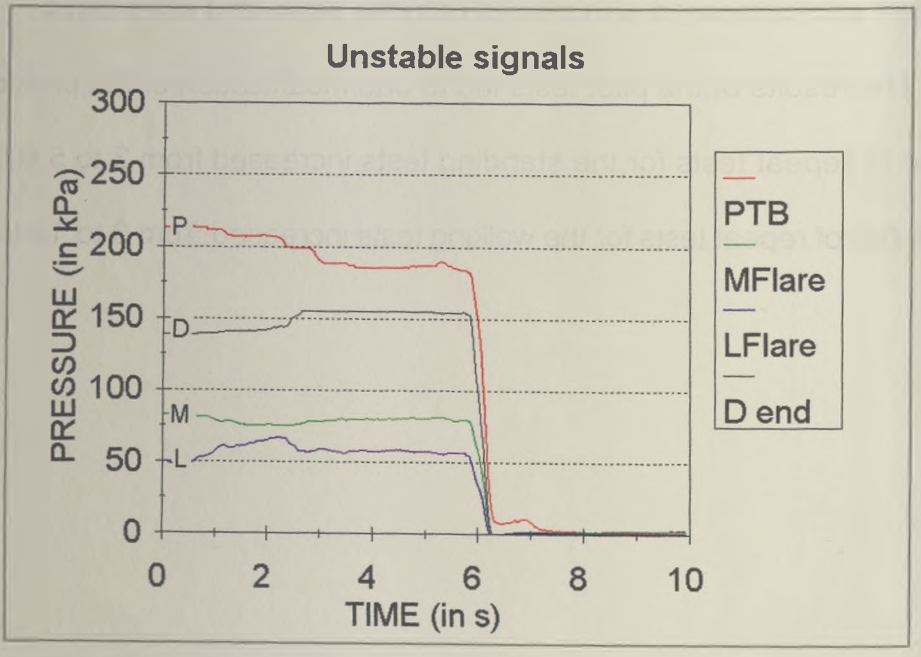

Fig 4.7.2

4.7 Data analysis

The aim of the data reduction and analysis was to arrive at sets of data representative of the different socket designs. Two conditions needed to be fulfilled for this:

1) the test results needed to be repeatable over at least a limited period of time
2) the data had to reflect and discriminate between the various socket designs

By placing the transducers in both modified areas (PTB, medial tibial flare, lateral tibial flare) and areas of particular interest (distal end), some consequences of the variations in socket design were measured as changes in pressure levels.

The static and dynamic tests each had their own problems in terms of reproducibility and data reduction. The subject *initially* had most difficulties with the single support test. Although he was able to stand on his prosthetic leg without discomfort, it took a while before he achieved stability relatively easily. The figures 4.7.1 and 4.7.2 show the difference between a stable and an unstable single support test. Data collections of the latter quality were rejected whereas data such as in figure 4.7.1 were accepted.

For the single and double support tests, two-second intervals were selected from each pressure signal and an average value was calculated from it. The results from each test were then combined and averaged. For the walking tests, the peak pressures arising during stance phase were used for

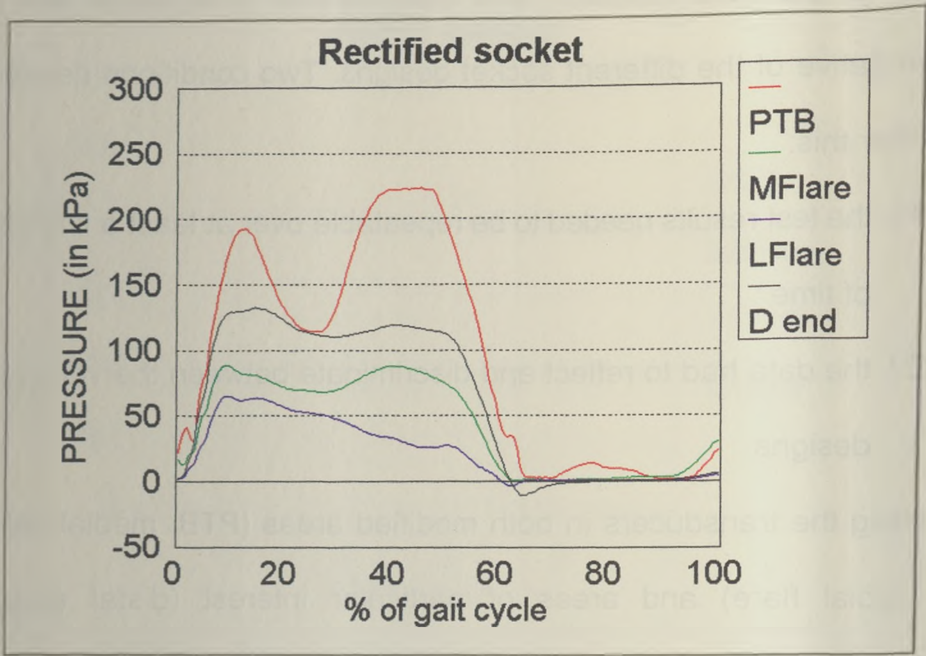

Fig 4.7.3

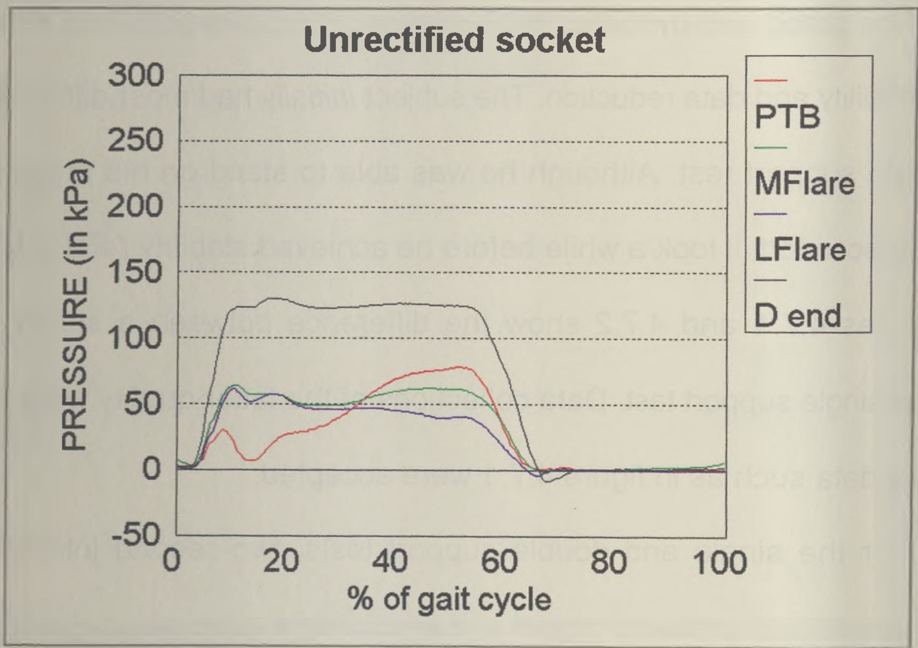

Fig 4.7.4

comparative purposes. This was because they are easy to determine and they represent critical moments in the stump-socket interaction. Most of the pressure sites showed a distinct double peak pattern during stance phase (fig 4.7.3). Peak 1 occurred early in stance phase, just after heel strike and peak 2 occurred just after heel off. Because of the possible differences in consistency and socket design specificity, it was decided to monitor their characteristics separately.

The lateral flare pressure pattern was the only one that did not show a clear peak in the second half of stance phase (fig 4.7.3) so it was only determined early in stance phase. The PTB area usually presented a double peak pattern except for the sockets that were completely unmodified in this area. In those cases, the first peak sometimes disappeared whereas the second one remained distinct (fig 4.7.4).

CHAPTER 5

THE PILOT TESTS

5.1 Introduction

The main aim of the pilot tests was to investigate whether the two conditions stated in section 4.7 could be fulfilled:

1) are the test results repeatable over at least a limited period of time
2) does the data reflect and discriminate between various socket designs.

The reproducibility of the results was checked by testing the reference socket on different days. The tests were also conducted with an *un*rectified socket to check whether the patient could cope with the kind of sockets he would be fitted with and to assess whether the pressures measured were significantly different from reference socket pressures.

The pilot tests also served as a testing ground for both the equipment and the protocol. The findings of the pilot tests led to slight changes in the protocol for the six sockets comparison tests.

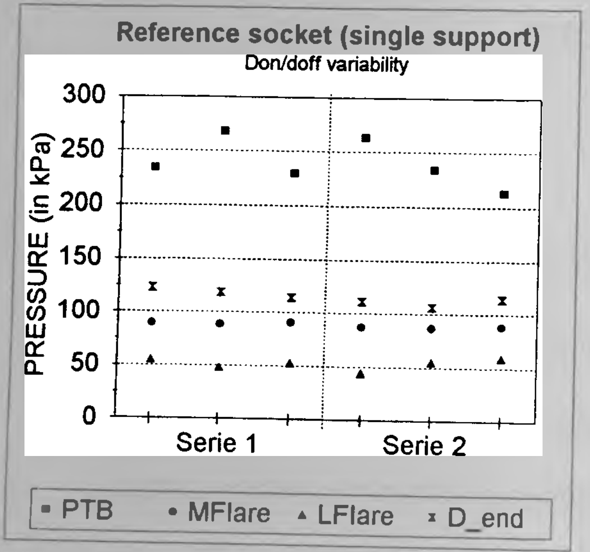

Fig 5.2.1

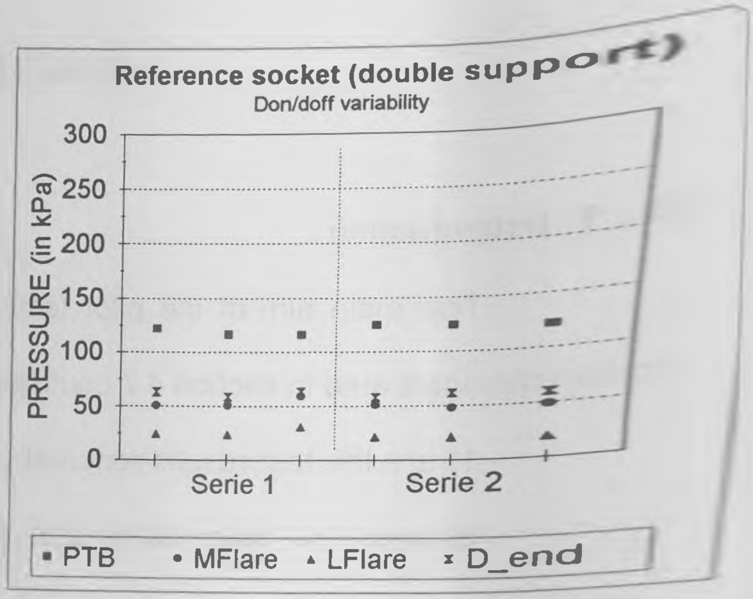

Fig 5.2.2

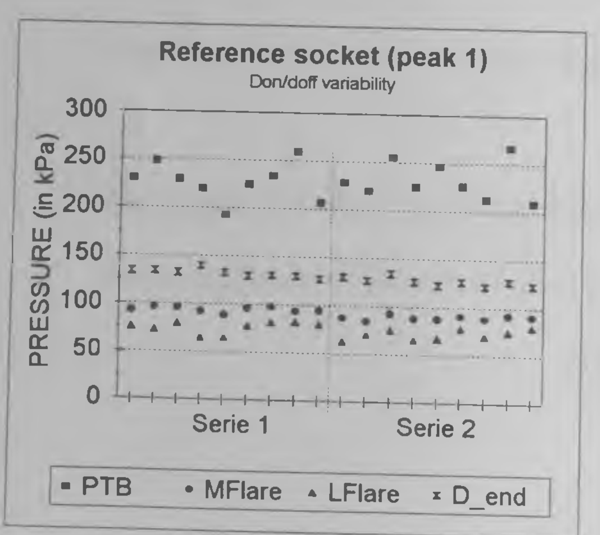

Fig 5.2.3

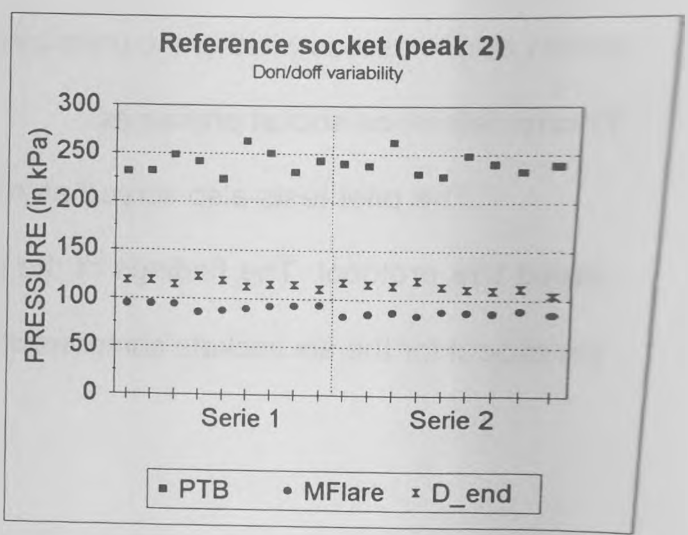

Fig 5.2.4

5.2 Pilot tests results

On the first day of the tests, the subject was allowed to practice on the test procedures before the first measurements were done. It took a while before the patient could easily stand still on his prosthesis, but he did not find the 'single support' tests uncomfortable. The double support test posed no problems. The walking test required a few practice runs for the subject to land on the force plate without deliberately aiming for it, but once the right starting point was found, no further problems were encountered.

On the first day, two series of tests were conducted. In between the series, the subject was asked to doff and don the experimental prosthesis to check whether the donning and doffing procedure itself would have any effect on the pressures. The figures 5.2.1 to 5.2.4 show the results of both series (a listing of all test results can be found in appendix 5.2). There were no obvious differences between the two series, but there were clear differences in the pressure variability of the four sites.

The patellar tendon pressure showed large variations in the single support and the dynamic tests. Only in the double support tests were the PTB-variations fairly small. The level of PTB pressure (about 240 kPa) was almost twice that of the other sites.

The medial flare pressure was quite stable at about 90 kPa in both the single support and dynamic tests. In the double support tests, the medial flare pressure varied around 50 kPa.

The second peak lateral flare pressure was not determined because it did not show a second peak (see section 4.7). In the other three tests, it showed the lowest pressure of the four sites.

The distal end pressure varied around 115 kPa in both the single support and the second peak tests. The first peak distal end pressures were slightly higher, around 130 kPa.

It was important to see that there were no significant upward or downward trends of the distal end pressures over the two sets of tests as this might have indicated that the subject was not settled in his prosthesis.

The ranges of pressure were within the capacity of the transducers and they were not dissimilar from pressure ranges that have been reported by other investigators (see section 3.2.1).

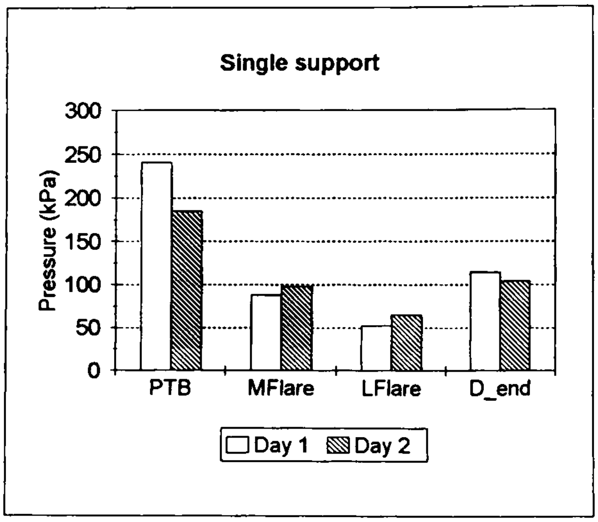

Fig. 5.2.5

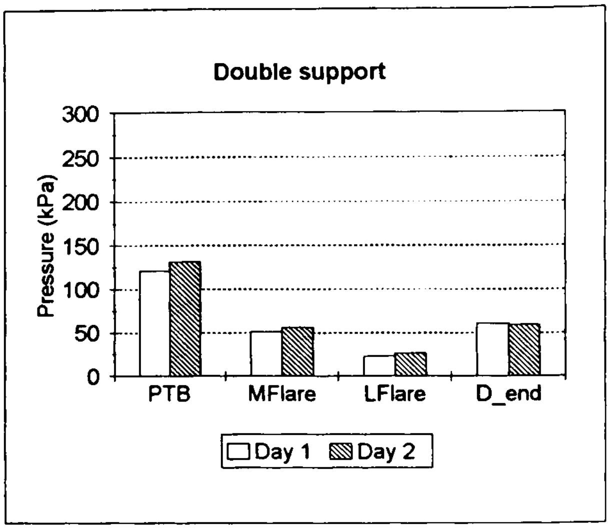

Fig. 5.2.6

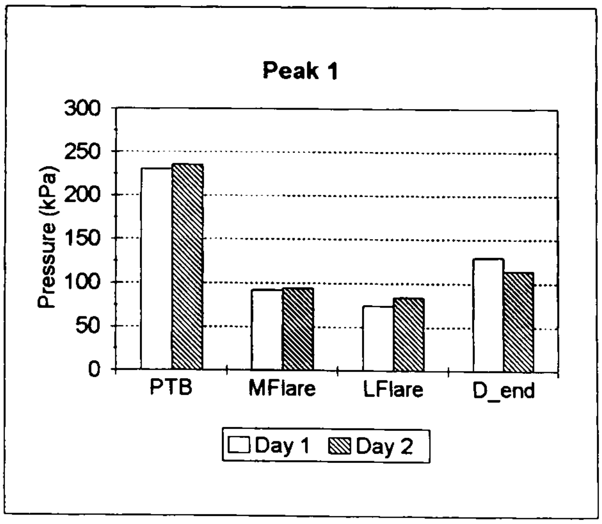

Fig. 5.2.7

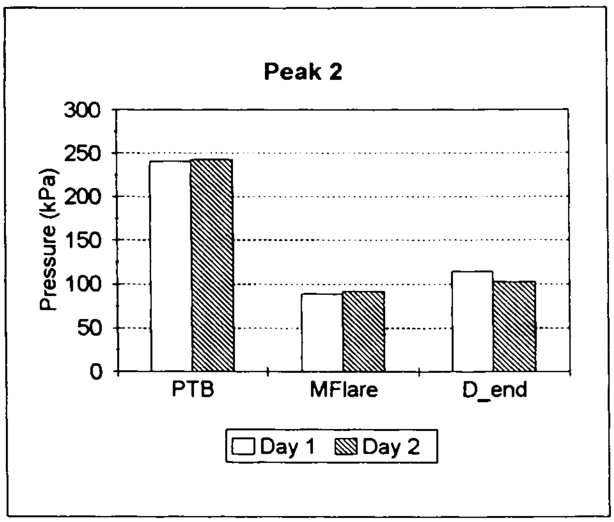

Fig. 5.2.8

On the second day, the reference socket was tested again with two sets of tests. The figures 5.2.5 to 5.2.8 show the mean pressures measured on day one and day two. The graphs show that the results were not exactly the same but similar on the two different days.

The double support and second peak tests appeared to be more repeatable than the single support and first peak tests. The largest difference was measured at the patellar tendon bar in the single support tests. The increase in familiarity with the testing procedure might have led to a lower level of tension in the patellar tendon on the second day.

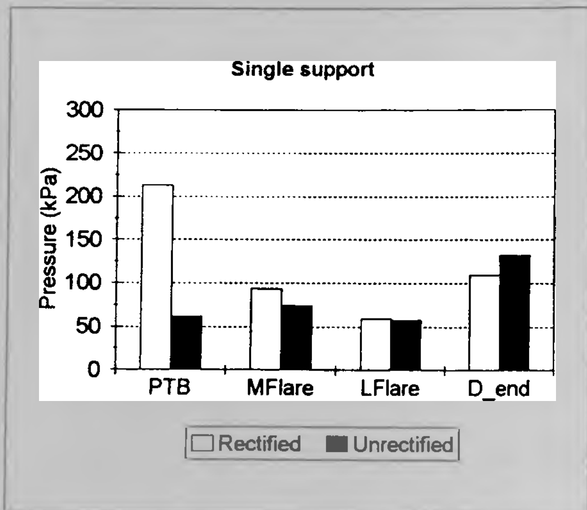

Fig. 5.2.9

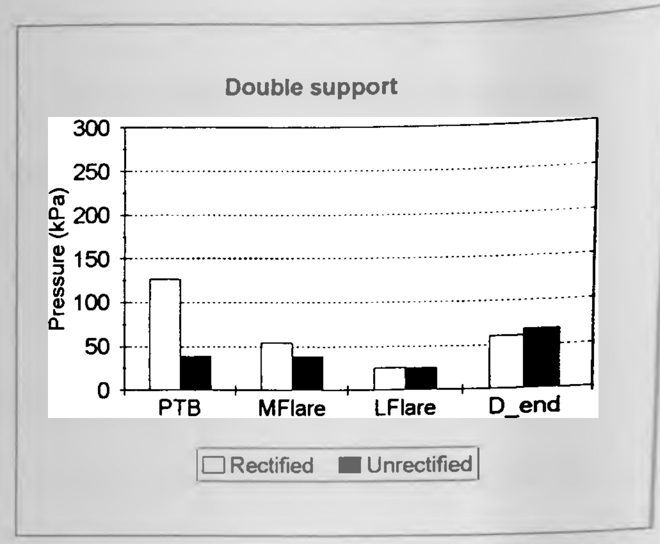

Fig. 5.2.10

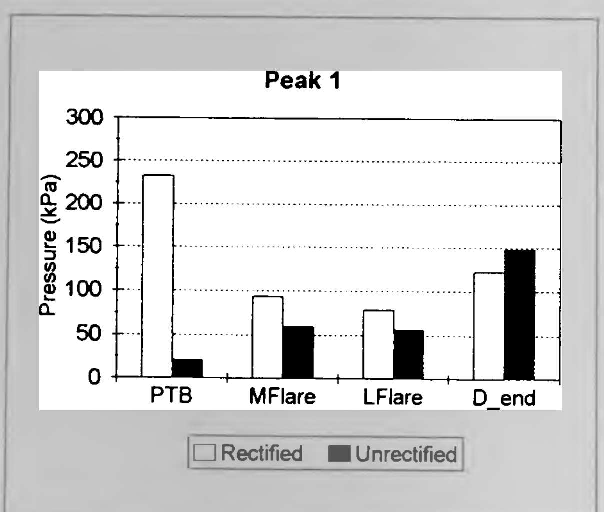

Fig. 5.2.11

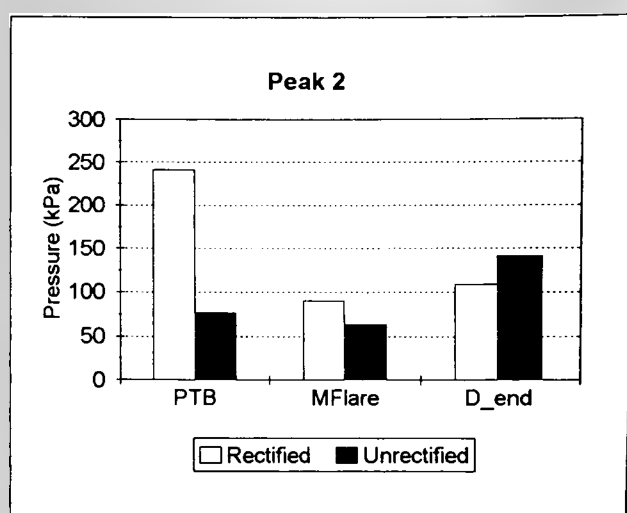

Fig. 5.2.12

To assess how significant these variations were compared to the pressures measured in a different socket, an unrectified socket was instrumented and tested. Two sets of tests were conducted and the results averaged and compared with the combined results of the reference socket.

The figures 5.2.9 to 5.2.12 show the rectified (reference) socket results as white bars and the unrectified socket results as black bars. The pressure differences between the two sockets were clearly larger than the differences between two days of reference socket tests.

The PTB pressures differed the most, but almost all other sites showed large differences as well. The lateral flare was the only site that did not show rectification related differences in the standing tests. In the comparison tests, these observations were further investigated.

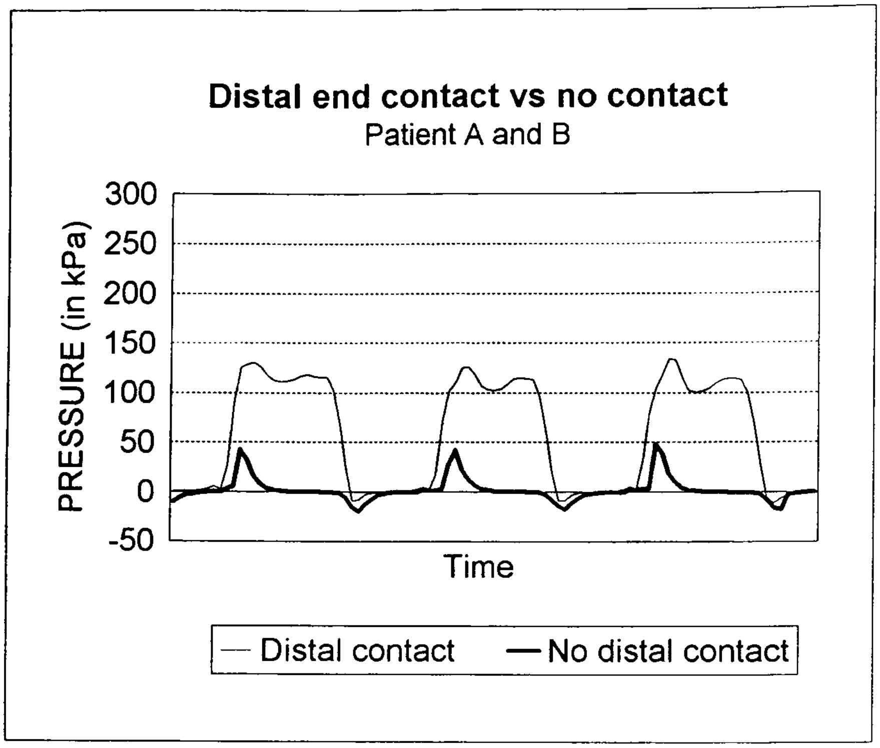

Fig. 5.2.13

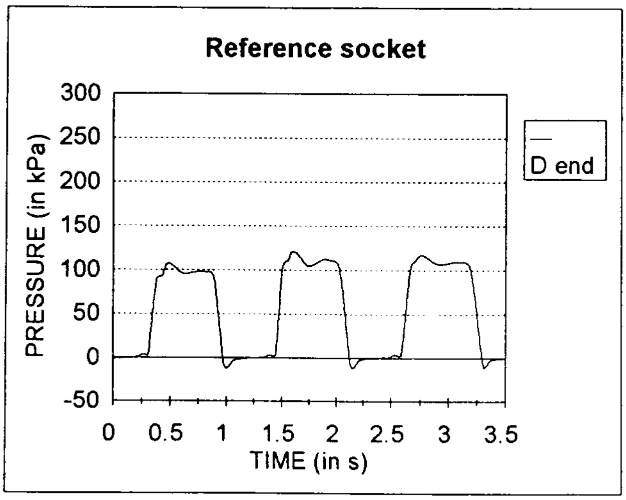

Fig. 5.2.14

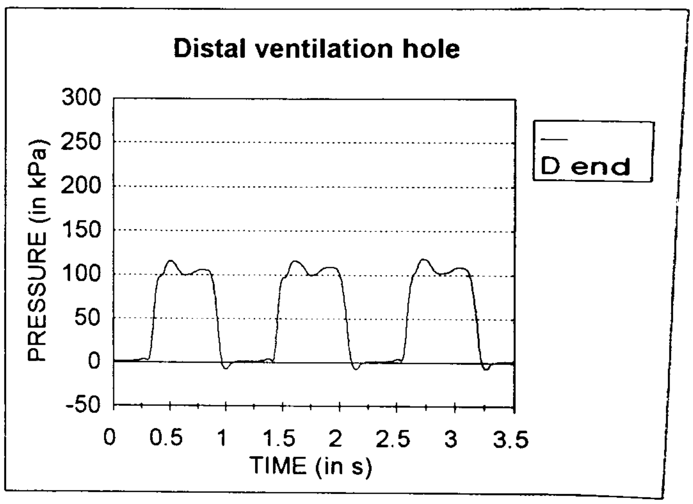

Fig. 5.2.15

Because the distal end pressure was of particular interest in this project additional tests were done to check whether there really was distal end contact between the stump and the transducer. Before these pilot tests, some tests were conducted on a patient without distal end contact. Figure 5.2.13 shows the distal end pressures of the current subject and the previous one. The time scale has been adjusted to let the three gait cycles be in phase with each other. The sample frequency used with the first patient was only 25 Hz instead of 250 Hz, so the signal looks more angular.)

The difference in the two signals is significant: the subject without distal end contact showed a sharp rise and fall of 'distal end' pressure due to the momentary compression of air whereas the subject with distal end contact showed the double peak pattern also seen at the other pressure sites.

To check whether there really was no significant influence of compressed air on the distal end pressure from the pilot tests subject, a ventilation hole was drilled into the distal end of the reference socket. The complete test sequence was repeated and the distal end pressures compared. The figures 5.2.14 and 5.2.15 show the results from the reference sockets without and with the ventilation hole. There was no difference between the two results apart from the smaller negative pressure at the start of swing phase. As the peak pressures were the measurements of interest, this did not interfere with the results.

5.3 Conclusion

The pilot tests results showed that the double support and second peak results were more repeatable than the single support and first peak results. Because the pilot test subject would also take part in the comparison tests, it was expected that the testing experience acquired in the pilot tests, would reduce the variability of the measurements in the comparison tests. In the comparison tests, each socket could only be tested on one day, so it was decided to increase the number of repeat tests to five for the standing tests and ten for the walking tests (see also section 4.7 and 7.2).

The pressure differences between the rectified and unrectified sockets were considerable. This suggested that these tests could reflect and discriminate between different socket designs.

Sockets increasing in depth of rectification				
Socket identification number	Percentage of **P/M/L** rectification	Depth of rectification (in mm)		
		PTB	**MFlare**	**LFlare**
1	0%	0	0	0
2	50%	-4.5	-2.5	-1.9
3	100%	-9	-5	-3.8
4	150%	-14	-7.5	-5.7

Socket identification number	Percentage of **P/M/L** rectification	Volumes in cc (cm^3)				
		PTB	**MFlare**	**LFlare**	**P+M+L**	Total socket
1	0%	0	0	0	0	1100
2	50%	-1.9	-4	-3.9	-9.8 (1%)	1090.2
3	100%	-3.7	-8.1	-7.5	-19.3 (2%)	1080.7
4	150%	-5.4	-12.2	-11	-28.6 (3%)	1071.4

Table 6.1.1

CHAPTER 6

THE COMPARISON TESTS RESULTS

6.1 Introduction

In March 1994, six sockets were instrumented and tested over a two week period. To simplify the presentation and discussion of the results, all sockets have been given a socket identification number. Table 6.1.1 gives an overview of the sockets 1 to 4. The reference socket described in the pilot tests has number 3, the unrectified socket number 1.

The percentage of **P**(atellar tendon), **M**(edial tibial flare) and **L**(ateral tibial flare) rectification was set at 100% for the reference socket. The rectifications of the other sockets were scaled to 0%, 50% and 150% of those of the reference socket. The deepest point or apex of the rectifications is also listed in the top section of table 6.1.1. Prosthetists currently working in the field will find it easier to relate to the depth of rectification than the volume of it, simply because such detailed knowledge of volume changes has only become available fairly recently with the arrival of CAD/CAM systems.

The total volumes of the sockets were measured on the computer model from the posterior shelf to the distal end. In other words, the section of the socket that enclosed the stump was measured. This volume was 1100 cc for the unrectified socket and decreased to 1071.4 cc for the 150% rectified socket, a 3% reduction of volume. Table 6.1.1 also lists the volumes of the individual

Volume equivalent pairs of sockets						
Socket identification number	Percentage of **P/M/L** rectification	Depth of rectification (in mm)				
		PTB	**M**Flare	**L**Flare	Posterior aspect	
1	0%	0	0	0	0	
5	100%	-9	-5	-3.8	+1.4	
3	100%	-9	-5	-3.8	0	
6	0%	0	0	0	-1.4	
Socket identification number	Percentage of **P/M/L** rectification	Volumes in cc (cm^3)				
		PTB	**M**Flare	**L**Flare	Posterior aspect	Total socket volume
1	0%	0	0	0	0	1100
5	100%	-3.7	-8.1	-7.5	+19.3	1100
3	100%	-3.7	-8.1	-7.5	0	1080.7
6	0%	0	0	0	-19.3	1080.7

Table 6.1.2

rectifications. The PTB volume listed, is the volume of the section of the PTB rectification that was located below the level of the posterior shelf.

Table 6.1.2 presents the characteristics of two volume-equivalent pairs of sockets. Socket 5 was created to match socket 1 in volume but to differ in shape. Whereas socket 1 was unrectified at the PML-areas, socket 5 was 100% rectified. To compensate for the volume loss, a volume *addition* of the required 19.3 cc was made to the posterior aspect of the socket. This rectification was spread over 160 cm^2, so that the depth needed was only 1.4 mm (with the edges tapering to 0 mm). In this way the posterior socket remained virtually unchanged in shape.

Socket 6 was created to match socket 3 in volume but to differ in shape. The PML-rectifications of socket 6 were reduced from 100% to 0%. The resulting volume addition was compensated for by *subtracting* the posterior aspect modification.

This created two sets of volume-equivalent sockets, one set consisting of socket 1 and 5 with a total volume of 1100 cc and one set of socket 3 and 6 with a total volume of 1080.7 cc. These socket pairs helped to determine whether a possible reduction in distal end pressure was either due to the effectiveness of PML-rectifications or the accompanying volume reductions. The results of these tests are presented in chapter 6.2 and discussed in chapter 7.

6.2 Results of the comparison tests

In section 6.2.1, the results of socket 1 are presented in detail to illustrate the format of the tests and the way the results have been summarised. The results from the other five sockets are presented in a summarised form. A full description of all the results can be found in appendix 6.2.

In the sections 6.2.2 to 6.2.6, the results of the first four sockets are presented and discussed. All four types of results (single/double support, peak 1 and 2) are reported, first the standing tests and then the walking tests.

In the sections 6.2.7 to 6.2.10, the results from socket 5 and 6 are presented and contrasted with their volume-equivalent counterparts (socket 1 and 3 respectively). In section 6.2.11, the results of both the sockets increasing in rectification and the volume-equivalent pairs are summarised. Please note that when the test results are described and discussed, terms such as 'the distal pressure' are used as an abbreviated version of: the *mean* distal end pressure *of the test results under discussion.*

Single support	Fy	PTB	MFlare	LFlare	D_end
Unit of measurement	Newtons	kPascals	kPascals	kPascals	kPascals
Stand1	879	62	90	71	103
Stand2	879	61	88	72	102
Stand3	880	64	90	76	105
Stand4	880	65	84	69	100
Stand5	878	61	90	75	107
Mean	879	63	89	72	103
Standard Dev's	0.7	1.3	2.3	2.7	2.5
% SD of Mean	0.1%	2.0%	2.6%	3.8%	2.4%

Table 6.2.1.1

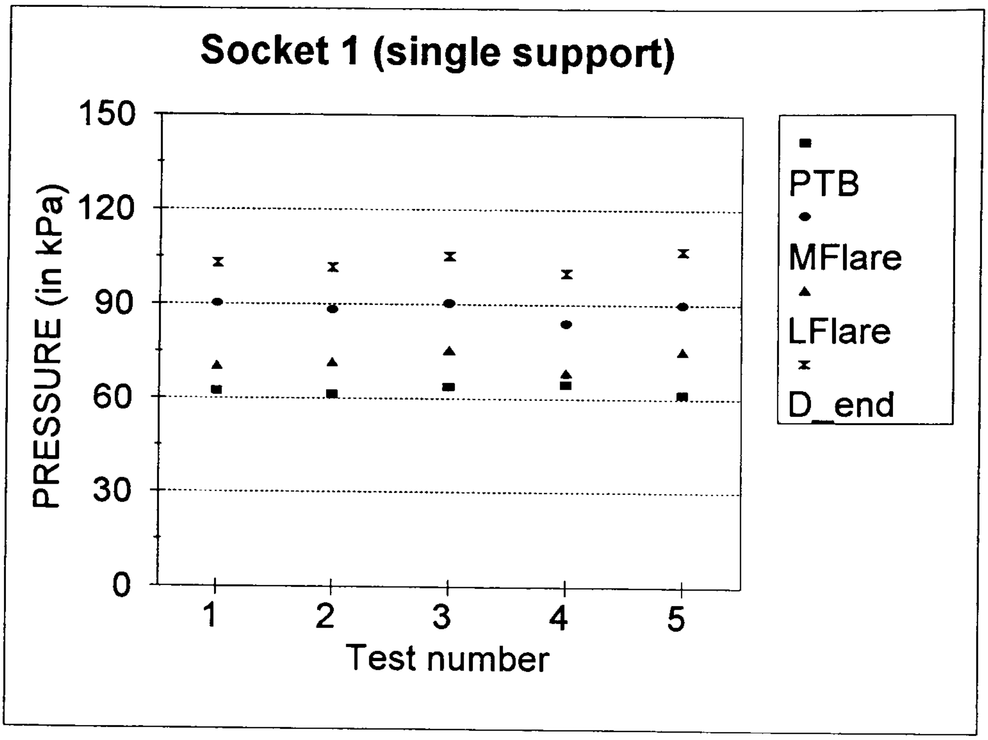

Fig. 6.2.1.1

6.2.1 Socket 1 results

Table 6.2.1.1 summarises the single support results of the unrectified socket no.1. The mean values have been calculated over five tests. Standard deviations have been calculated to give some indication of the variability of the measurements. To simplify comparisons in pressure variability, the standard deviations have also been expressed as a percentage of the mean value.

The highest pressures (in the single support tests) were measured at the distal end: 103 kPa. The PTB pressure was only 63 kPa and the medial and lateral flare pressure 89 and 72 kPa respectively. The double support tests showed a similar picture: the highest pressure at the distal end, 63 kPa, and pressures of 35, 49 and 33 kPa for the patellar tendon, medial and lateral flare (see table 6.2.1.2).

Double support	Fy	PTB	MFlare	LFlare	D_end
Unit of measurement	Newtons	kPascals	kPascals	kPascals	kPascals
Stand1	444	38	47	34	67
Stand2	457	31	51	33	64
Stand3	437	33	47	31	60
Stand4	468	35	50	33	61
Stand5	464	36	50	34	61
Mean	454	34	49	33	63
Standard Dev's	11.5	2.2	1.7	0.9	2.6
% SD of Mean	2.5%	6.4%	3.5%	2.6%	4.2%

Table 6.2.1.2

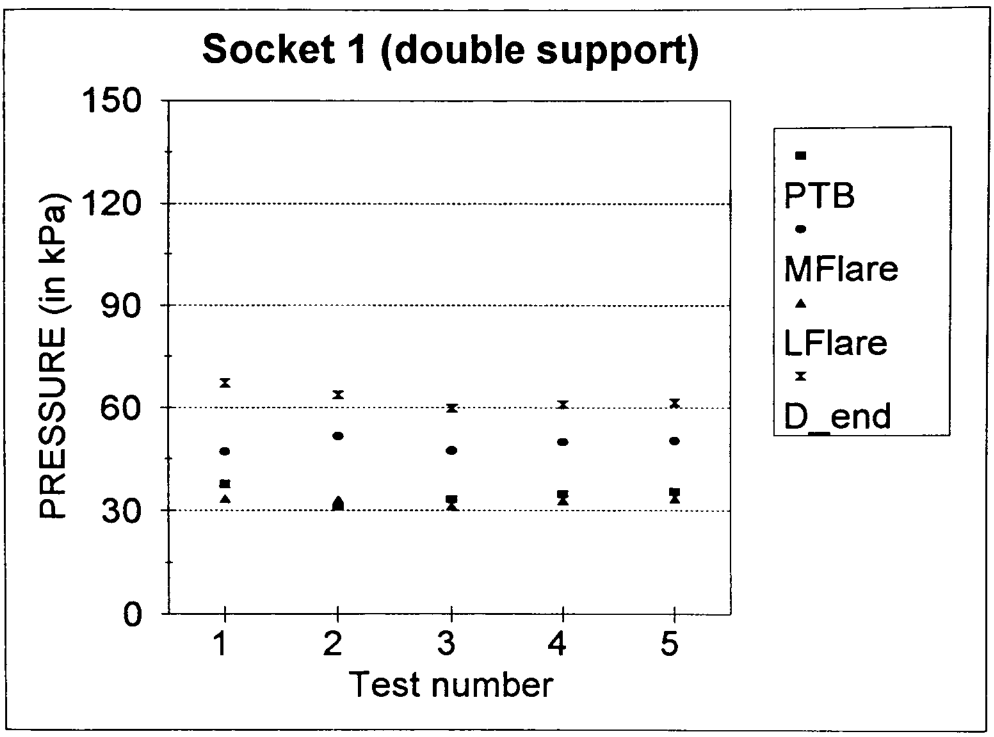

Fig. 6.2.1.2

The vertical support force (Fy) as measured by the forceplate showed a larger variability for the double support than for the single support tests, although it was still at a low level: 2.5%. The standard deviations of the pressure measurements varied between 2 and 3.8% for the single support and between 2.6 and 6.4% for the double support tests. In both the single and the double support tests, there was no indication of an upward or downward trend in pressure levels over the five tests performed (see fig. 6.2.1.1 and fig. 6.2.1.2).

Peak1 Values	Fy	PTB	MFlare	LFlare	D_end
Unit of measurement	Newtons	kPascals	kPascals	kPascals	kPascals
Mean values	911	21	78	74	114
Standard Dev's	40.4	4.5	3.8	4.2	5.3
% SD of Mean	4.4%	22.1%	4.8%	5.8%	4.7%

Table 6.2.1.3

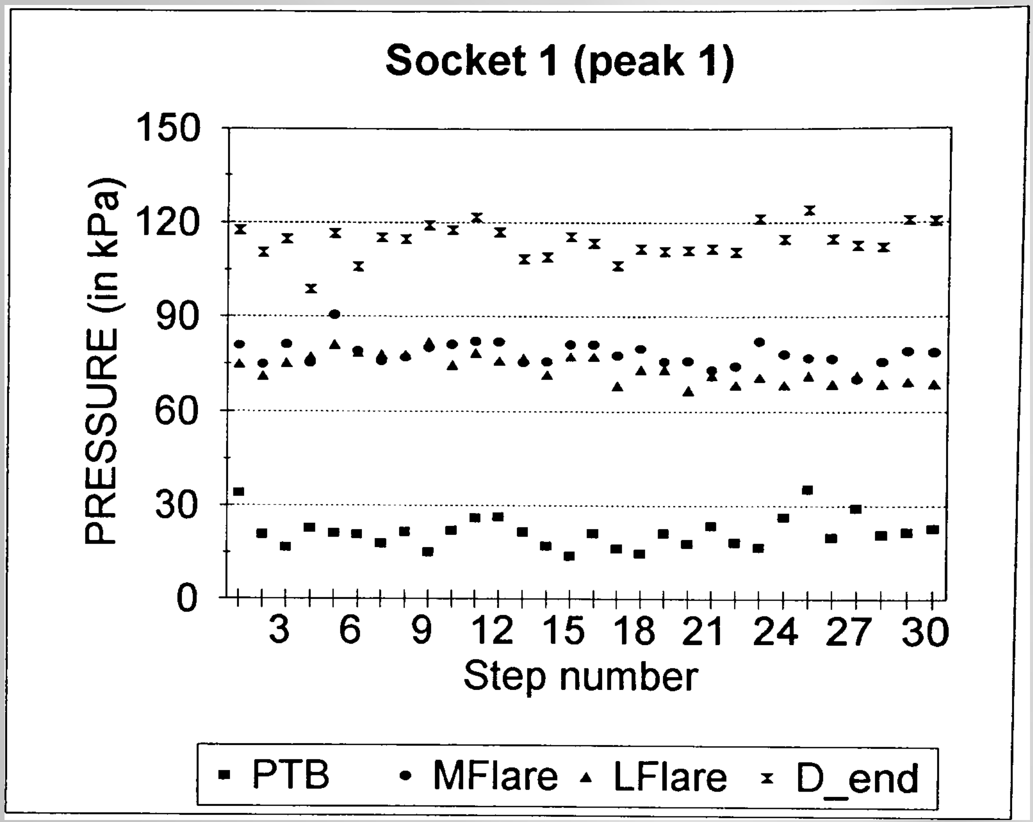

Fig. 6.2.1.3

In the dynamic tests, the subject's gait was monitored over a series of ten walks. Each walk contributed three steps of which the middle one landed on the force plate. This means that the vertical support force (Fy) was averaged over ten steps while the pressure measurements were averaged over thirty steps. From each gait cycle, the first and second peak pressure were determined. A full listing of those results can be found in appendix 6.2. The summarised results of the first and second peak results are displayed in the tables 6.2.1.3 and 6.2.1.4 respectively.

At the first peak measurements, the mean Fy value (911 N) was a little higher than that of the single support test (879 N). The variability of the Fy-values was much higher at the first peak (4.4%) than in the single support tests (0.1%). At the second peak the Fy-variability dropped to 1.5%.

The variability of the peak 1 PTB pressures was also high, especially in relation to the pressure levels measured. However, in the sockets that were unrectified in this area (1 and 6), the first PTB peak was not always clearly identifiable. When the first PTB peak was not clear, a representative value was selected at the same instant in time that the other pressure sites peaked. This allowed some comparison between the PTB pressures of the unrectified and rectified sockets early in stance phase. Even though the standard deviations were calculated for the first peak PTB pressures of socket 1, the limitations outlined above have to be born in mind when comparisons are made and the results interpreted.

Peak 2 Values	Fy	PTB	MFlare	D_end
Unit of measurement	Newtons	kPascals	kPascals	kPascals
Averages	890	66	79	106
Standard Dev's	13	4	3	4
% SD of Mean	1.5%	6.5%	4.0%	3.4%

Table 6.2.1.4

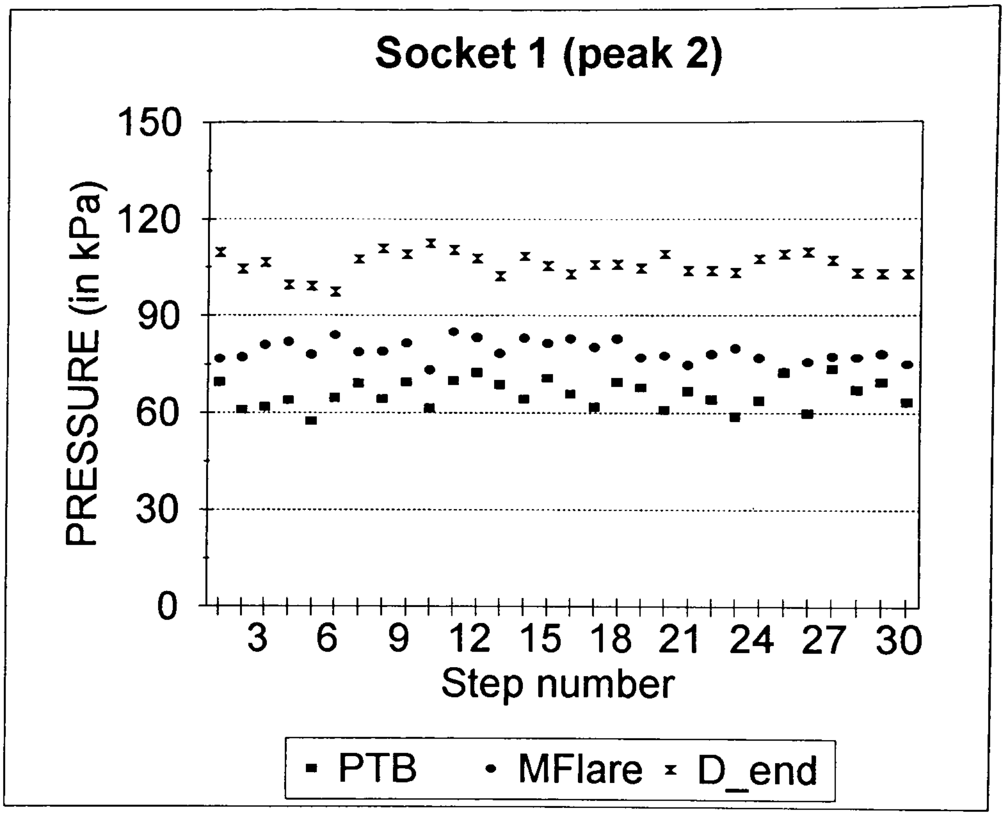

Fig. 6.2.1.4

The medial flare pressures were virtually the same at the first and the second peak: 78 and 79 kPa respectively. This was lower than the single support value (89 kPa). The lateral flare pressure at the first peak was 74 kPa compared to 72 kPa in the single support tests. The lateral flare pressure did not peak in any socket in the second half of stance phase, so no second peak measurements were determined (see section 4.6).

The distal end pressure was higher at the first peak than at the second peak: 114 and 106 kPa respectively. The second peak pressure did not differ much from the single support pressure (103 kPa).

The figures 6.2.1.3 and 6.2.1.4 illustrate that although there was some variability in the measurements, there was no upward or downward trend in the pressure levels. This was important as an upward or downward trend of the distal end pressure in particular could have indicated that the patient was not settled in the prosthesis, thereby compromising the accuracy of the measurements.

Single support, mean values	Fy	PTB	MFlare	LFlare	D_end
Unit of measurement	Newtons	kPascals	kPascals	kPascals	kPascals
Socket 1 (0%)	879	63	89	72	103
Socket 2 (50%)	869	115	93	64	97
Socket 3 (100%)	882	198	113	65	95
Socket 4 (150%)	874	232	122	66	70

Table 6.2.2A

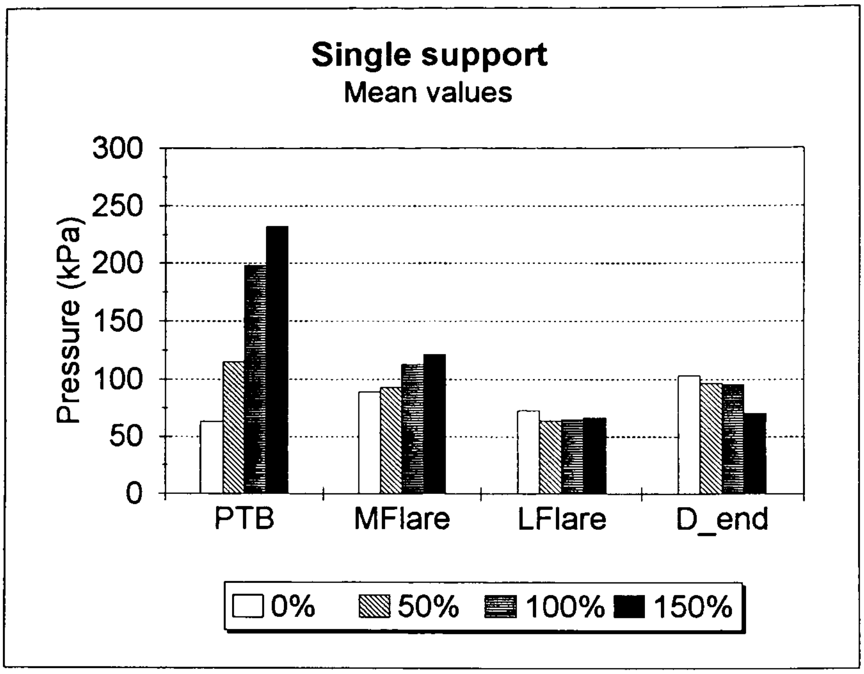

Fig 6.2.2

Single support	Fy		PTB		MFlare		LFlare		D_end	
SD / %SD of Mean	SD	%SD	SD	%SD	SD	%SD	SD	%SD	SD	%SD
Socket 1 (0%)	0.7	0.1%	1.3	2.0%	2.3	2.6%	2.7	3.8%	2.5	2.4%
Socket 2 (50%)	1.1	0.1%	5.3	4.6%	1.8	2.0%	1.5	2.4%	1.0	1.0%
Socket 3 (100%)	3.2	0.4%	9.7	4.9%	2.9	2.6%	2.4	3.7%	3.7	3.9%
Socket 4 (150%)	2.0	0.2%	12.4	5.3%	1.0	0.8%	1.7	2.6%	1.3	1.9%

Table 6.2.2B

6.2.2 Single support results of the sockets 1, 2, 3 and 4

Table 6.2.2A and figure 6.2.2 give an overview of the mean single support pressures measured in the sockets 1, 2, 3 and 4. While the rectifications in each of the PML-areas increased by the same percentage, the pressure levels at these sites did not necessarily reflect this.

The area that was most affected by the rectifications was the patellar tendon area. Figure 6.2.2 illustrates how the PTB pressure rose from 63 kPa in socket 1 to 232 kPa in socket 4.

The rise in medial flare pressure was less dramatic: from 89 kPa in socket 1 to 122 kPa in socket 4.

The lateral flare area showed a more ambiguous pattern: although the depth of rectification increased, the pressure decreased from socket 1 to socket 2 and stabilised around 65 kPa for the sockets 2, 3 and 4.

The distal end pressure showed little change initially, from socket 1 to 3 it decreased from 103 to 95 kPa. However, in socket 4 the distal end pressure fell to 70 kPa, a 26% reduction in pressure.

The vertical component of the ground reaction force (Fy) varied little from socket to socket (from 869 to 882 N). The Fy-variability per socket was particularly low; the standard deviations never exceeded 0.4% of the mean values (see table 6.2.2B).

The pressure sites' standard deviations varied between 1 and 5% of the mean values, with the medial flare showing the lowest and the PTB the highest variabilities.

Double support, mean values	Fy	PTB	MFlare	LFlare	D_end
Unit of measurement	Newtons	kPascals	kPascals	kPascals	kPascals
Socket 1 (0%)	454	34	49	33	63
Socket 2 (50%)	437	55	50	28	55
Socket 3 (100%)	440	119	59	23	50
Socket 4 (150%)	441	129	64	29	38

Table 6.2.3A

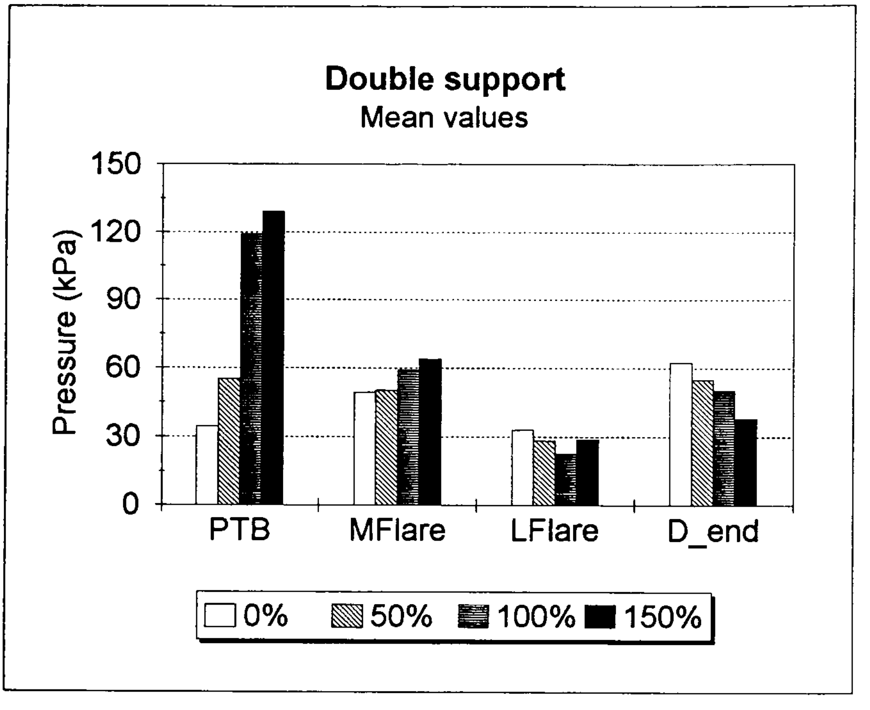

Fig 6.2.3

Double support	Fy		PTB		MFlare		LFlare		D_end	
SD / %SD of Mean	SD	%SD	SD	%SD	SD	%SD	SD	%SD	SD	%SD
Socket 1 (0%)	11.5	2.5%	2.2	6.4%	1.7	3.5%	0.9	2.6%	2.6	4.2%
Socket 2 (50%)	14.2	3.3%	6.2	11.2%	1.6	3.2%	1.0	3.5%	1.3	2.4%
Socket 3 (100%)	9.2	2.1%	9.4	7.9%	2.0	3.5%	2.2	9.7%	1.9	3.8%
Socket 4 (150%)	36.9	8.3%	9.6	7.4%	1.4	2.3%	1.6	5.4%	1.2	3.1%

Table 6.2.3B

6.2.3 Double support results of the sockets 1, 2, 3 and 4

The double support test results generally showed similar patterns as the single support test results. The PTB pressure demonstrated the largest increase in pressure; from 34 kPa in socket 1 to 129 kPa in socket 4. The largest rise was between socket 2 and 3, the smallest between socket 3 and 4, just as in the single support tests (cf. fig. 6.2.2 and fig. 6.2.3).

The medial flare pressure increased moderately from 49 kPa in socket 1 to 64 kPa in socket 4.

The lateral flare pressure fell again from socket 1 to socket 2, but this time it continued to fall from socket 2 to socket 3: from 28 to 23 kPa. In socket 4, it rose again to 29 kPa.

The distal end pressure dropped more significantly between socket 1, 2 and 3 than before: from 63 to 50 kPa. However, the largest drop was still from socket 3 to 4: from 50 to 38 kPa.

Fy varied little between the sockets: from 437 to 454N. The variability of Fy per socket was considerably larger in the double support tests than in the single support tests: it varied between 2.1 and 8.3% of the mean values. All pressure sites showed a percentagewise larger variability as well.

Peak 1, mean values	Fy	PTB	MFlare	LFlare	D_end
Unit of measurement	Newtons	kPascals	kPascals	kPascals	kPascals
Socket 1 (0%)	911	21	78	74	114
Socket 2 (50%)	951	88	81	78	119
Socket 3 (100%)	971	231	113	97	117
Socket 4 (150%)	945	462	116	91	110

Table 6.2.4A

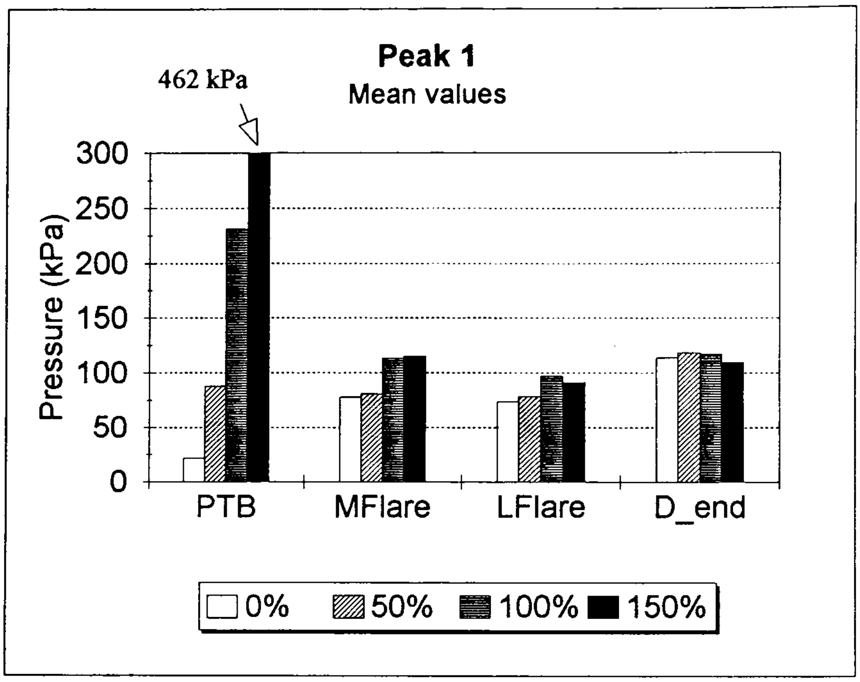

Fig 6.2.4

Peak 1	Fy		PTB		MFlare		LFlare		D_end	
SD / %SD of Mean	SD	%SD	SD	%SD	SD	%SD	SD	%SD	SD	%SD
Socket 1 (0%)	40.4	4.4%	4.5	22.1%	3.8	4.8%	4.2	5.8%	5.3	4.7%
Socket 2 (50%)	26.9	2.8%	6.2	7.0%	2.8	3.4%	4.2	5.3%	5.7	4.8%
Socket 3 (100%)	35.4	3.6%	9.4	4.1%	4.4	3.9%	4.2	4.4%	3.9	3.3%
Socket 4 (150%)	38.6	4.1%	9.6	2.1%	3.8	3.3%	3.9	4.3%	4.8	4.4%

Table 6.2.4B

6.2.4 Peak 1 results of the sockets 1, 2, 3 and 4

The dynamic tests presented somewhat different patterns than the static tests. The rise in PTB pressure was more pronounced: the first peak pressure in the gait cycle reached a mean socket 4 value of 462 kPa; *double* the pressure of the single support test (the scale of the Y-axis in fig. 6.2.4 has not been adjusted to this value as it would complicate visual comparisons between the static and dynamic tests). In contrast to this, the first peak PTB pressures measured in the first two sockets were *lower* than those measured in the single support tests.

The medial flare pressures followed the pattern set in the static tests: a moderate increase in pressure from socket 1 to socket 4 (from 78 to 116 kPa).

The lateral flare pressure did not decrease this time, it *in*creased from 74 to 91 kPa. However, the socket 3 pressure (97 kPa) was higher than the socket 4 pressure.

The distal end pressure did not show any correlation with the amount of rectification: it varied between 110 and 119 kPa without any recognisable pattern (see fig. 6.2.4).

The Fy forces and variations were larger than in the single support tests: the peak 1 values varied between 911 and 971N (in the single support tests 869 to 882 N). While the variability of all results apart from the PTB was very similar (between 3 and 5%), the PTB variability dropped from 22.1 to 2.1%.

Peak 2, mean values	Fy	PTB	MFlare	D_end
Unit of measurement	Newtons	kPascals	kPascals	kPascals
Socket 1 (0%)	890	66	79	106
Socket 2 (50%)	872	135	80	98
Socket 3 (100%)	896	220	107	99
Socket 4 (150%)	877	280	110	94

Table 6.2.5A

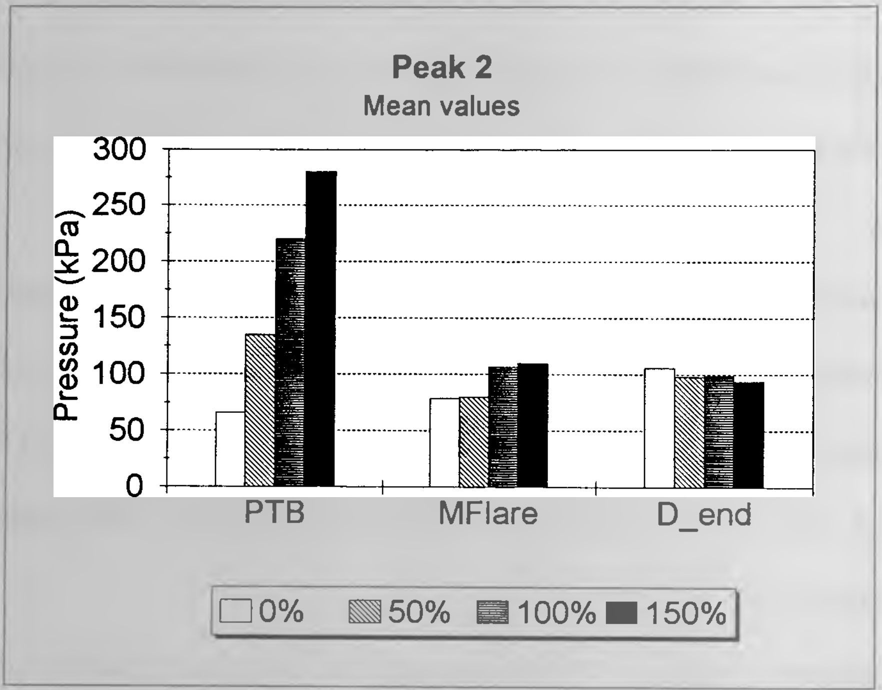

Fig 6.2.5

Peak 2	Fy		PTB		MFlare		D_end	
SD / %SD of Mean	SD	%SD	SD	%SD	SD	%SD	SD	%SD
Socket 1 (0%)	13.4	1.5%	4.3	6.5%	3.1	4.0%	3.6	3.4%
Socket 2 (50%)	14.5	1.7%	15.0	11.1%	3.3	4.1%	3.2	3.2%
Socket 3 (100%)	9.7	1.1%	6.9	3.1%	3.6	3.3%	3.9	4.0%
Socket 4 (150%)	16.0	1.8%	17.4	6.2%	2.0	1.8%	3.6	3.9%

Table 6.2.5B

6.2.5 Peak 2 results of the sockets 1, 2, 3 and 4

The second peak in a gait cycle did not occur at the lateral flare (see section 4.7) so the tables and figure on the opposite page only show the results for the PTB, medial flare and distal end measurements.

At the second peak of the gait cycle, the Fy values were very similar to the single support measurements (the Fy-average over the sockets 1, 2, 3 and 4 was 876 N at single support and 884 N at the second peak).

The PTB pressures increased from 66 to 280 kPa. The medial flare pressures increased over almost the same range as in the first peak: from 79 to 110 kPa. The distal end pressure decreased slightly from 106 kPa to 94 kPa.

The variability of the second peak Fy measurements (1.1 to 1.8%) was less than those of the first peak measurements (2.8 to 4.4%). Of the pressure sites, the PTB variability was erratic again: it varied from 3.1% in socket 3 to 11.1% in socket 2. The medial flare and distal end variability was similar to that measured previously (around 4%).

6.2.6 The socket 1, 2, 3 and 4 results summarised

The most important differences between the static and dynamic test results from the sockets 1, 2, 3 and 4 appeared to be:

1) the very high PTB value early in the gait cycle in socket 4
2) the considerable decrease in distal end pressure in socket 4 in the static tests
3) the lack of correlation between distal end pressure and the amount of proximal rectification in the dynamic tests

In the static tests of the first four sockets, there were indications that an increase in proximal rectifications led to a decrease in distal end pressure. Whether this effect was shape or volume related will depend on the results of the volume-equivalent pairs of sockets. These are present in the next four sections, 6.2.7 to 6.2.10

	Single support Unit of measurement	Fy Newtons	PTB kPascals	MFlare kPascals	LFlare kPascals	D_end kPascals
Pair A	0% (Socket 6)	879	62	101	80	103
	100% (Socket 3)	882	198	113	65	95
Pair B	0% (Socket 1)	879	63	89	72	103
	100% (Socket 5)	874	203	92	61	95

Table 6.2.7

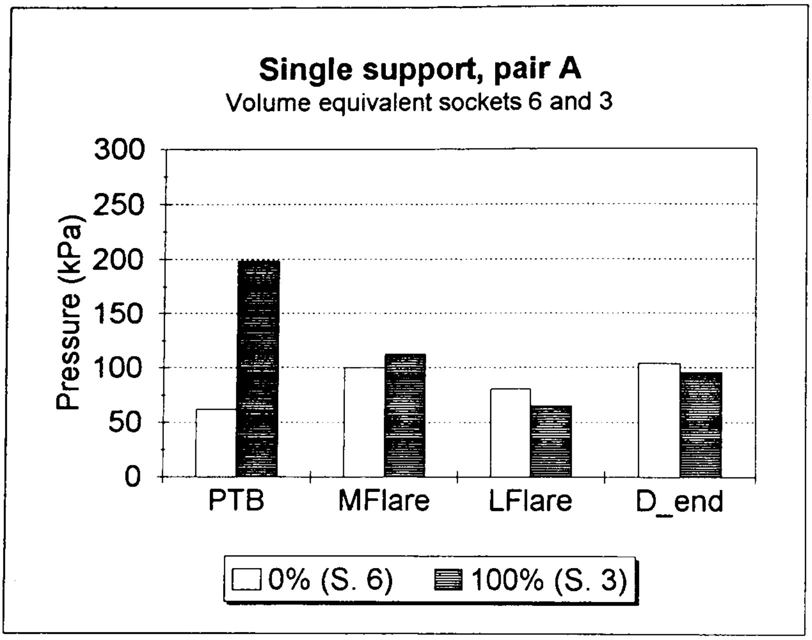

Fig. 6.2.7A

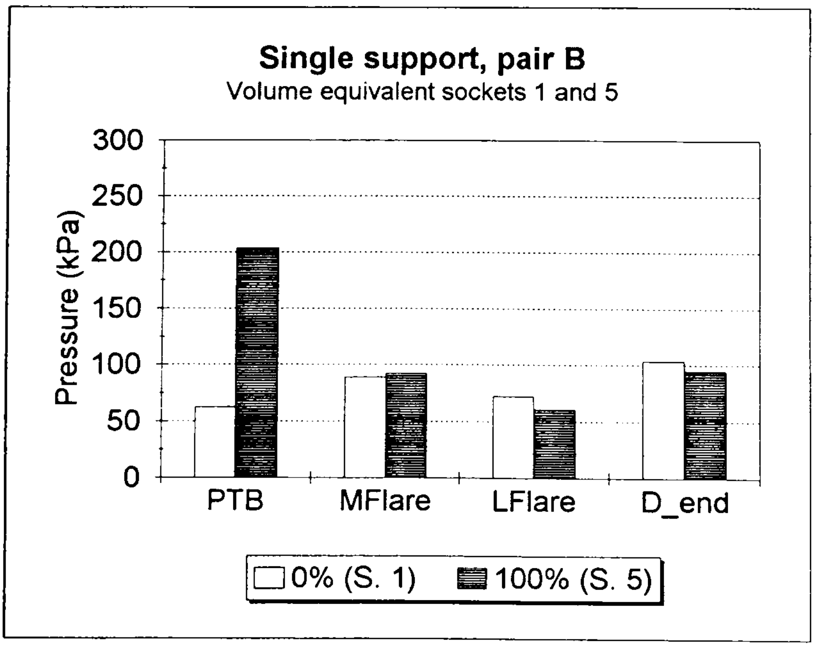

Fig. 6.2.7B

6.2.7 Single support results of the sockets 5 and 6

The single support test results of the sockets 5 and 6 are presented with the results of their volume-equivalent sockets 1 and 3 in table 6.2.7. The sockets 6 and 3 formed pair A, the 'small' pair, with a volume of 1080.7 cc and the sockets 1 and 5 formed pair B, the 'large' pair, with a volume of 1100 cc (see also table 6.1.2). In the figures 6.2.6A and 6.2.6B, the data from the PML-*un*rectified sockets is displayed as white bars and the PML-rectified socket data as horizontally striped bars. A complete listing of the socket 5 and 6 results can be found in appendix 6.2.

At the single support tests, the vertical loading conditions were virtually the same for all sockets. The difference in Fy between the sockets 6 and 3 was only 3N (~0.3 kg) and between the sockets 1 and 5, 5N (~0.5 kg).

As before, the PTB area was influenced the most by rectifications in that area. The PTB-pressure in pair A increased from 62 to 198 kPa and in pair B from 63 to 203 kPa. The medial flare pressure also increased, although considerably more in pair A than in pair B (from 101 to 113 kPa and from 89 to 92 kPa respectively).

The lateral flare pressure decreased again despite the removal of the undercut in that area: from 80 to 65 kPa in pair A and from 72 to 61 kPa in pair B. The distal end pressure decreased in both pairs from 103 to 95 kPa, despite their difference in volume. The medial and lateral flare pressure were higher on average in the smaller pair A.

	Double support Unit of measurement	Fy Newtons	PTB kPascals	MFlare kPascals	LFlare kPascals	D_end kPascals
Pair A	0% (Socket 6)	437	26	54	35	55
	100% (Socket 3)	440	119	59	23	50
Pair B	0% (Socket 1)	454	34	49	33	63
	100% (Socket 5)	441	114	49	27	53

Table 6.2.8

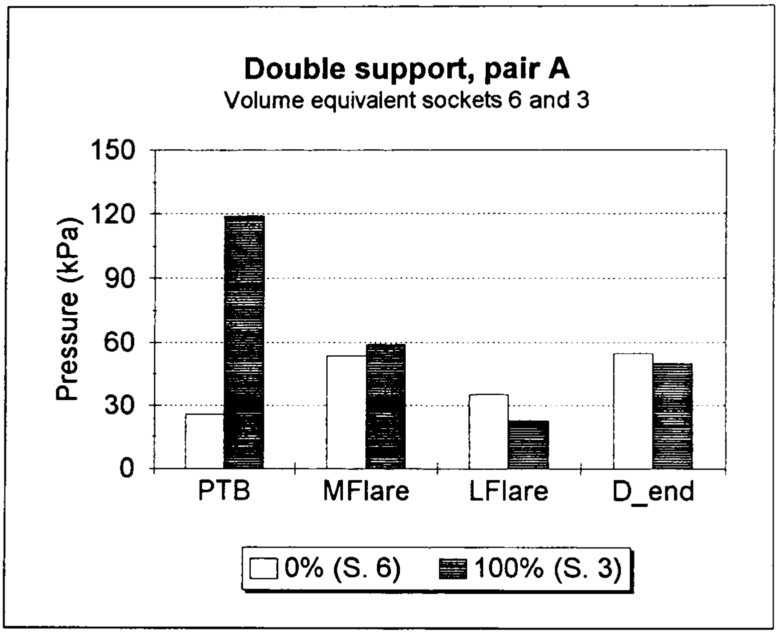

Fig. 6.2.8A

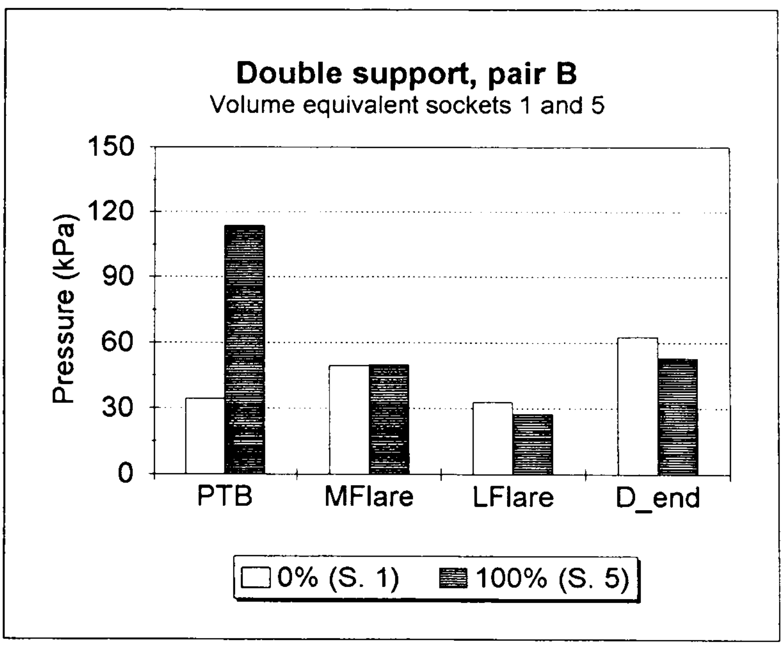

Fig. 6.2.8B

6.2.8 Double support results of the sockets 5 and 6

The double support test results showed similar patterns as the single support test results. The PTB pressure increased significantly in both pairs; the medial flare pressure increased in pair A, but stayed the same in pair B; the lateral flare pressure fell in both pairs as did the distal end pressure.

One difference between the single and double support test results was that the distal end pressure was generally higher in pair B than in pair A.

The vertical support force Fy differed between the sockets 5 and 1 by 13N, but percentagewise this was not more than 3%.

	Peak 1	Fy	PTB	MFlare	LFlare	D_end
	Unit of measurement	Newtons	kPascals	kPascals	kPascals	kPascals
Pair A	0% (Socket 6)	893	26	86	90	107
	100% (Socket 3)	971	231	113	97	117
Pair B	0% (Socket 1)	911	21	78	74	114
	100% (Socket 5)	950	272	78	80	109

Table 6.2.9

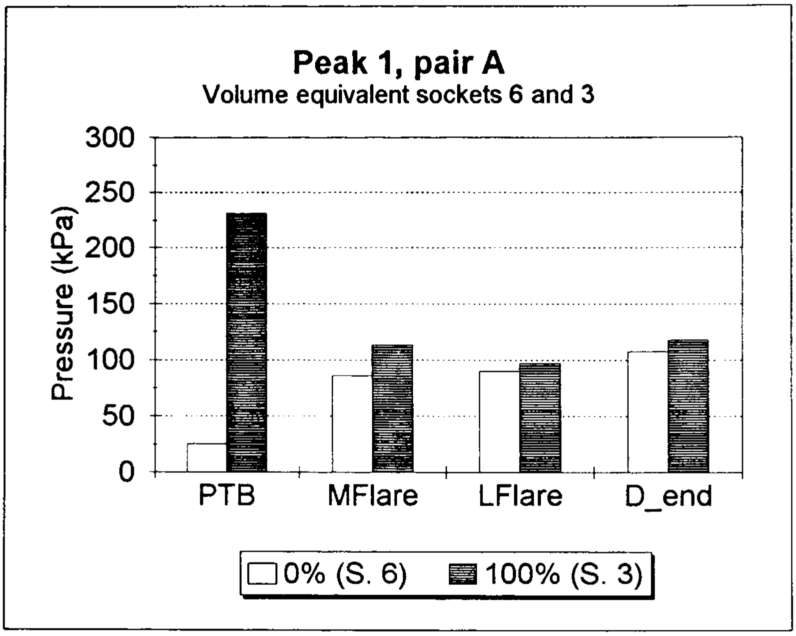

Fig. 6.2.9A

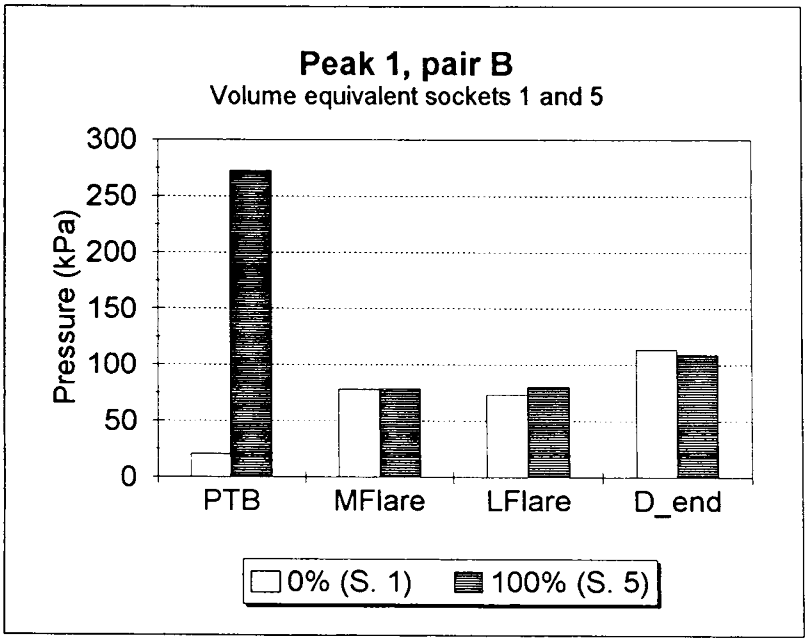

Fig. 6.2.9B

6.2.9 Peak 1 results of the sockets 5 and 6

The vertical component of the ground reaction force (Fy) varied more in the dynamic tests than in the static tests. The differences in Fy were particularly large at the first peak in the gait cycle: in pair A, a difference of 78 N was measured, about 9% of the mean value. In pair B, the difference was 39 N or about 4% of the mean value.

The differences in PTB pressures were larger than in the single support tests: in pair A, the PTB pressure increased from 26 to 231 kPa and in pair B from 21 to 272 kPa. The medial flare pressures were lower on average than those measured at single support but the pattern was similar as before: in pair A, the pressure increased (from 86 to 113 kPa) and in pair B, the pressure remained virtually the same (78 kPa).

In the dynamic tests, the lateral flare pressure *in*creased in both pairs with the increase in rectification instead of decreasing with the increase in rectification as it did in the static tests.

The distal end pressure rose in pair A but fell in pair B with the increase in the PML-rectifications. However, the difference in loading conditions as indicated by the difference in Fy values has to be taken into account when these pressure test results are interpreted.

	Peak 2	Fy	PTB	MFlare	D_end
	Unit of measurement	Newtons	kPascals	kPascals	kPascals
Pair A	0% (Socket 6)	878	56	87	100
	100% (Socket 3)	896	220	107	99
Pair B	0% (Socket 1)	890	66	79	106
	100% (Socket 5)	868	212	79	92

Table 6.2.10

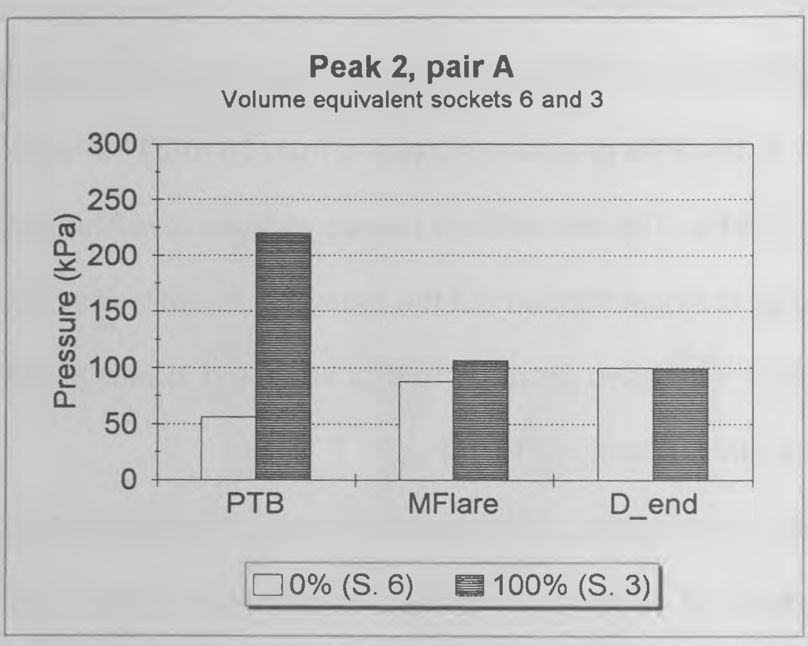

Fig. 6.2.10A

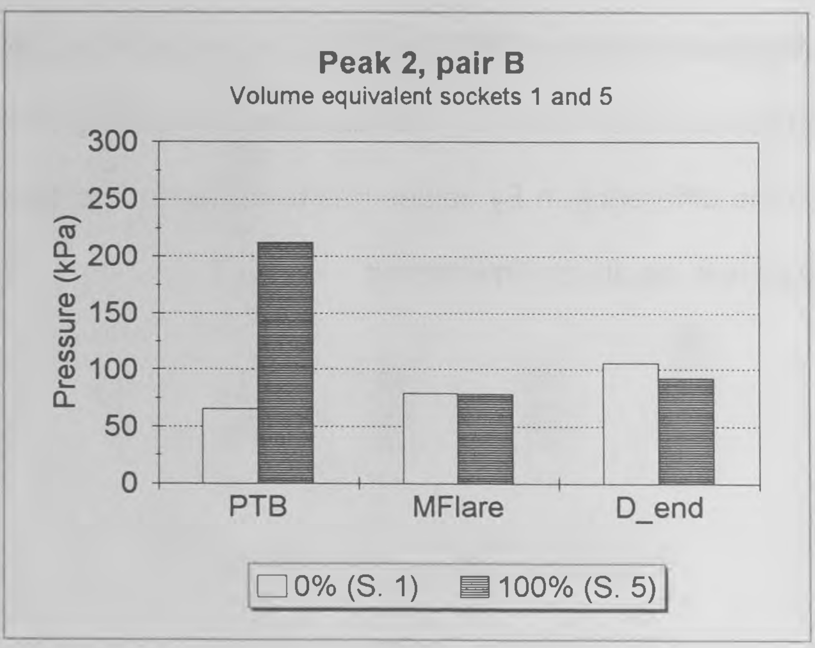

Fig. 6.2.10B

6.2.10 Peak 2 results of the sockets 5 and 6

In the second peak results, the differences in Fy measurements were smaller (3% in pair 1 and 2.5% in pair 2). The PTB pressures showed the same trend as before and the values were close to the results from the single support tests. The medial flare pressures were very similar to the ones measured at the first peak in the gait cycle. The distal end pressure in pair A varied very little (from 100 to 99 kPa) while in pair B it decreased from 106 to 92 kPa, a 14% decrease.

6.2.11 The comparison test results summarised

The pressure trends that were observed in first four sockets were also observed when the sockets 1 and 3 were compared with their volume-equivalent counterparts:

1) the PTB pressure increased considerably from an unrectified to a rectified socket
2) the medial flare pressure increased also but to a lesser extent
3) the lateral flare pressure either fell or stayed the same with an increase in rectification in the static tests but rose with an increase in rectification in the first peak results
4) the distal end pressure decreased with an increase in proximal rectification in the static tests, but not necessarily in the dynamic tests

This means that the effect of the PML-rectifications on the distal end pressure *in the static tests* was not caused by a socket volume reduction but by the shape and/or location of the rectifications.

The two percent volume difference between the two socket pairs did not affect the PTB pressure noticeably but the medial and lateral flare pressure were generally higher in (the smaller) pair A than in pair B. The distal end pressure was only higher in pair B in the double support tests, the other tests did not show a volume-related difference.

CHAPTER 7

DISCUSSION OF THE COMPARISON TEST RESULTS

7.1 Introduction

The main aim of this study was to test whether the amount of distal end loading correlates to proximal variations in socket design. The design of the six sockets described in section 6.1 allowed a distinction between volume- and shape-related effects. Both static and dynamic tests were performed to evaluate the effects of the rectifications. A secondary aim was to investigate the relationship between the amount of rectification in the modified areas and the pressure levels measured.

Before the significance of the results is discussed, the limitations of this project are assessed in section 7.2.

The evidence for a correlation between distal end pressure and proximal socket design is assessed and discussed in section 7.3 and the influence of rectification on pressure levels at the PML-sites in section 7.4.

In section 7.5, the main findings of this project are summarised and recommendations are made for future projects.

7.2 Limitations of the project

The factors influencing the accuracy of the data and the validity of the results can be separated in three categories:

1) technical accuracy

2) quality of method

3) patient variability

The first two categories can be controlled by the investigator, the last category can only be monitored (although the suitability of the method will have some influence on patient related variability).

The technical accuracy generally was of a high level. The transducers showed very low hysteresis and drift, and a high sensitivity, linearity and frequency response (see section 4.5). The sensing surface of the transducers was flush with the inner surface of the socket so that the presence of the transducers did not affect local pressure levels. The CNC-milling machine provided very consistent socket shapes, transducer locations and alignment coordinates.

The small size of the transducer (5mm diameter) made it fairly easy to blend it with the socket contours. The transducers were placed at the deepest points of rectification, assuming that at those points, the effects of changes in rectification would most noticeable. However, the small size of the transducer also meant that the pressure trends observed might not be representative for the whole area of rectification.

The main limitations in the method were the number of repeat tests that could be done per socket. To minimize the influence of patient related variations on the pressure patterns, the sockets had to be tested in as short a time span as possible. However, only one socket could be tested per day for two reasons:

1) it took a few hours to accurately transfer the pressure transducers from one socket to another
2) the complete testing procedure took up to two hours. To minimize the effect of diurnal stump volume changes, each socket was tested at the same time each day (see section 4.6).

Another limitation was the fact that the patient could only wear the instrumented sockets for the duration of the test procedure. It was not possible to let the patient get used to the sockets over a longer period of time as this would have interfered with the comparisons among the six sockets.

The weight of the instrumented prosthesis was higher than that of a normal prosthesis but not much above the weight of a fitting prosthesis with a Berkeley alignment unit (2 kg). The leads from the pressure transducers were channelled through a waist band, from which an 'umbilical cord' of 8m length was connected to the amplifiers. This allowed the subject to walk over the length of the walkway without too much restriction in his movements.

Single support, mean values	Fy	D_end	D_end:FyNormalised
Unit of measurement	Newtons	kPascals	kPascals
Socket 1 (0%)	879	103	103
Socket 2 (50%)	869	97	97
Socket 3 (100%)	882	95	95
Socket 4 (150%)	874	70	70

Table 7.2.1

Double support	Fy	D_end	D_end:FyNormalised
Unit of measurement	Newtons	kPascals	kPascals
Socket 1 (0%)	454	63	61
Socket 2 (50%)	437	55	56
Socket 3 (100%)	440	50	50
Socket 4 (150%)	441	38	38

Table 7.2.2

Peak1	Fy	D_end	D_end:FyNormalised
Unit of measurement	Newtons	kPascals	kPascals
Socket 1 (0%)	911	114	117
Socket 2 (50%)	951	119	117
Socket 3 (100%)	971	117	113
Socket 4 (150%)	945	110	109

Table 7.2.3

Peak2	Fy	D_end	D_end:FyNormalised
Unit of measurement	Newtons	kPascals	kPascals
Socket 1 (0%)	890	106	104
Socket 2 (50%)	872	98	99
Socket 3 (100%)	896	99	97
Socket 4 (150%)	877	94	94

Table 7.2.4

The validity of the socket comparisons depended mainly on the subject. To compare the sockets on equal terms, the loading conditions had to be as constant as possible. This means that in each socket, the patient had to stand and walk in the same way.

The distal end pressure would have been influenced mainly by the load acting along the long axis of the socket. Because the load cell was not able to register this axial force accurately (see section 4.5), the exact loading conditions along the socket axis can not be known. However, the ground reaction force (GRF) measurements from the force plate provided a good estimate of the loading conditions.

In the static tests, the vertical component of the GRF (Fy) was sufficient to monitor the axial load (Fz and Fx were negligible). In the dynamic tests, calculations showed that the Fy was a good approximation of the total load applied to the sockets at the moments of peak pressure (see appendix 7.2).

In section 6.2, the Fy-values were listed alongside the pressure data of each socket. The mean Fy-values differed from socket to socket in all types of tests, but the range of variation was much larger in e.g. the first peak results than in the single support results.

To check whether the differences in loading conditions could have affected the distal end pressures significantly, the distal end pressures have been normalised for the Fy-variations and printed alongside the original values. The tables 7.2.1 to 7.2.4 show that the distal end pressures of the static tests remained virtually unchanged but the dynamic distal end pressures showed

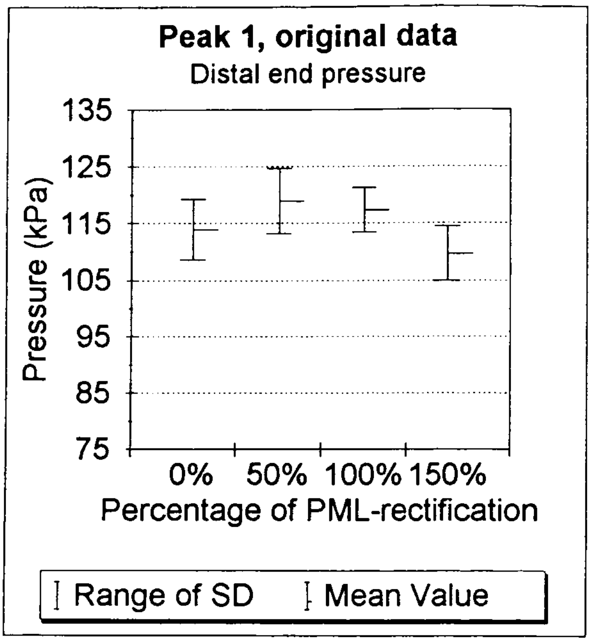

Fig. 7.2.1

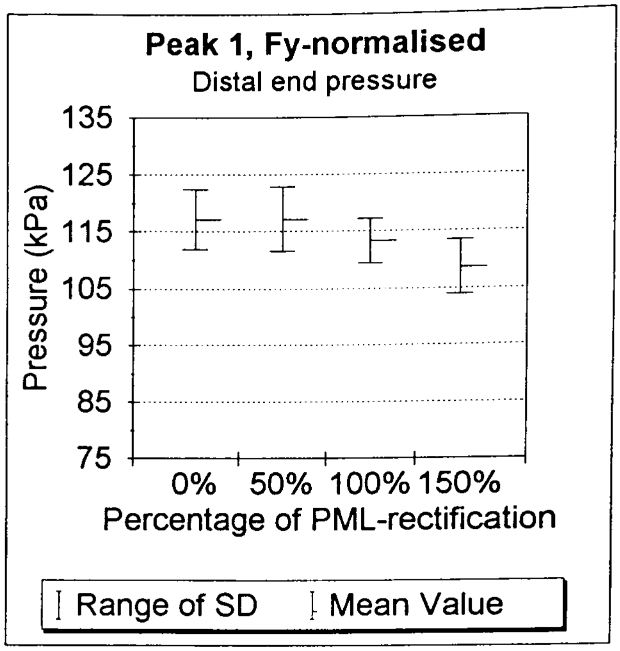

Fig. 7.2.2

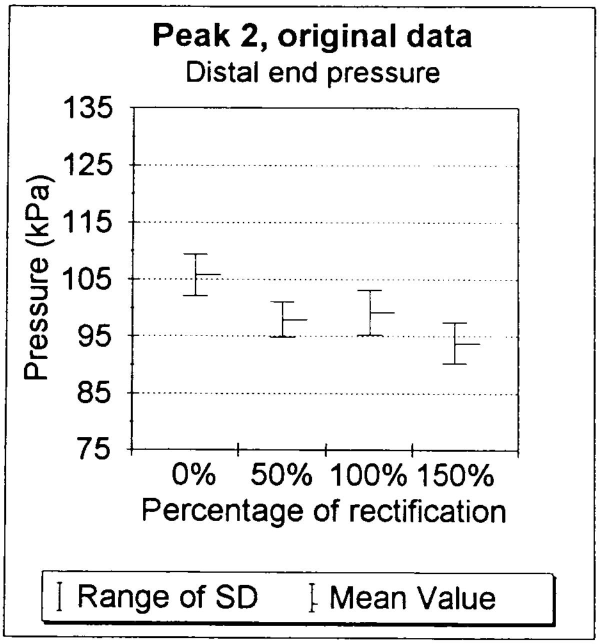

Fig. 7.2.3

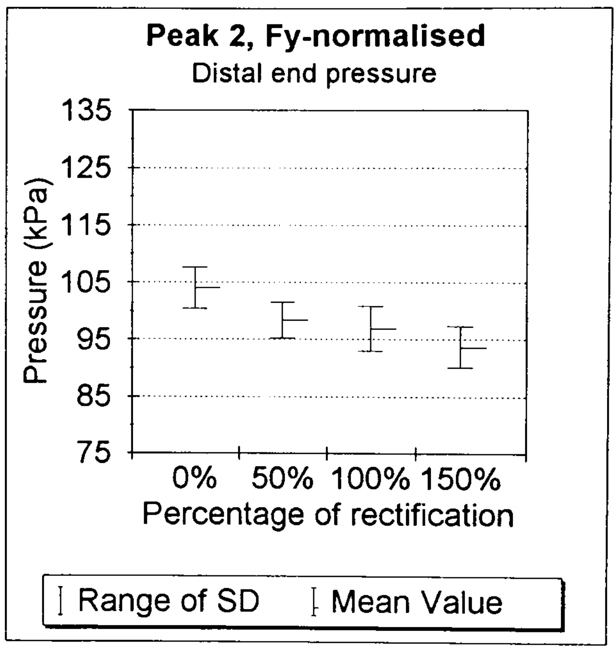

Fig. 7.2.4

some differences. At the first peak, the normalised distal end pressures showed a very slight downward trend instead of no pattern. The slight downward trend in the second peak data remained the same but the inverse correlation with the amount of rectification improved.

The figures 7.2.1 to 7.2.4 show both the original and the normalised distal end pressures with the original ranges of standard deviation. In the first peak data, the change from no clear pattern in fig. 7.2.1 to a slight decrease in distal end pressure in fig. 7.2.2 is visible, but the differences between the sockets are hardly significant. In the second peak data, the existing trend is clearer in fig. 7.2.4 than in fig. 7.2.3, but only the differences between the first and the fourth socket are significant, as they were in the original data.

Normalisation of the distal end pressures of the two volume equivalent pairs showed the same patterns: the static test and second peak distal end pressures remained virtually unchanged and the first peak data showed differences of between 1 and 5 kPa (see appendix 7.2).

From these simulations, it is clear that variations in loading conditions early in stance phase affected the first peak data to such an extent that they could not be regarded as reliable socket comparison indicators. However, the loading conditions variations in the static tests and at the second peak were small enough not to affect the socket comparisons significantly.

Finally, the tests in this project were performed on only one subject. Whether the relationship between distal end pressure and proximal rectification observed in this subject is true in general, can only be determined after trials with many patients with different types of trans-tibial stumps.

7.3 The effect of proximal rectifications on distal end pressure

In chapter 6.2, some correlation between proximal rectifications and distal end pressure was observed in the static tests, but little in the dynamic tests. To investigate how significant these results were, the mean distal end pressure of each test has been plotted with the corresponding standard deviation (SD). The Y-axis has a range of 60 kPa in each figure, but the pressure levels have been adapted to the results of each test: e.g. the Y-axis of the single support tests ranges from 55 to 115 kPa, the double support tests from 25 to 85 kPa (fig. 7.3.1 and 7.3.2).

Because the first peak distal end pressures were not reliable enough, they are not included in this section.

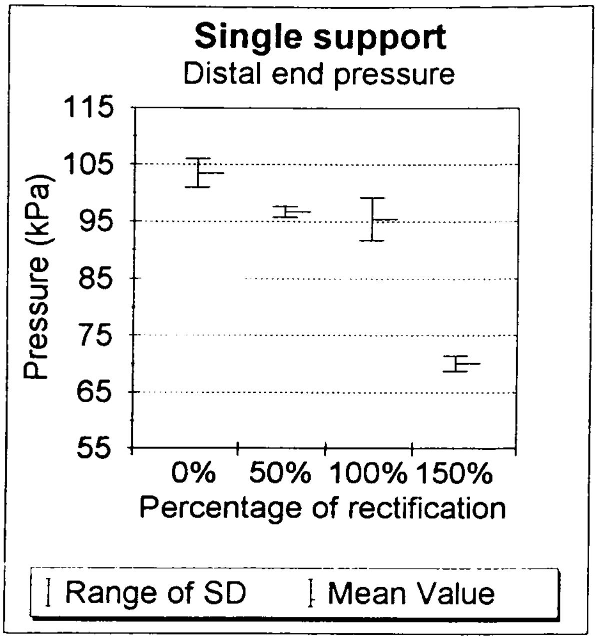

Fig. 7.3.1

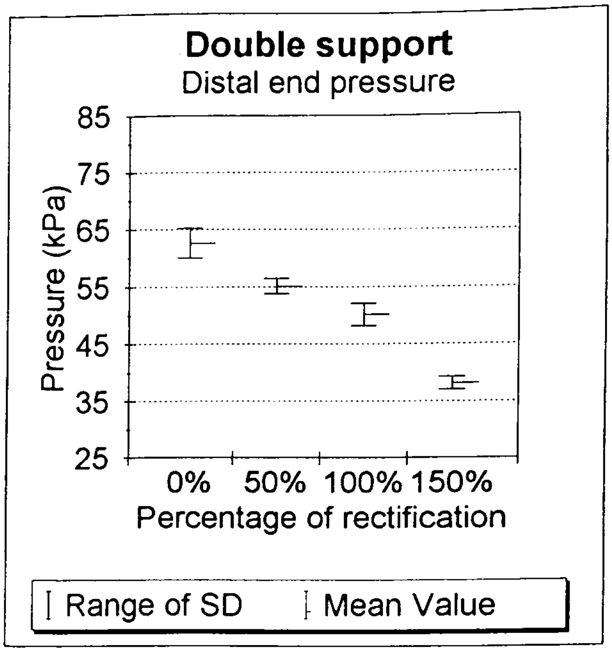

Fig. 7.3.2

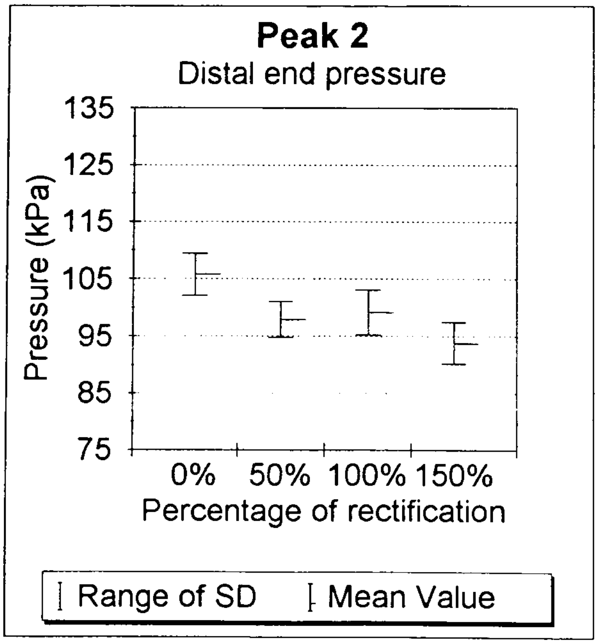

Fig. 7.3.3

7.3.1 Discussion of the socket 1, 2, 3 and 4 results

The figures 7.3.1 and 7.3.2 show the single and double support distal end pressures of the first four sockets. In the single support tests, the difference between the most rectified socket and the other three was very significant. However, there was no significant difference between the 50% and 100% rectified sockets. The difference between the 0% socket and the 50/100% rectified sockets was small, but significant. In the double support tests, there were significant differences between all sockets, but the largest difference was again between 100% and 150% rectified sockets (fig. 7.3.2).

The dynamic test result showed a somewhat different picture: at the second peak, the distal end pressure tended to decrease slightly with an increase in proximal rectification, but these differences were hardly significant (fig. 7.3.3).

To summarise the findings from the first four sockets:

Static tests:

1) the distal end pressure decreased significantly with an increase in the amount of patellar tendon, medial and lateral flare rectification
2) this effect was most pronounced in the 'overrectified' 150%-socket
3) the difference between no rectification (0%) and some rectification (50-100%) was small but significant
4) the difference between a small (50%) and an average (100%) amount of rectification was hardly significant

Dynamic tests:

5) at the weight-acceptance phase of the gait cycle (peak 1), no conclusion could be made about any correlation between distal end pressure and amount of proximal rectification
6) at heel-off (peak 2), the distal end pressure decreased slightly with increasing PML-rectification, but this trend was hardly significant

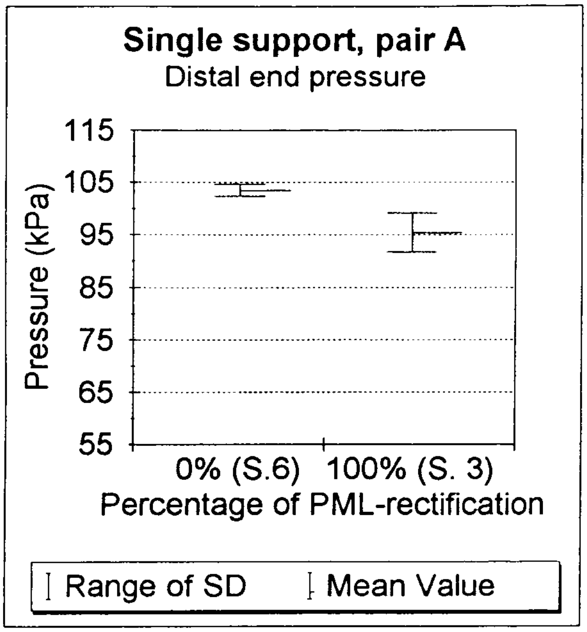

Fig. 7.3.4

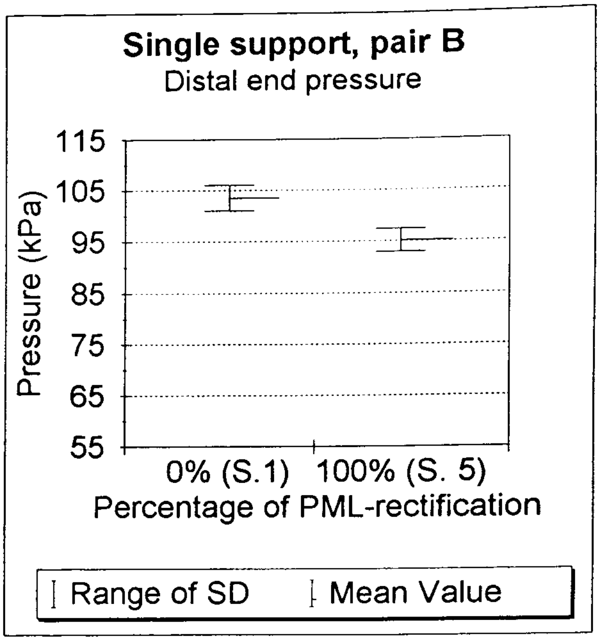

Fig. 7.3.5

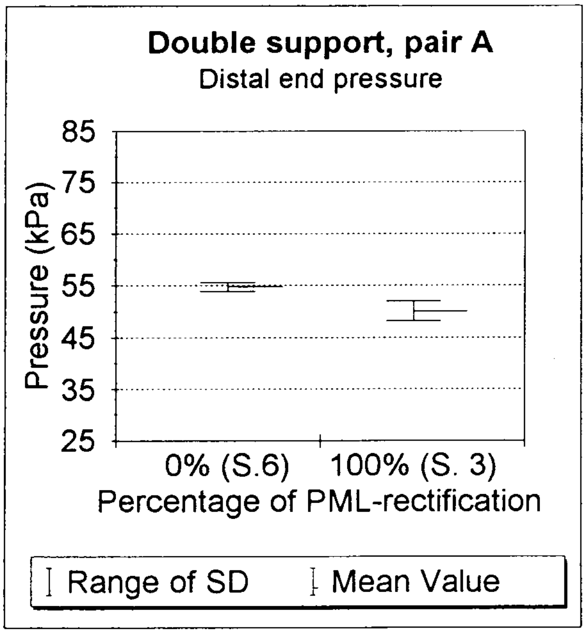

Fig. 7.3.6

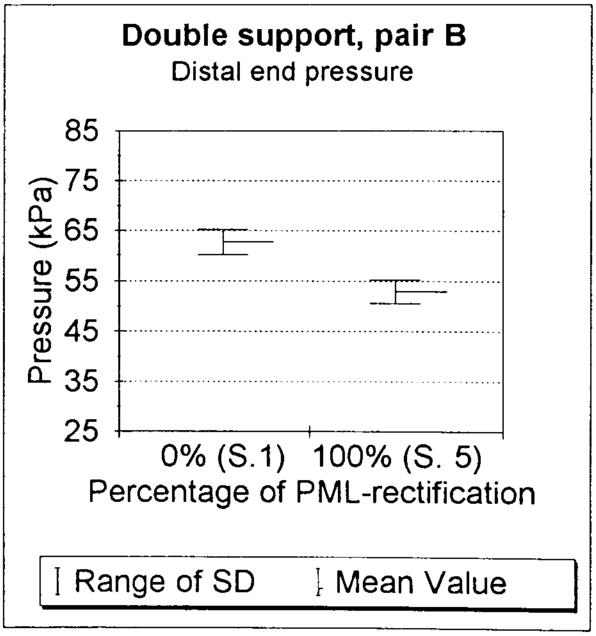

Fig. 7.3.7

7.3.2 Discussion of the volume equivalent sockets results

To assess whether the observed effects were volume- or shape-related, the results from the two volume-equivalent pairs have to be taken into account. The figures 7.3.4 to 7.3.7 show the single and double support results from pair A and pair B.

In all static tests, there was a significant difference in distal end pressure between the 0% and 100% PML-rectified sockets. This suggests that (in a static situation) the effectiveness of the PML-rectifications in decreasing the distal end pressure is not simply caused by a decrease in socket volume. However, the reductions in distal end pressure achieved by a standard rectification were fairly small: between 5 and 10 kPa.

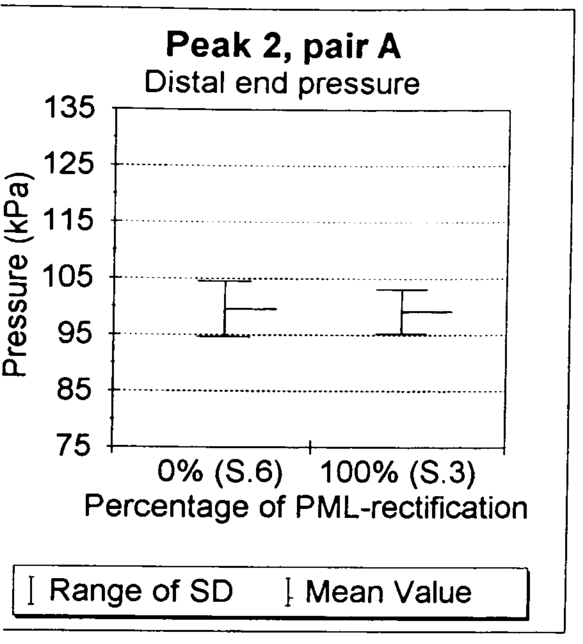

Fig. 7.3.8

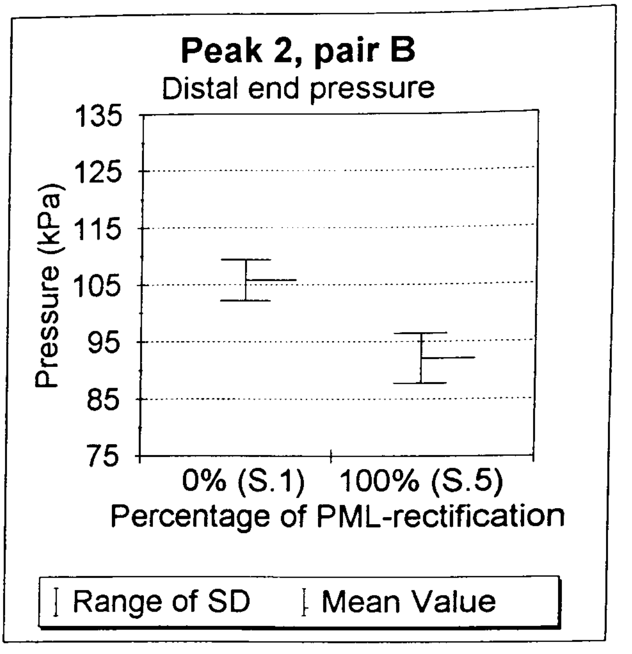

Fig. 7.3.9

In the dynamic tests, the second peak distal end pressures were virtually identical in pair A, while there was a significant decrease in pair B (fig. 7.3.8 and 7.3.9). From these results, it was not possible to determine whether there was any correlation between dynamic peak distal end pressures and an average PML-rectification.

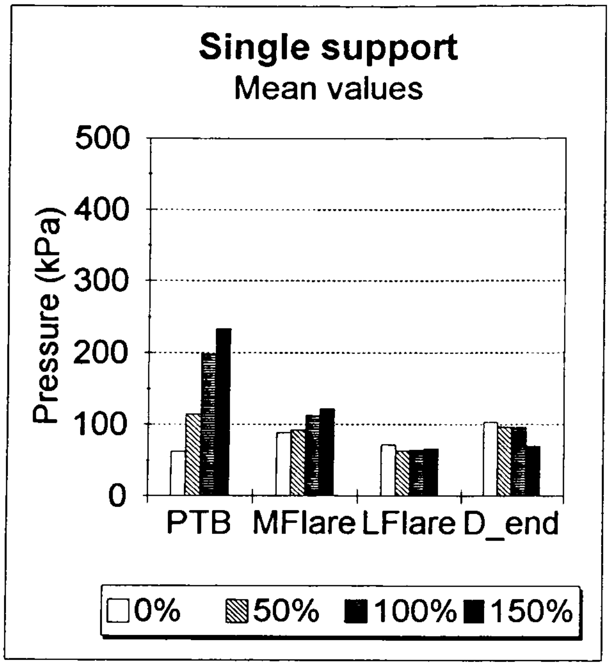

Fig. 7.4.1

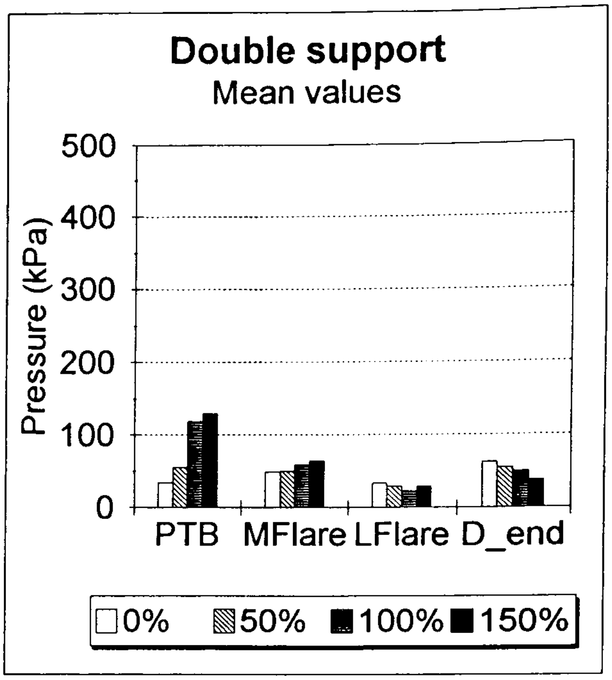

Fig. 7.4.2

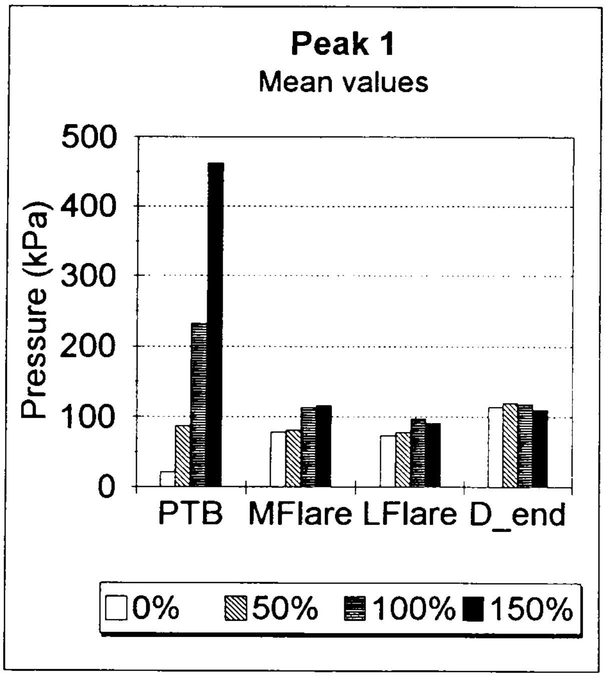

Fig 7.4.3

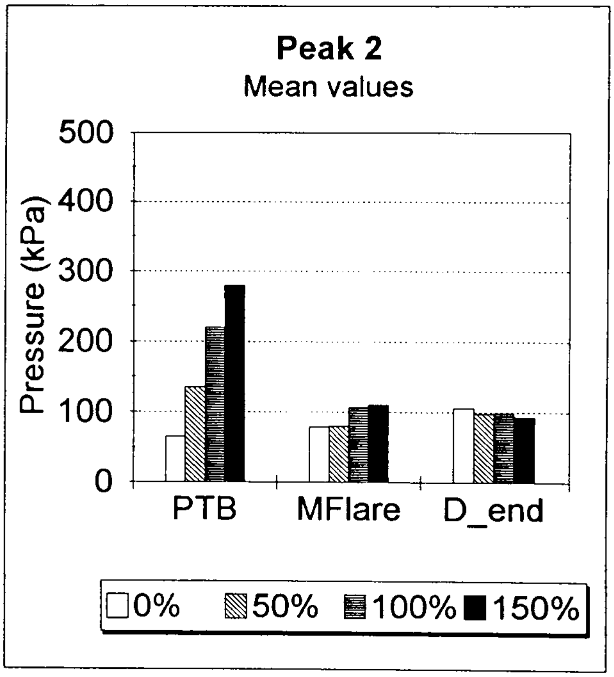

Fig. 7.4.4

7.4 PML-rectifications and resulting pressure levels

The figures 7.4.1 to 7.4.4 summarise the pressures measured in the first four sockets. The Y-axis range is increased to 500 kPa in all graphs to illustrate the increase in first peak PTB pressure and to simplify comparisons between the different tests. In nearly all tests, two significant trends were observed as far as the PML-pressures were concerned:

1) the PTB-pressure increased considerably with each increment of rectification
2) the lateral flare pressure generally did not increase with increasing rectification

The first peak PTB-pressures showed an interesting pattern: in the 0% and 50% rectified socket, they were lower than both the single support and double peak PTB pressures. This might be expected from a biomechanical point of view, as early in stance phase the ground reaction force tends to be directed posterior to the knee, thus decreasing the forces on the anterior-proximal and posterior-distal part of the stump.

However, the first peak 150% PTB-pressure is the highest PTB-pressure of all measurements. This could well be caused by the tensioning of the patellar tendon early in stance phase, when the rate of knee flexion needs to be controlled. Figure 7.4.3 illustrates that at the weight-acceptance stage of the gait cycle, even a very high pressure on the patellar tendon has no effect on the distal end pressure. This appears to confirm the theoretical analysis in section 2.4.1 about the effects of quadriceps activity on the usefulness of a patellar

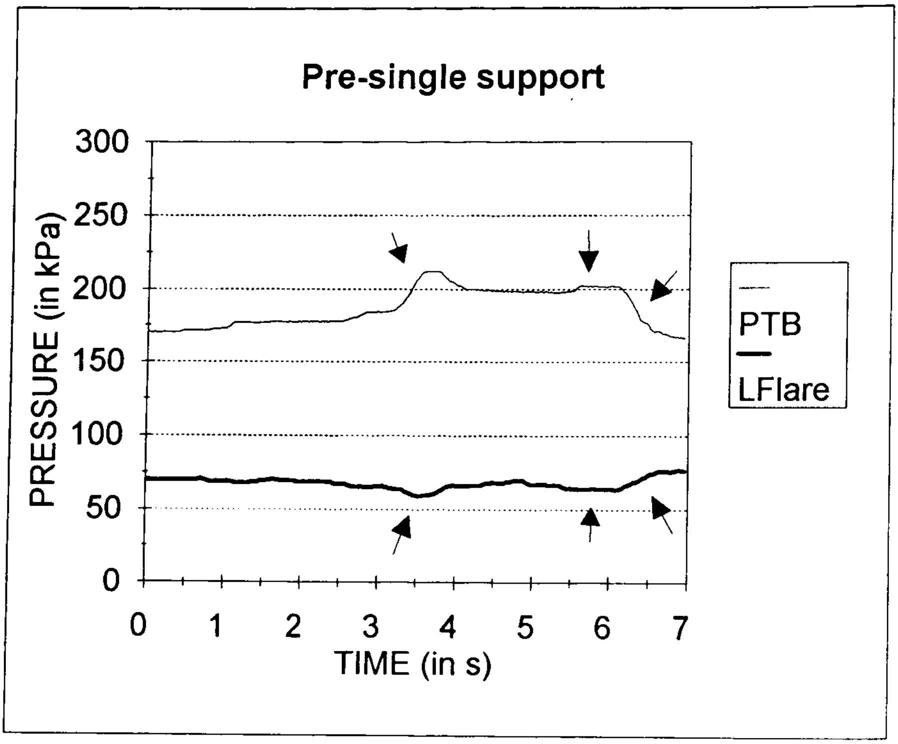
Pre-single support
300
250
200
150
100
50
0
PRESSURE (in kPa)
0
1
2
3
4
5
6
7
TIME (in s)
PTB
LFlare

Fig. 7.4.5

tendon bar.

At the second peak in stance phase, a biomechanical analysis would suggest that the pressures at the anterior-proximal and posterior-distal end of the stump should rise because of the direction of the ground reaction force (in front of the knee). The second peak PTB-pressures appeared to confirm this, the second peak PTB-pressures for all sockets were larger than the single support PTB-pressures.

There was some indication that the lateral flare pressure was directly influenced by the patellar tendon pressure. When the patient was just finding his balance before a single support test, the lateral flare pressure would decrease when the PTB pressure increased (see fig. 7.4.5). This relationship was not observed between the PTB and medial flare or distal end pressure.

In section 2.4.1, the anatomical reasons for this relationship were explained: the posterior displacement of the proximal end of the stump resulting from an increase in PTB-rectification could possibly lead to a decrease in contact with the *antero*-lateral location of the lateral tibial flare support area. This process might explain why the lateral flare pressure did not increase with a general increase in PML-rectification. However, to be certain about how the PML-rectifications influence each other, each rectification should be changed separately.

7.5 Conclusions and recommendations

With the creation of CAD/CAM systems such as the Strathclyde system, a new era in prosthetic socket research has arrived. For the first time, it has become easy to numerically define and store socket shapes and the modifications made to them. This technology made it possible to create six versions of one socket, defined both in shape and volume. With these sockets, it was possible to distinguish volume from shape effects on the support forces at four separate socket locations.

The technical accuracy of this project was greatly enhanced by the combination of the CAD design system with a CNC-machine as a manufacturing *and positioning* tool. The recording capabilities of the CAD system make it possible for subsequent researchers to repeat the original experiments and build on the existing experience.

This means that it is now possible to investigate prosthetic socket design in a methodical and controlled manner. Models created by the prosthetist-computer operator or created by e.g. finite element modelling can be machined and instrumented to investigate the pressure patterns arising in the designs.

The results from this project suggest that the traditional patellar tendon, medial flare and lateral flare rectifications *can* reduce the distal end pressure when an amputee is standing. However, the reduction in distal end pressure is fairly small for an average rectification. In the overrectified socket, the distal end pressure dropped considerably more, but the skin condition of the patient in the patellar tendon area after the tests, suggested that a rectification of this severity would not be tolerated for a long time. Further tests are required to determine the possible contribution from each rectification site to the support forces.

In this project, there was a difference between the static and the dynamic test results. During walking, there was no clear evidence that the PML-rectifications had a significant effect on the distal end pressure. This suggests that either the tests were not sensitive enough or that other mechanisms play a more important role in providing dynamic support than the PML-rectifications. Some authors also suggest that during stance phase, different force transfer mechanisms play a role at different stages (Klasson, 1994).

At this moment in time, the exact nature of force transfer between socket and stump is poorly understood. Soft tissue mechanics is a very complicated subject and the ability of tissues to change their mechanical characteristics over short and long periods of time complicates research considerably. In the long term, only a complete understanding of all the processes involved in stump-socket force transfer can lead to a rational socket design. In the short term, investigations into the effectiveness of currently used socket design concepts can improve the quality of current prosthetic practice.

However, a theoretically sound biomechanical force transfer is just one of the patient's requirements. For the current amputee population, the effect of socket design on the stump circulation needs to be researched. The walking range of a patient suffering from peripheral vascular disease is usually limited by the onset of ischaemic pain after a certain walking distance. By paying attention to this aspect of socket design, we can try to make sure that the prosthetic leg does not become the limiting factor.

REFERENCES

Appoldt, F.A. et al. (1970)
Tangential pressures measurements in above-knee suction sockets
Bulletin of Prosthetics Research, 1970, BPR 10:13, pp 70-86

Bennett, L. et al. (1979)
Shear vs pressure as causative factor in skin blood flow occlusion
Arch. Phys. Med. Rehabil., 1979, 60, July, pp 309-314

Besser, M.P. et al. (1992)
Loading at the patellar tendon and distal end in the PTB prosthesis
Proceedings Seventh World Congress of ISPO, 1992, Chicago, Illinois, USA

Bleck, E.E., Canty, T.J. (1963)
Below-the-knee, closed-end, soft socket
Journal of Bone and Joint Surgery, 1963, 45A, pp 967-976

Breakey, J. (1976)
Gait of unilateral below-knee amputees
Orthotics and Prosthetics, 1976, 30 (3), pp 17-24

Burgess, E.M., Moore, A.J. (1977)
A study of interface pressures in the below-knee prosthesis - Physiological suspension: an interim report
Bulletin of Prosthetics Research, 1977, BPR 10:28, Fall, pp 55-70

Foort, J. (1965)
The Patellar-Tendon-Bearing Prosthesis for Below-Knee Amputees, a Review of Technique and Criteria
Artificial Limbs, 1965, Vol. 9, No.1, pp 4-13

Foort, J. (1984)
Adjustable sockets and significant regions for modularization
Strathclyde papers, 1984, 2, pp 9-10

Foort, J. (1986)
The Knud Jansen Lecture: Innovation in prosthetics and orthotics
Prosthetics and Orthotics International, 1986, 10, pp 61-71

Gardner, H. (1968)
A pneumatic system for below-knee casting
Prosthetics International, 1968, 3 (4/5), pp 12-14

Gowitzke, B.A. et al. (1988)
Scientific basis of human movement (third edition)
Baltimore, 1988, Williams & Wilkins

Grevsten, S. (1978)
Ideas on the suspension of the below-knee prosthesis
Prosthetics and Orthotics International, 1978, 2, pp 3-7

Hayes, R.F. (1975)
A below-knee weight bearing, pressure-formed socket
Orthotics and Prosthetics, 1975, 29 (4), pp 37-40

Inman, V.T. et. al (1981)
Human walking
Baltimore, 1981, Williams & Wilkins

Isherwood, P.A. (1971)
The Controlled Pressure Casting procedure for Patellar Tendon Sockets
BRADU Bulletin No. 4, July 1971, pp 30-33

Isherwood, P.A. (1978)
Simultaneous PTB Socket Pressures and Force Plate values.
BRADU Report 1978, pp 45-49

Katz, K. et al. (1979)
End-bearing characteristics of patellar-tendon-bearing prostheses - a preliminary report
Bulletin of prosthetics research, BPR 10:32, Fall 1979, pp 55-68

Klasson, B. (1994)
Appreciation of prosthetic socket fitting from basic engineering principles
National Centre for Training and Education in Prosthetics and Orthotics
University of Strathclyde, Oct. 1994, Glasgow, Scotland (to be published)

Kristinsson, Ö (1993)
The ICEROSS concept: a discussion of a philosophy
Prosthetics and Orthotics International, 1993, 17 ,pp 49-55

Mizrahi, J. et al. (1985)
Gait performance and dynamic characteristics of weightbearing on the patellar tendon in a patellar tendon bearing prosthesis
Biomechanics IXA, 1985, (Ed. D. Winter), Human Kinetic Publishers, Champain, Illinois

Murdoch, G. (1965)
The "Dundee" socket: a total contact socket for the below-knee amputation
Inter-clinic information bulletin, 1965, 5 (3), pp 13-15

Murdoch, G. (1968)
The "Dundee" socket for the below-knee amputation
Prosthetics International, 1968, 3 (4/5), 15-21

Murphy, E. F. (1954)
"The Fitting of Below-knee Prostheses"
In: Human Limbs and their Substitutes, New York, 1954, pp 693-735

Murphy, E.F., Wilson, A.B. (1961)
Anatomical and physiological considerations in below-knee prosthetics
Artificial Limbs, 1961, 6 (2), pp 4-15

Pearson, J.R. et al. (1973)
"Pressures in critical regions of the below-knee Patellar-Tendon-Bearing prosthesis"
Bulletin of Prosthetic Research, BPR 10:19, Spring 1973, pp 52-76

Pinzur, M.S. et al. (1991)
Dynamic Electromyography in Active and Limited Walking Below-Knee Amputees
Orthopedics, 1991, 14, pp 535-538

Radcliffe, C.W.; Foort, J. (1961)
"The patellar-tendon-bearing below-knee prosthesis"
University of California, Berkeley 1961

Radcliffe, C.W (1961)
The biomechanics of below-knee prostheses in normal, level, bipedal walking.
Artificial Limbs, 1961, 6 (2), pp 16-24

Rae, J.W.; Cockrell, J.L. (1971)
Interface pressures and stress distribution in prosthetic fitting
Bulletin of Prosthetic Research, 1969, 10:12,pp 8-14

Redhead, R.G. (1979)
Total surface bearing self suspending above-knee sockets
Prosthetics and Orthotics International, 1979, 3, pp 126-136

APPENDIX

The appendices have been given the numbers of the sections they are connected with.

Appendix 4.2

Alignment transfer procedure

Socket 1, the reference socket, is fitted and aligned as usual. If the fit is completely satisfactory, it is set up in the transfer jig.

There are two differences with the standard transfer procedure:

1) before setting it up the socket is filled with plaster to prevent the occurrence of any compression by the clamping screws
2) the eight clamping screws have to contact the socket, not the foam as usually happens at the distal end.

The socket is removed by cutting the foam and releasing the clamping screws on one side only. This leaves us with eight indentations on the socket indicating the position of the clamping screws. (These points will be the reference points for positioning the other three sockets in the same alignment configuration.)

The socket is then cut along the posterior aspect and fitted over a duplicate of the original cast. The pole used for this cast is either marked or it is a square pole to indicate the point of 0 degrees of rotation. The top of the pole serves as the reference point for the Z-axis on the CNC-machine (Deckel). The height at which the cast is positioned relative to the Deckel.

The indicator fitted in the Deckers' drillhead is positioned at the eight indentations and the three-dimensional coordinates of each point are recorded.

Then next step is positioning the duplicate of the first cast + socket and the other three casts + sockets in the Deckel in the same zero position as the first cast, again by using square or marked poles and using the top of the poles as the height-zero. The Deckers' indicator re-establishes the position of the eight points on each of the three sockets.

When the duplicate of the first socket is aligned in the transfer jig, a container connected to the transfer jig by sliding clamps will be positioned so that it encloses the casting pole. This container will then be filled with high density Pedilen 700 foam thereby making a mould of the pole and fixing its' position relative to the transfer jig. The next cast can then be positioned accurately by retracting the first cast and inserting the (square) pole of the next cast. The position of the foot and the alignment jigs can be copied on the transfer jig itself.

Summary:

- the eight indentations made by the transfer jig on the first socket are used for aligning the other sockets in the same position
- the deckers' 3D measurement capabilities and the identical socket axes are used to achieve this

Appendix 5.2

Pilot test results

Reference socket, day 1 (Static tests)

Single support	Fy	PTB	MFlare	LFlare	D_end
Unit of measurement	Newtons	kPascals	kPascals	kPascals	kPascals
Serie 1, Stand1	858.1	234.4	89.4	55.1	123.0
Stand2	860.6	267.9	88.3	48.3	118.9
Stand3	858.5	229.7	90.6	53.1	114.4
Serie 2, Stand1	860.8	263.1	87.3	44.5	111.6
Stand2	857.2	234.6	87.0	55.2	106.9
Stand3	855.7	213.1	88.3	59.7	114.7

	Fy	PTB	MFlare	LFlare	D_end
Mean values	858.5	240.5	88.5	52.7	114.9
Standard Dev's	1.8	19.1	1.2	5.0	5.1

Double support	Fy	PTB	MFlare	LFlare	D_end
Unit of measurement	Newtons	kPascals	kPascals	kPascals	kPascals
Serie 1, Stand1	395.4	122.0	50.6	24.2	63.2
Stand2	426.4	116.5	50.5	23.8	58.7
Stand3	492.0	116.3	59.5	30.7	63.1
Serie 2, Stand1	438.9	125.1	51.1	21.2	58.1
Stand2	410.7	124.7	48.1	21.0	61.6
Stand3	407.7	121.8	48.3	19.0	59.7

	Fy	PTB	MFlare	LFlare	D_end
Mean values	428.5	121.1	51.3	23.3	60.7
Standard Dev's	31.6	3.5	3.8	3.7	2.0

Reference socket, day 1 (Dynamic tests)

Peak 1	Fy	PTB	MFlare	LFlare	D_end
Unit of measurement	Newtons	kPascals	kPascals	kPascals	kPascals
Serie 1, Walk1, Step1		229.8	92.8	76.0	133.8
Step2	944.9	248.1	96.4	72.9	134.3
Step3		229.4	96.2	80.1	132.5
Walk2, Step1		219.7	92.6	65.0	139.6
Step2	881.7	192.4	88.7	65.2	133.0
Step3		224.9	96.0	77.7	130.1
Walk3, Step1		233.9	97.7	81.5	130.9
Step2	929.8	259.5	93.4	82.6	130.4
Step3		206.7	94.4	80.7	127.5
Serie 2, Walk1, Step1		228.6	87.8	63.1	130.7
Step2	917.1	219.7	84.3	70.3	127.0
Step3		255.5	92.7	76.1	134.7
Walk2, Step1		225.0	88.0	66.1	126.8
Step2	926.0	246.5	88.0	67.8	123.3
Step3		226.2	91.2	78.8	127.0
Walk3, Step1		212.7	88.4	70.3	122.6
Step2	947.5	266.4	92.0	75.0	127.6
Step3		209.1	91.2	80.2	123.7

Peak 1	Fy	PTB	MFlare	LFlare	D_end
Mean values	924.5	229.7	91.8	73.9	129.7
Standard Dev's	21.8	18.9	3.6	6.2	4.4

Reference socket, day 1 (Dynamic tests)

Peak 2	Fy	PTB	MFlare	D_end
Unit of measurement	Newtons	kPascals	kPascals	kPascals
Serie 1, Walk1, Step1		231.0	94.6	118.7
Step2	893.1	231.9	94.6	119.2
Step3		248.5	94.2	115.0
Walk2, Step1		242.0	85.9	123.2
Step2	860.2	223.3	87.7	119.0
Step3		263.2	89.7	112.9
Walk3, Step1		250.6	92.4	115.0
Step2	881.7	231.1	93.0	115.0
Step3		242.9	93.4	110.5
Serie 2, Walk1, Step1		240.4	82.3	117.8
Step2	891.8	238.0	84.8	115.7
Step3		262.4	86.6	114.6
Walk2, Step1		229.9	82.9	119.9
Step2	908.3	227.0	87.8	113.8
Step3		248.6	86.6	110.9
Walk3, Step1		240.0	85.9	110.2
Step2	912.0	232.7	88.6	112.0
Step3		238.8	84.9	105.2

Peak 2	Fy	PTB	MFlare	D_end
Mean values	891.2	240.1	88.7	114.9
Standard Dev's	17.2	10.9	4.0	4.2

Reference socket, day 2 (Static tests)

Single support	Fy	PTB	MFlare	LFlare	D_end
Unit of measurement	Newtons	kPascals	kPascals	kPascals	kPascals
Serie 1, Stand1	859.4	167.7	103.5	63.4	109.5
Stand2	860.1	181.8	104.7	68.3	100.4
Stand3	859.1	200.1	100.9	63.6	103.8
Serie 2, Stand1	857.6	202.7	91.7	67.6	100.1
Stand2	856.8	159.1	87.4	68.7	111.3
Stand3	857.8	199.8	97.1	61.4	103.6

	Fy	PTB	MFlare	LFlare	D_end
Mean values	858.5	185.2	97.6	65.5	104.8
Standard Dev's	1.2	17.0	6.3	2.8	4.3

Double support	Fy	PTB	MFlare	LFlare	D_end
Unit of measurement	Newtons	kPascals	kPascals	kPascals	kPascals
Serie 1, Stand1	456.3	130.5	54.9	19.7	47.5
Stand2	454.8	139.0	54.8	21.7	52.6
Stand3	502.6	156.8	59.8	23.4	54.0
Serie 2, Stand1	433.5	129.0	52.5	27.9	66.7
Stand2	525.9	122.9	64.4	38.5	67.6
Stand3	431.4	112.4	53.3	29.5	67.9

	Fy	PTB	MFlare	LFlare	D_end
Mean values	467.4	131.8	56.6	26.8	59.4
Standard Dev's	35.1	13.8	4.2	6.3	8.3

Reference socket, day 2 (Dynamic tests)

Peak 1 Values	Fy	PTB	MFlare	LFlare	D_end
Unit of measurement	Newtons	kPascals	kPascals	kPascals	kPascals
Serie 1, Walk1, Step1		223.72	92.47	81.36	115.14
Step2	896.87	239.18	93.89	87.15	116.73
Step3		220.06	95.93	82.74	118.84
Walk2, Step1		173.39	91.74	89.48	115.67
Step2	853.86	200.24	93.57	84.79	115.67
Step3		198.61	102.11	96.65	118.84
Walk3, Step1		249.06	98.42	82.30	118.87
Step2	914.58	264.52	98.01	83.12	116.75
Step3		280.79	107.77	92.50	138.68
Serie 2, Walk1, Step1		236.04	83.39	81.25	99.03
Step2	933.55	238.89	87.66	85.66	102.19
Step3		247.02	90.10	89.79	104.84
Walk2, Step1		220.56	91.09	74.62	103.81
Step2	955.06	244.16	93.94	81.79	112.26
Step3		236.02	91.09	83.17	106.71
Walk3, Step1		248.67	93.98	77.66	107.23
Step2	939.88	267.38	93.77	79.31	121.49
Step3		249.08	93.16	77.11	117.79

Peak 1	Fy	PTB	MFlare	LFlare	D_end
Mean values	915.6	235.4	94.0	83.9	113.9
Standard Dev's	33.2	25.5	5.2	5.4	8.9

Reference socket, day 2 (Dynamic tests)

Peak 2 Values	Fy	PTB	MFlare	D_end
Unit of measurement	Newtons	kPascals	kPascals	kPascals
Serie 1, Walk1, Step1		258.71	89.42	105.37
Step2	880.42	240.40	92.27	107.22
Step3		219.66	87.80	109.33
Walk2, Step1		237.66	97.43	105.90
Step2	885.48	238.07	98.85	108.80
Step3		233.19	99.06	108.54
Walk3, Step1		240.11	91.31	104.07
Step2	872.83	258.01	91.31	98.53
Step3		253.95	92.12	104.07
Serie 2, Walk1, Step1		249.06	87.05	92.42
Step2	884.22	233.19	85.22	92.42
Step3		234.82	86.23	90.84
Walk2, Step1		220.56	91.09	103.81
Step2	884.22	250.26	93.53	100.11
Step3		253.92	91.30	96.68
Walk3, Step1		253.96	92.96	98.51
Step2	888.01	236.47	94.99	112.51
Step3		259.25	95.20	109.87

Peak 2	Fy	PTB	MFlare	D_end
Mean values	882.5	242.8	92.1	102.7
Standard Dev's	4.9	12.0	3.9	6.4

Unrectified socket (static tests)

Single support	Fy	PTB	MFlare	LFlare	D_end
Unit of measurement	Newtons	kPascals	kPascals	kPascals	kPascals
Serie 1, Stand1	863.8	60.0	72.0	51.9	142.7
Stand2	858.9	70.1	75.7	59.1	127.8
Stand3	861.1	68.0	74.2	62.0	121.4
Serie 2, Stand1	858.6	56.8	73.9	58.0	130.0
Stand2	862.8	63.0	72.3	58.3	148.8
Stand3	862.2	52.2	77.6	55.9	121.9

	Fy	PTB	MFlare	LFlare	D_end
Mean values	861.2	61.7	74.3	57.5	132.1
Standard Dev's	1.9	6.2	1.9	3.1	10.3

Double support	Fy	PTB	MFlare	LFlare	D_end
Unit of measurement	Newtons	kPascals	kPascals	kPascals	kPascals
Serie 1, Stand1	405.3	35.1	37.9	25.1	56.9
Stand2	448.7	43.1	39.6	26.3	64.3
Stand3	427.9	41.0	37.5	23.9	58.7
Serie 2, Stand1	434.4	35.3	38.8	28.9	71.0
Stand2	437.6	38.4	36.8	22.5	75.7
Stand3	469.7	38.5	41.4	26.7	79.0

	Fy	PTB	MFlare	LFlare	D_end
Mean values	437.3	38.6	38.7	25.6	67.6
Standard Dev's	19.6	2.9	1.5	2.0	8.3

Unrectified socket (dynamic tests)

Peak 1 Values	Fy	MFlare	LFlare	D_end
Unit of measurement	Newtons	kPascals	kPascals	kPascals
Serie 1, Walk1, Step1		56.7	50.5	141.6
Step2	880.4	57.9	56.5	136.3
Step3		52.6	53.8	136.8
Walk2, Step1		62.4	62.3	129.7
Step2	885.5	63.8	60.9	130.2
Step3		63.4	62.3	140.5
Walk3, Step1		53.5	56.0	137.4
Step2	881.7	60.4	59.0	143.7
Step3		55.5	63.4	161.7
Serie 2, Walk1, Step1		61.6	51.3	182.0
Step2	877.9	55.0	48.5	174.3
Step3		60.5	52.1	169.8
Walk2, Step1		58.7	58.7	145.5
Step2	876.6	58.9	56.5	143.4
Step3		60.0	59.0	152.9
Walk3, Step1		60.3	54.3	146.6
Step2	885.5	59.1	55.9	141.9
Step3		62.6	58.4	160.1

Peak 1	Fy	MFlare	LFlare	D_end
Mean values	881.3	59.1	56.6	148.6
Standard Dev's	3.4	3.2	4.2	14.7

Unrectified socket (dynamic tests)

Peak 2 Values	Fy	PTB	MFlare	D_end
Unit of measurement	Newtons	kPascals	kPascals	kPascals
Serie 1, Walk1, Step1		86.2	61.4	139.7
Step2	875.4	77.7	64.6	138.4
Step3		80.1	62.8	133.9
Walk2, Step1		81.8	62.6	130.7
Step2	850.1	78.1	61.8	126.5
Step3		78.9	63.8	126.3
Walk3, Step1		82.6	60.8	134.2
Step2	846.3	81.0	59.8	137.1
Step3		74.5	61.6	139.2
Serie 2, Walk1, Step1		77.3	64.8	173.3
Step2	870.3	68.7	63.2	169.6
Step3		76.9	63.8	155.8
Walk2, Step1		76.1	65.2	135.8
Step2	845.0	76.5	65.7	135.2
Step3		76.1	66.7	139.7
Walk3, Step1		73.6	67.0	145.1
Step2	846.3	71.2	67.7	139.8
Step3		75.7	66.2	144.5

Peak 2	Fy	PTB	MFlare	D_end
Mean values	855.5	77.4	63.9	141.4
Standard Dev's	12.4	4.0	2.2	12.5

Appendix 6.2

Comparison test results

Static test results (socket 1)

Single support	Fy	PTB	MFlare	LFlare	D_end
Unit of measurement	Newtons	kPascals	kPascals	kPascals	kPascals
Stand1	879.5	62.4	90.3	70.5	103.1
Stand2	879.2	61.4	88.2	71.8	101.7
Stand3	879.6	63.8	90.4	75.7	105.4
Stand4	879.7	64.7	84.2	68.6	100.1
Stand5	877.8	61.5	90.0	75.3	107.0

	Fy	PTB	MFlare	LFlare	D_end
Mean values	879.2	62.7	88.6	72.4	103.5
Standard Dev's	0.7	1.3	2.3	2.7	2.5

Double support	Fy	PTB	MFlare	LFlare	D_end
Unit of measurement	Newtons	kPascals	kPascals	kPascals	kPascals
Stand1	444.3	37.7	47.1	33.6	67.2
Stand2	457.3	31.1	51.5	33.2	63.7
Stand3	437.4	33.3	47.4	31.2	59.8
Stand4	467.7	34.9	49.9	32.9	60.9
Stand5	463.6	35.6	50.3	33.5	61.5

	Fy	PTB	MFlare	LFlare	D_end
Mean values	454.1	34.5	49.2	32.9	62.6
Standard Dev's	11.5	2.2	1.7	0.9	2.6

Dynamic test results (socket 1, peak 1)

Peak1 Values	Fy	PTB	MFlare	LFlare	D_end
Unit of measurement	Newtons	kPascals	kPascals	kPascals	kPascals
Walk1,Step1		34.1	80.8	74.9	117.6
Walk1,Step2	886.7	20.7	74.8	71.1	110.3
Walk1,Step3		16.6	81.0	75.2	114.7
Walk2,Step1		22.8	75.2	77.4	98.7
Walk2,Step2	946.2	21.1	90.4	81.2	116.5
Walk2,Step3		20.7	79.0	78.7	105.9
Walk3,Step1		17.9	75.8	78.2	115.3
Walk3,Step2	912.0	21.5	77.0	77.9	114.7
Walk3,Step3		15.0	80.2	82.0	119.1
Walk4,Step1		21.9	81.2	74.6	117.6
Walk4,Step2	942.4	26.0	82.2	78.5	121.7
Walk4,Step3		26.4	82.0	76.0	116.8
Walk5,Step1		21.5	75.4	76.8	108.5
Walk5,Step2	880.4	17.1	75.6	71.6	109.0
Walk5,Step3		13.8	81.2	77.4	115.5
Walk6,Step1		21.1	81.2	77.4	113.4
Walk6,Step2	841.2	16.2	77.8	68.1	106.4
Walk6,Step3		14.6	79.8	73.3	111.6
Walk7,Step1		21.1	75.6	73.3	110.9
Walk7,Step2	871.6	17.9	75.8	66.7	111.1
Walk7,Step3		23.6	73.0	71.4	111.6
Walk8,Step1		18.2	74.2	68.4	110.6
Walk8,Step2	974.0	16.6	82.2	70.8	121.2
Walk8,Step3		26.3	78.0	68.4	114.7
Walk9,Step1		35.3	76.8	71.3	124.1
Walk9,Step2	901.9	19.9	76.6	68.6	114.7
Walk9,Step3		29.2	70.0	71.3	112.7
Walk10,Step1		20.7	75.6	68.6	112.2
Walk10,Step2	956.3	21.5	79.0	69.5	120.7
Walk10,Step3		22.7	78.6	68.6	120.4

Peak1 Values	Fy	PTB	MFlare	LFlare	D_end
Mean values	911.3	20.5	78.2	73.6	113.9
Standard Dev's	40.4	4.5	3.8	4.2	5.3

Dynamic test results (socket 1, peak 2)

Peak2 Values	Fy	PTB	MFlare	D_end
Unit of measurement	Newtons	kPascals	kPascals	kPascals
Walk1,Step1		69.4	76.6	109.6
Walk1,Step2	880.4	60.9	77.0	104.4
Walk1,Step3		61.7	80.8	106.5
Walk2,Step1		63.7	81.8	99.5
Walk2,Step2	871.6	57.2	77.8	99.2
Walk2,Step3		64.6	83.8	97.4
Walk3,Step1		69.0	78.6	107.5
Walk3,Step2	912.0	64.1	78.8	110.9
Walk3,Step3		69.4	81.4	109.0
Walk4,Step1		61.3	73.2	112.4
Walk4,Step2	894.3	69.8	84.8	110.4
Walk4,Step3		72.3	83.2	107.8
Walk5,Step1		68.6	78.2	102.3
Walk5,Step2	908.3	64.1	83.0	108.5
Walk5,Step3		70.6	81.4	105.4
Walk6,Step1		65.7	82.8	102.8
Walk6,Step2	875.4	61.7	80.2	105.9
Walk6,Step3		69.4	82.8	105.9
Walk7,Step1		67.8	77.0	104.7
Walk7,Step2	894.3	60.9	77.6	109.1
Walk7,Step3		66.6	74.8	103.9
Walk8,Step1		64.1	78.0	103.9
Walk8,Step2	890.5	58.8	79.8	103.3
Walk8,Step3		63.7	76.8	107.5
Walk9,Step1		72.3	72.6	109.0
Walk9,Step2	900.7	59.7	75.6	109.6
Walk9,Step3		73.5	77.2	107.0
Walk10,Step1		67.0	77.0	103.1
Walk10,Step2	876.6	69.4	78.0	102.8
Walk10,Step3		63.3	75.0	102.8

Peak2 Values	Fy	PTB	MFlare	D_end
Mean values	890.4	65.7	78.9	105.7
Standard Dev's	13.4	4.3	3.1	3.6

Static test results (socket 2)

Single support	Fy	PTB	MFlare	LFlare	D_end
Unit of measurement	Newtons	kPascals	kPascals	kPascals	kPascals
Stand1	867.2	116.8	90.4	66.2	98.1
Stand2	869.6	121.4	94.3	62.1	95.2
Stand3	869.8	117.6	93.6	62.6	96.8
Stand4	870.1	110.5	90.9	62.8	96.0
Stand5	870.4	106.8	94.9	64.5	97.2

	Fy	PTB	MFlare	LFlare	D_end
Mean values	869.4	114.6	92.8	63.6	96.7
Standard Dev's	1.1	5.3	1.8	1.5	1.0

Double support	Fy	PTB	MFlare	LFlare	D_end
Unit of measurement	Newtons	kPascals	kPascals	kPascals	kPascals
Stand1	428.1	52.3	48.5	26.8	57.7
Stand2	429.5	50.6	50.9	29.3	54.5
Stand3	421.8	49.1	48.4	27.9	54.0
Stand4	461.2	66.0	52.6	29.5	54.5
Stand5	444.9	57.8	50.9	28.6	54.7

	Fy	PTB	MFlare	LFlare	D_end
Mean values	437.1	55.2	50.3	28.4	55.1
Standard Dev's	14.2	6.2	1.6	1.0	1.3

Dynamic test results (socket 2, peak 1)

Peak1 Values	Fy	PTB	MFlare	LFlare	D_end
Unit of measurement	Newtons	kPascals	kPascals	kPascals	kPascals
Walk1,Step1		89.68	80.16	68.87	105.59
Walk1,Step2	905.72	80.75	81.56	68.33	106.11
Walk1,Step3		86.44	82.36	72.15	111.28
Walk2,Step1		91.73	82.15	77.90	113.08
Walk2,Step2	941.14	87.67	88.16	72.44	116.96
Walk2,Step3		84.02	85.55	75.99	114.11
Walk3,Step1		85.62	78.75	80.62	116.44
Walk3,Step2	950.00	72.63	82.75	76.26	115.41
Walk3,Step3		77.91	85.36	77.07	125.24
Walk4,Step1		86.05	78.94	81.73	119.31
Walk4,Step2	999.33	73.47	82.95	79.00	127.85
Walk4,Step3		85.24	83.35	79.55	122.16
Walk5,Step1		87.23	74.32	78.20	118.50
Walk5,Step2	942.41	83.17	81.94	73.29	117.98
Walk5,Step3		82.36	79.33	77.93	118.24
Walk6,Step1		91.32	84.33	83.91	119.32
Walk6,Step2	952.53	89.69	82.33	80.64	116.99
Walk6,Step3		89.69	82.33	84.73	124.23
Walk7,Step1		100.61	80.36	86.39	124.73
Walk7,Step2	967.71	78.69	79.35	79.29	126.03
Walk7,Step3		91.27	76.55	81.75	123.70
Walk8,Step1		93.31	79.96	80.09	114.65
Walk8,Step2	922.17	86.41	79.96	75.72	115.68
Walk8,Step3		95.75	80.76	81.73	120.08
Walk9,Step1		89.26	78.34	76.54	115.95
Walk9,Step2	941.14	86.42	79.54	80.36	121.38
Walk9,Step3		89.66	78.54	80.09	121.38
Walk10,Step1		99.80	78.73	79.53	120.59
Walk10,Step2	989.21	94.52	82.94	81.72	127.31
Walk10,Step3		99.80	81.53	80.63	128.61

Peak1 Values	Fy	PTB	MFlare	LFlare	D_end
Mean values	951.14	87.67	81.11	78.41	118.96
Standard Dev's	26.88	6.83	2.76	4.18	5.68

Dynamic test results (socket 2, peak 2)

Peak2 Values	Fy	PTB	MFlare	D_end
Unit of measurement	Newtons	kPascals	kPascals	kPascals
Walk1,Step1		173.69	83.36	91.88
Walk1,Step2	867.77	140.00	81.36	93.17
Walk1,Step3		156.24	80.76	91.62
Walk2,Step1		138.80	86.76	95.23
Walk2,Step2	889.28	122.98	87.36	100.40
Walk2,Step3		132.31	86.16	97.81
Walk3,Step1		120.52	79.15	94.71
Walk3,Step2	837.42	91.30	75.74	104.80
Walk3,Step3		109.15	81.95	101.43
Walk4,Step1		119.33	74.54	101.98
Walk4,Step2	865.24	128.26	79.75	94.47
Walk4,Step3		134.34	81.35	97.58
Walk5,Step1		125.78	81.14	104.01
Walk5,Step2	894.34	125.38	79.73	99.61
Walk5,Step3		124.97	76.73	98.06
Walk6,Step1		131.09	81.12	96.29
Walk6,Step2	870.30	137.17	78.12	97.58
Walk6,Step3		141.23	79.52	96.81
Walk7,Step1		141.19	77.15	95.75
Walk7,Step2	874.10	137.13	77.75	99.63
Walk7,Step3		140.38	77.75	100.67
Walk8,Step1		150.13	81.96	96.79
Walk8,Step2	871.57	129.43	80.16	100.16
Walk8,Step3		152.56	81.16	94.47
Walk9,Step1		127.41	78.34	99.39
Walk9,Step2	875.36	138.77	78.74	99.91
Walk9,Step3		141.61	73.93	97.32
Walk10,Step1		140.79	79.73	98.08
Walk10,Step2	876.63	142.41	78.73	99.89
Walk10,Step3		153.37	73.92	99.11

Peak2 Values	Fy	PTB	MFlare	D_end
Unit of measurement	Newtons	kPascals	kPascals	kPascals
Mean values	872.20	134.92	79.80	97.95
Standard Dev's	14.48	14.98	3.29	3.16

Static test results (socket 3)

Single support	**Fy**	**PTB**	**MFlare**	**LFlare**	**D_end**
Unit of measurement	**Newtons**	**kPascals**	**kPascals**	**kPascals**	**kPascals**
Stand1	886.6	214.8	113.6	61.2	102.7
Stand2	885.2	199.7	118.0	66.2	95.4
Stand3	880.2	185.4	110.0	68.1	92.7
Stand4	877.7	193.0	110.7	64.0	93.3
Stand5	881.9	197.5	111.5	63.1	93.1

	Fy	**PTB**	**MFlare**	**LFlare**	**D_end**
Mean values	882.3	198.1	112.7	64.5	95.4
Standard Dev's	3.2	9.7	2.9	2.4	3.7

Double support	**Fy**	**PTB**	**MFlare**	**LFlare**	**D_end**
Unit of measurement	**Newtons**	**kPascals**	**kPascals**	**kPascals**	**kPascals**
Stand1	424.7	131.0	57.3	18.6	49.4
Stand2	453.0	122.9	62.2	22.8	52.0
Stand3	439.5	112.6	56.6	23.7	47.0
Stand4	444.5	124.2	60.5	24.1	52.3
Stand5	439.1	104.2	58.4	25.0	49.9

	Fy	**PTB**	**MFlare**	**LFlare**	**D_end**
Mean values	440.2	119.0	59.0	22.8	50.1
Standard Dev's	9.2	9.4	2.0	2.2	1.9

Dynamic test results (socket 3, peak 1)

Peak1 Values	Fy	PTB	MFlare	LFlare	D_end
Unit of measurement	Newtons	kPascals	kPascals	kPascals	kPascals
Walk1,Step1		233.3	116.7	93.7	113.2
Walk1,Step2	970.2	277.5	118.3	94.8	120.2
Walk1,Step3		234.9	113.7	98.9	112.7
Walk2,Step1		224.0	119.2	98.3	118.5
Walk2,Step2	936.1	225.2	112.6	95.0	112.5
Walk2,Step3		228.9	122.0	104.8	119.8
Walk3,Step1		226.8	112.7	100.9	115.2
Walk3,Step2	1003.1	265.4	122.1	105.5	121.7
Walk3,Step3		217.5	112.5	98.1	112.9
Walk4,Step1		231.3	109.5	100.6	112.9
Walk4,Step2	972.8	247.5	114.3	103.3	118.6
Walk4,Step3		211.4	110.7	98.4	112.1
Walk5,Step1		226.8	109.7	91.6	118.6
Walk5,Step2	944.9	235.3	105.7	89.1	117.1
Walk5,Step3		242.2	117.7	100.1	124.3
Walk6,Step1		222.0	110.7	94.6	118.6
Walk6,Step2	991.7	241.4	114.1	99.2	119.6
Walk6,Step3		229.7	112.3	97.3	118.6
Walk7,Step1		238.2	112.9	96.5	121.2
Walk7,Step2	1038.5	242.7	115.1	100.1	127.4
Walk7,Step3		217.5	109.3	92.4	117.3
Walk8,Step1		241.1	114.5	92.1	115.0
Walk8,Step2	927.2	201.3	102.1	89.4	112.1
Walk8,Step3		217.1	113.5	93.8	115.5
Walk9,Step1		219.1	107.3	93.8	111.9
Walk9,Step2	999.3	235.7	114.3	100.3	122.0
Walk9,Step3		225.6	114.3	97.1	118.9
Walk10,Step1		229.8	114.1	99.8	119.6
Walk10,Step2	927.2	220.5	107.7	90.2	113.9
Walk10,Step3		232.3	115.3	96.2	120.9

Peak1 Values	Fy	PTB	MFlare	LFlare	D_end
Mean values	971.1	231.4	113.1	96.9	117.4
Standard Dev's	35.4	14.7	4.4	4.2	3.9

Dynamic test results (socket 3, peak 2)

Peak2 Values	Fy	PTB	MFlare	D_end
Unit of measurement	Newtons	kPascals	kPascals	kPascals
Walk1,Step1		223.2	111.3	98.2
Walk1,Step2	896.9	221.9	110.7	98.7
Walk1,Step3		230.1	108.5	95.3
Walk2,Step1		214.7	110.8	97.5
Walk2,Step2	896.9	208.2	110.4	98.3
Walk2,Step3		209.4	111.0	96.0
Walk3,Step1		219.5	112.3	97.9
Walk3,Step2	918.4	219.5	112.5	99.5
Walk3,Step3		226.8	107.1	96.4
Walk4,Step1		215.0	106.7	96.1
Walk4,Step2	905.7	217.9	108.7	100.2
Walk4,Step3		221.1	105.5	108.5
Walk5,Step1		233.7	102.3	97.4
Walk5,Step2	881.7	226.4	99.5	95.1
Walk5,Step3		225.6	104.5	97.9
Walk6,Step1		209.8	103.5	99.4
Walk6,Step2	896.9	217.9	103.7	103.6
Walk6,Step3		226.4	106.7	115.0
Walk7,Step1		221.6	103.9	101.8
Walk7,Step2	895.6	215.5	101.0	100.5
Walk7,Step3		204.5	101.0	98.9
Walk8,Step1		226.9	110.7	99.2
Walk8,Step2	886.7	208.2	105.3	96.3
Walk8,Step3		217.9	107.7	98.9
Walk9,Step1		227.6	109.7	100.7
Walk9,Step2	893.1	216.7	107.7	98.9
Walk9,Step3		220.3	104.5	97.1
Walk10,Step1		217.7	105.1	98.7
Walk10,Step2	889.3	217.2	103.3	97.4
Walk10,Step3		224.1	104.5	96.3

Peak2 Values	Fy	PTB	MFlare	D_end
Mean values	896.1	219.5	106.6	99.2
Standard Dev's	9.7	6.9	3.6	3.9

Static test results (socket 4)

Single support	Fy	PTB	MFlare	LFlare	D_end
Unit of measurement	Newtons	kPascals	kPascals	kPascals	kPascals
Stand1	876.8	253.9	120.9	63.0	71.1
Stand2	876.5	219.1	121.4	67.9	71.0
Stand3	873.2	222.7	123.6	67.0	69.8
Stand4	871.6	236.6	121.3	66.2	67.7
Stand5	873.3	228.7	121.0	67.2	71.3

	Fy	PTB	MFlare	LFlare	D_end
Mean values	874.3	232.2	121.6	66.3	70.2
Standard Dev's	2.0	12.4	1.0	1.7	1.3

Double support	Fy	PTB	MFlare	LFlare	D_end
Unit of measurement	Newtons	kPascals	kPascals	kPascals	kPascals
Stand1	407.3	120.9	62.8	27.7	38.7
Stand2	405.6	127.3	63.0	30.0	36.0
Stand3	423.5	120.9	63.2	31.1	39.0
Stand4	477.6	147.0	63.4	26.7	39.2
Stand5	493.5	129.2	66.7	29.1	37.8

	Fy	PTB	MFlare	LFlare	D_end
Mean values	441.5	129.0	63.8	28.9	38.2
Standard Dev's	36.9	9.6	1.4	1.6	1.2

Dynamic test results (socket 4, peak 1)

Peak1 Values	Fy	PTB	MFlare	LFlare	D_end
Unit of measurement	Newtons	kPascals	kPascals	kPascals	kPascals
Walk1,Step1		458.1	114.2	86.8	104.5
Walk1,Step2	1009.5	539.3	123.6	95.3	114.8
Walk1,Step3		472.7	120.0	93.4	109.2
Walk2,Step1		511.8	119.2	89.8	107.1
Walk2,Step2	984.2	526.8	121.2	94.8	113.8
Walk2,Step3		455.3	117.4	95.0	108.4
Walk3,Step1		436.6	111.6	85.7	101.2
Walk3,Step2	919.6	512.1	114.4	86.5	104.8
Walk3,Step3		434.6	113.6	90.1	106.9
Walk4,Step1		431.4	110.2	87.4	102.9
Walk4,Step2	912.0	483.7	111.8	86.3	104.8
Walk4,Step3		463.8	116.2	91.7	113.8
Walk5,Step1		506.1	119.2	98.5	120.0
Walk5,Step2	969.0	534.5	119.6	95.8	116.1
Walk5,Step3		455.7	114.0	91.7	108.4
Walk6,Step1		447.6	115.2	97.2	112.5
Walk6,Step2	948.7	489.8	114.8	92.6	107.6
Walk6,Step3		454.9	116.2	94.2	108.7
Walk7,Step1		407.4	112.0	89.0	107.1
Walk7,Step2	981.6	511.7	120.2	98.1	120.0
Walk7,Step3		405.0	112.4	94.8	111.0
Walk8,Step1		454.1	111.6	88.2	109.2
Walk8,Step2	879.2	446.0	105.4	85.2	105.3
Walk8,Step3		426.9	113.8	94.2	115.1
Walk9,Step1		426.5	117.6	91.2	108.2
Walk9,Step2	910.8	461.4	113.4	85.2	103.5
Walk9,Step3		403.3	116.2	93.6	106.9
Walk10,Step1		431.4	116.0	88.7	109.9
Walk10,Step2	939.9	459.4	118.8	90.7	114.9
Walk10,Step3		422.5	118.0	87.1	113.1

Peak1 Values	Fy	PTB	MFlare	LFlare	D_end
Mean values	945.4	462.3	115.6	91.3	109.7
Standard Dev's	38.6	38.2	3.8	3.9	4.8

Dynamic test results (socket 4, peak 2)

Peak2 Values	Fy	PTB	MFlare	D_end
Unit of measurement	Newtons	kPascals	kPascals	kPascals
Walk1,Step1		265.8	108.4	89.5
Walk1,Step2	885.5	284.0	113.4	89.2
Walk1,Step3		286.5	109.6	88.5
Walk2,Step1		284.1	112.8	89.8
Walk2,Step2	893.1	268.7	113.0	92.4
Walk2,Step3		294.2	111.6	90.5
Walk3,Step1		292.6	108.8	89.8
Walk3,Step2	864.0	280.8	109.4	88.2
Walk3,Step3		287.7	109.4	94.4
Walk4,Step1		301.1	107.8	91.3
Walk4,Step2	853.9	265.4	107.4	91.0
Walk4,Step3		305.6	107.8	93.1
Walk5,Step1		339.7	113.0	96.5
Walk5,Step2	899.4	298.7	113.2	99.1
Walk5,Step3		295.0	108.8	94.9
Walk6,Step1		270.2	110.4	94.9
Walk6,Step2	880.4	285.3	112.2	90.8
Walk6,Step3		275.9	111.8	91.8
Walk7,Step1		259.7	110.8	98.5
Walk7,Step2	896.9	283.2	112.0	99.3
Walk7,Step3		273.5	108.8	96.7
Walk8,Step1		269.1	107.8	96.5
Walk8,Step2	874.1	253.6	108.2	98.8
Walk8,Step3		276.8	107.4	100.1
Walk9,Step1		277.5	111.4	95.7
Walk9,Step2	865.2	258.5	111.0	90.8
Walk9,Step3		271.8	107.0	92.6
Walk10,Step1		260.9	112.0	93.1
Walk10,Step2	855.1	259.3	110.0	98.8
Walk10,Step3		275.2	108.2	97.5

Peak2 Values	Fy	PTB	MFlare	D_end
Mean values	876.8	280.0	110.1	93.8
Standard Dev's	16.0	17.4	2.0	3.6

Static test results (socket 5)

Single support	Fy	PTB	MFlare	LFlare	D_end
Unit of measurement	Newtons	kPascals	kPascals	kPascals	kPascals
Stand1	875.2	190.4	91.1	60.6	97.2
Stand2	873.1	209.9	91.4	60.9	95.7
Stand3	872.6	216.8	93.4	59.9	96.3
Stand4	877.1	200.9	90.9	64.3	95.9
Stand5	871.8	198.7	92.9	57.0	90.9

	Fy	PTB	MFlare	LFlare	D_end
Mean values	874.0	203.4	91.9	60.5	95.2
Standard Dev's	1.9	9.1	1.0	2.3	2.2

Double support	Fy	PTB	MFlare	LFlare	D_end
Unit of measurement	Newtons	kPascals	kPascals	kPascals	kPascals
Stand1	406.7	104.5	44.3	25.2	49.5
Stand2	434.3	138.6	47.1	21.8	50.9
Stand3	461.3	112.5	53.6	30.5	55.0
Stand4	450.3	101.8	50.9	29.5	54.2
Stand5	451.1	111.4	51.2	29.3	54.9

	Fy	PTB	MFlare	LFlare	D_end
Mean values	440.7	113.8	49.4	27.3	52.9
Standard Dev's	19.1	13.1	3.3	3.3	2.3

Dynamic test results (socket 5, peak1)

Peak1 Values	Fy	PTB	MFlare	LFlare	D_end
Unit of measurement	Newtons	kPascals	kPascals	kPascals	kPascals
Walk1,Step1		238.8	77.8	70.7	103.6
Walk1,Step2	947.5	246.5	82.2	73.7	103.6
Walk1,Step3		226.6	81.2	75.6	100.8
Walk2,Step1		251.0	74.0	75.4	94.6
Walk2,Step2	885.5	239.6	74.8	73.4	95.4
Walk2,Step3		246.9	80.2	78.6	101.8
Walk3,Step1		243.6	73.2	69.6	99.8
Walk3,Step2	926.0	284.2	84.1	74.5	110.9
Walk3,Step3		241.2	78.2	75.9	101.3
Walk4,Step1		299.6	78.6	90.4	111.4
Walk4,Step2	966.4	302.9	79.4	87.9	112.9
Walk4,Step3		275.7	77.6	85.7	106.0
Walk5,Step1		296.8	77.4	90.1	103.1
Walk5,Step2	953.8	294.4	80.4	88.2	102.1
Walk5,Step3		258.7	75.2	85.5	97.9
Walk6,Step1		275.7	79.8	80.5	113.5
Walk6,Step2	937.3	281.8	79.8	81.6	105.5
Walk6,Step3		250.9	77.0	82.1	109.1
Walk7,Step1		274.9	79.4	81.3	119.4
Walk7,Step2	963.9	283.8	78.0	82.4	114.3
Walk7,Step3		261.9	76.0	80.8	113.7
Walk8,Step1		282.6	71.0	77.5	110.1
Walk8,Step2	977.8	296.8	76.2	80.0	116.8
Walk8,Step3		293.1	82.2	83.5	125.6
Walk9,Step1		284.2	73.8	77.5	106.7
Walk9,Step2	948.7	297.2	72.8	75.6	111.9
Walk9,Step3		282.6	73.8	77.3	115.5
Walk10,Step1		298.8	86.0	81.6	123.0
Walk10,Step2	993.0	291.9	84.6	84.6	124.0
Walk10,Step3		270.8	84.8	84.6	119.6

Peak1 Values	Fy	PTB	MFlare	LFlare	D_end
Mean values	950.0	272.5	78.3	80.2	109.1
Standard Dev's	28.3	22.2	3.8	5.4	8.3

Dynamic test results (socket 5, peak 2)

Peak2 Values	Fy	PTB	MFlare	D_end
Unit of measurement	Newtons	kPascals	kPascals	kPascals
Walk1,Step1		213.6	80.4	89.6
Walk1,Step2	862.7	215.3	81.4	83.4
Walk1,Step3		201.5	79.0	92.7
Walk2,Step1		217.3	82.8	84.7
Walk2,Step2	848.8	177.9	78.2	86.6
Walk2,Step3		210.4	84.6	87.6
Walk3,Step1		208.3	81.2	94.6
Walk3,Step2	861.4	178.3	78.8	99.5
Walk3,Step3		203.1	82.8	94.6
Walk4,Step1		258.6	79.4	91.5
Walk4,Step2	876.6	221.3	78.8	95.3
Walk4,Step3		218.5	75.0	85.0
Walk5,Step1		220.1	78.6	87.1
Walk5,Step2	889.3	209.2	80.2	86.8
Walk5,Step3		216.9	76.6	86.0
Walk6,Step1		200.2	75.8	99.2
Walk6,Step2	876.6	197.0	78.0	92.3
Walk6,Step3		207.5	80.4	97.2
Walk7,Step1		230.2	79.2	93.3
Walk7,Step2	865.2	201.8	76.4	93.0
Walk7,Step3		216.4	79.8	97.2
Walk8,Step1		209.9	76.4	94.3
Walk8,Step2	858.9	216.8	74.8	92.7
Walk8,Step3		212.0	76.4	92.5
Walk9,Step1		204.7	76.8	93.0
Walk9,Step2	872.8	209.6	75.6	95.1
Walk9,Step3		203.5	73.0	96.4
Walk10,Step1		238.4	80.0	94.3
Walk10,Step2	862.7	222.5	77.6	96.1
Walk10,Step3		229.4	77.6	92.5

Peak2 Values	Fy	PTB	MFlare	D_end
Mean values	867.5	212.3	78.5	92.1
Standard Dev's	10.9	15.3	2.6	4.3

Static test results (socket 6)

Single support	Fy	PTB	MFlare	LFlare	D_end
Unit of measurement	Newtons	kPascals	kPascals	kPascals	kPascals
Stand1	878.5	56.1	105.8	80.1	104.1
Stand2	883.0	61.6	99.2	78.8	101.3
Stand3	878.2	64.1	100.6	81.4	103.4
Stand4	875.5	60.7	100.8	79.2	103.6
Stand5	877.8	68.3	96.7	82.2	104.7

	Fy	PTB	MFlare	LFlare	D_end
Mean values	878.6	62.1	100.6	80.4	103.4
Standard Dev's	2.4	4.0	3.0	1.3	1.2

Double support	Fy	PTB	MFlare	LFlare	D_end
Unit of measurement	Newtons	kPascals	kPascals	kPascals	kPascals
Stand1	443.0	24.8	56.0	38.0	54.7
Stand2	426.0	25.7	51.6	33.4	53.5
Stand3	448.6	25.9	55.1	35.7	54.5
Stand4	427.1	26.4	52.5	33.8	54.8
Stand5	440.5	25.9	53.3	35.1	56.2

	Fy	PTB	MFlare	LFlare	D_end
Mean values	437.1	25.7	53.7	35.2	54.7
Standard Dev's	9.0	0.5	1.6	1.6	0.9

Dynamic test results (socket 6, peak 1)

Peak1 Values	Fy	PTB	MFlare	LFlare	D_end
Unit of measurement	Newtons	kPascals	kPascals	kPascals	kPascals
Walk1,Step1		25.6	81.5	84.5	99.2
Walk1,Step2	838.7	24.8	82.5	87.5	100.2
Walk1,Step3		31.2	82.3	78.8	94.5
Walk2,Step1		26.0	85.4	101.2	105.6
Walk2,Step2	855.1	27.6	83.0	92.7	101.2
Walk2,Step3		28.8	88.0	95.2	101.5
Walk3,Step1		25.9	82.4	86.7	100.2
Walk3,Step2	853.9	26.8	80.2	93.0	96.9
Walk3,Step3		28.0	87.2	84.5	97.9
Walk4,Step1		30.0	80.8	79.8	94.8
Walk4,Step2	905.7	28.4	87.0	99.8	111.3
Walk4,Step3		31.6	86.0	86.1	104.1
Walk5,Step1		26.4	81.4	85.3	98.7
Walk5,Step2	904.5	29.6	91.4	96.0	115.5
Walk5,Step3		26.8	82.2	87.0	105.4
Walk6,Step1		20.7	98.6	99.5	127.4
Walk6,Step2	975.3	24.7	97.4	94.6	127.1
Walk6,Step3		22.7	90.0	91.6	121.2
Walk7,Step1		19.5	81.0	90.8	110.6
Walk7,Step2	903.2	19.9	85.6	92.9	112.1
Walk7,Step3		27.2	86.2	91.3	112.6
Walk8,Step1		22.7	84.0	85.1	110.3
Walk8,Step2	858.9	25.5	84.6	83.7	106.4
Walk8,Step3		28.8	88.8	89.2	110.1
Walk9,Step1		23.1	90.6	91.8	116.5
Walk9,Step2	928.5	18.2	85.5	98.4	109.6
Walk9,Step3		24.3	86.2	89.1	103.9
Walk10,Step1		20.3	87.7	92.1	108.8
Walk10,Step2	904.5	24.3	87.1	88.8	105.9
Walk10,Step3		26.3	85.9	91.8	106.2

Peak1 Values	Fy	PTB	MFlare	LFlare	D_end
Mean values	892.8	25.5	86.0	90.3	107.2
Standard Dev's	39.5	3.4	4.4	5.5	8.4

Dynamic test results (socket 6, peak 2)

Peak2 Values	Fy	PTB	MFlare	D_end
Walk1,Step1		57.6	86.1	97.9
Walk1,Step2	884.2	56.4	86.7	98.4
Walk1,Step3		56.0	89.8	93.7
Walk2,Step1		60.5	93.2	97.1
Walk2,Step2	888.0	60.1	90.2	96.3
Walk2,Step3		62.5	90.0	97.1
Walk3,Step1		62.1	89.2	91.7
Walk3,Step2	880.4	59.2	84.0	93.8
Walk3,Step3		60.8	92.2	94.3
Walk4,Step1		59.6	88.0	91.2
Walk4,Step2	886.7	56.8	88.0	95.3
Walk4,Step3		62.9	90.2	99.2
Walk5,Step1		58.5	89.8	97.4
Walk5,Step2	877.9	55.6	87.2	102.0
Walk5,Step3		58.9	90.8	105.1
Walk6,Step1		59.2	84.4	105.4
Walk6,Step2	856.4	48.7	82.4	106.2
Walk6,Step3		51.1	87.2	111.1
Walk7,Step1		53.2	86.2	108.0
Walk7,Step2	876.6	51.5	84.6	105.6
Walk7,Step3		55.2	90.4	106.7
Walk8,Step1		52.7	85.2	103.1
Walk8,Step2	857.7	51.9	84.0	101.3
Walk8,Step3		59.2	87.8	102.0
Walk9,Step1		55.5	86.4	102.3
Walk9,Step2	872.8	46.2	82.3	97.4
Walk9,Step3		55.5	86.4	97.9
Walk10,Step1		49.9	87.9	96.3
Walk10,Step2	894.3	51.1	85.9	96.6
Walk10,Step3		54.7	86.3	97.6

Peak2 Values	Fy	PTB	MFlare	D_end
Mean values	877.5	56.1	87.4	99.6
Standard Dev's	11.8	4.2	2.7	5.0

Appendix 7.2

Fy-GRF comparisons

Fy-normalised distal end values of volume equivalent sockets

To calculate how Fy related to the total ground reaction force (Ftot), the Fx, Fy and Fz of the first five walks on the reference socket have been converted to Ftot.
The tables below show that at the first peak, the difference between Fy and Ftot is only 1.4 % of the Fy value.
At the second peak, that difference is only 0.7% of the Fy value.

Peak1	**Fx**	**Fy**	**Fz**	**Ftot**
Unit of measurement	**Newtons**	**Newtons**	**Newtons**	**Newtons**
Walk1	138	970	68	982
Walk2	132	936	68	948
Walk3	152	1003	95	1019
Walk4	145	973	83	987
Walk5	132	945	76	957

For the first peak values, Ftot is on average 13 N larger than Fy (1.4 % of the Fy value)

Peak2	**Fx**	**Fy**	**Fz**	**Ftot**
Unit of measurement	**Newtons**	**Newtons**	**Newtons**	**Newtons**
Walk1	68	897	62	902
Walk2	62	897	75	902
Walk3	61	918	85	924
Walk4	58	906	75	911
Walk5	79	882	79	889

For the second peak values, Ftot is on average 6 N larger than Fy (0.7 % of the Fy value)

	Single support	Fy	D_end	D_end:FyNormalised
	Unit of measurement	Newtons	kPascals	kPascals
Pair A	100% (Socket 3)	882	95	95
	0% (Socket 6)	879	103	103
Pair B	100% (Socket 5)	874	95	95
	0% (Socket 1)	879	103	103

	Double support	Fy	D_end	D_end:FyNormalised
	Unit of measurement	Newtons	kPascals	kPascals
Pair A	100% (Socket 3)	440	50	50
	0% (Socket 6)	437	55	55
Pair B	100% (Socket 5)	441	53	53
	0% (Socket 1)	454	63	61

	Peak 1	Fy	D_end	D_end:FyNormalised
	Unit of measurement	Newtons	kPascals	kPascals
Pair A	100% (Socket 3)	971	117	113
	0% (Socket 6)	893	107	112
Pair B	100% (Socket 5)	950	109	108
	0% (Socket 1)	911	114	117

	Peak 2	Fy	D_end	D_end:FyNormalised
	Unit of measurement	Newtons	kPascals	kPascals
Pair A	100% (Socket 3)	896	99	97
	0% (Socket 6)	878	100	100
Pair B	100% (Socket 5)	868	92	93
	0% (Socket 1)	890	106	104